

VOLUME 43 (2011)

ISSN 1016-2526

PUNJAB UNIVERSITY **JOURNAL** **OF** **MATHEMATICS**

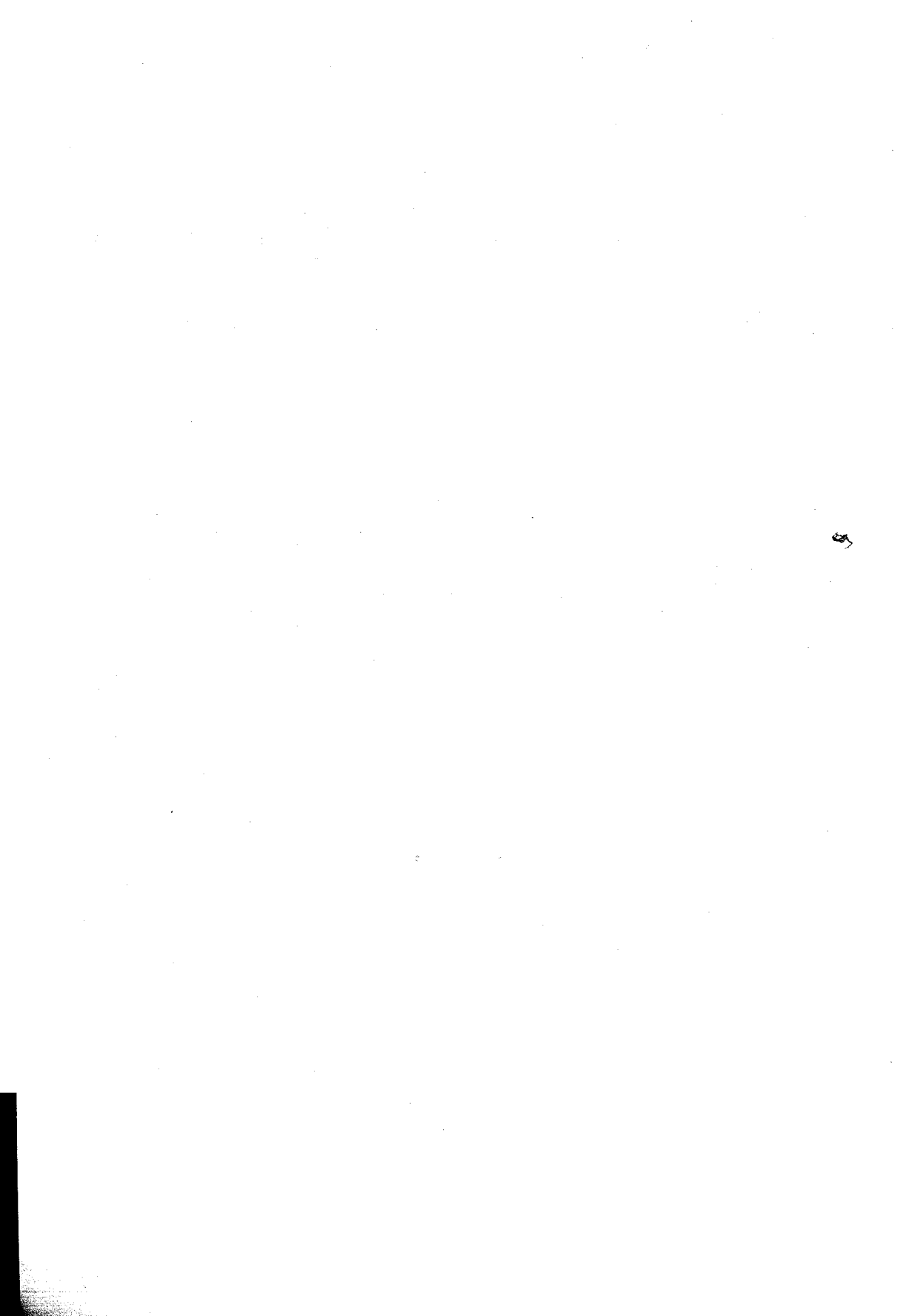


DEPARTMENT OF MATHEMATICS

UNIVERSITY OF THE PUNJAB

LAHORE - 54000 PAKISTAN

www.punjabu.edu.pk/mathjournal



Editorial Board

Chief Editor

Shahid S. Siddiqi
Department of Mathematics
University of the Punjab
Lahore - Pakistan
Email: shahid_siddiqi@math.pu.edu.pk
Shahidsiddiqimath@yahoo.co.uk

Editor

Muhammad Sharif
Department of Mathematics
University of the Punjab
Lahore - Pakistan

Managerial Secretary

Zahid Hussain Shamsi
Department of Mathematics
University of the Punjab
Lahore - Pakistan

Associate Editors

Ghazala Akram
Department of Mathematics
University of the Punjab
Lahore - Pakistan

Robert Cripps
School of Engineering Mechanical Engineering
The University of Birmingham
B15 2TT
UK

Ioannis K. Argyros
Department of Mathematics
Cameron University
Lawton, OK 73505
USA

B. Davvaz
Department of Mathematics
Yazd University Yazd Iran

René de Borst
Department of Mechanical Engineering
Eindhoven University of Technology
P.O. Box 513, NL-5600 MB Eindhoven The
Netherlands

Qi Duan
School of Mathematics and System Science
Shandong University Jinan, 250100
China

Kung-Ching Chang
Department of Mathematics
Peking University
Beijing 100871
China

Sebastien Ferenczi
Institut de Mathematiques de Luminy
CNRS-UPR 9016
Case 930-163 avenue de Luminy
F13288 Marseille Cedex 9
France

Yuqun Chen
Department of Mathematics South China Normal
University
Guangzhou 510631
China

Brian Fisher
Department of Mathematics and Computer Science
University of Leicester
Leicester, LE1 7RH
England

A. D. R. Choudary
School of Mathematical Sciences (SMS)
Lahore - Pakistan

Malik Zawwar Hussain
Department of Mathematics
University of the Punjab
Lahore - Pakistan

P. Corsini
Dept of Mathematics and CS Via delle Science 206
33100 Udine
Italy

Palle Jorgensen
Department of Mathematics
14 MLH
The University of Iowa
Iowa City, IA 52242-1419
USA

Young Bae Jun
Department of Mathematics Education
Gyeongsang Natl University
Chinju 660-701
Korea

Abdul Qayyum M. Khaliq
Department of Mathematical Sciences
Middle Tennessee State University
Murfreesboro, TN 37132
USA

Manabu Sakai
Department of Mathematics and Computer Science
Kagoshima University
1-22-36, Kagoshima city Kagoshima, 890-0065
Japan

Muhammad Sarfraz
Department of Information Science
Kuwait University Kuwait

Walter Schempp
Lehrstuhl fuer Mathematik I
University of Siegen
Walter-Flex-Strasse 3
57068 Siegen
Germany

Muhammad Aslam Malik
Department of Mathematics
University of the Punjab
Lahore - Pakistan

Ratnasingham Shivaji
Department of Mathematics and Statistics
Mississippi State University
Mississippi State, MS 39762
USA

Hari M. Srivastava
Department of Mathematics and Statistics
University of Victoria
Victoria, British Columbia V8W 3P4
Canada

Jieqing Tan
Director, Institute of Applied Mathematics
Hefei University of Technology
Hefei 230009
China

E. H. Twizell
School of Information Systems
Computing and Mathematics
Brunel University
Uxbridge, Middlesex
UB8 3PH
England

E. M. E. Zayed
Department of Mathematics
Zagazig University
Zagazig
Egypt

CONTENTS

1. Chromatic Uniqueness of Complete Bipartite Graphs with Certain Edges Deleted II 1-8
by R. Hasni and Y.H. Peng
2. Newton-Like Methods with At least Quadratic Order of Convergence for the Computation of Fixed Points 9-18
by Ioannis K. Argyros
3. On the Semilocal Convergence of Werner's Method for Solving Equations Using Recurrent Functions 19-28
by Ioannis K. Argyros and Said Hilout
4. Simulation of Rotational Flows in Cylindrical Vessel with Double Rotating Stirrers; Part-A: Analysis of Flow Structure and Pressure Differentials 29-45
by Ahsanullah Baloch, Rafique Ahmed Memon and M.A. Solangi
5. Analysis of Stresses and Power Consumption of Mixing Flow in Cylindrical Container 47-67
by Ahsanullah Baloch, Rafique Ahmed Memon and M.A. Solangi
6. Convolution of Salagean-type Harmonic Univalent Functions 69-73
by Saurabh Porwal, K. K. Dixit and S. B. Joshi
7. G -Subsets and G -Orbits of $Q^*(\sqrt{n})$ Under Action of the Modular Group 75-84
by M. Riaz and M. Aslam Malik
8. Anti Fuzzy Implicative Ideals in BCK-Algebras 85-91
by Nora. O. Al-Shehri

Chromatic Uniqueness of Complete Bipartite Graphs with Certain Edges Deleted II

R. Hasni

School of Mathematical Sciences
Universiti Sains Malaysia
11800 USM, Penang, Malaysia
Email: hroslan@cs.usm.my

Y. H. Peng

Department of Mathematics, and
Institute for Mathematical Research
Universiti Putra Malaysia
43400 UPM Serdang, Malaysia
Email: yhpeng@fsas.upm.edu.my

Abstract. For integers p, q, s with $p \geq q \geq 2$ and $s \geq 0$, let $\mathcal{K}_2^{-s}(p, q)$ denote the set of 2-connected bipartite graphs which can be obtained from $K_{p,q}$ by deleting a set of s edges. In this paper, we prove that for any graph $G \in \mathcal{K}_2^{-s}(p, q)$ with $p \geq q \geq 3$, if $11 \leq s \leq q - 1$ and $\Delta(G') = s - 4$, where $G' = K_{p,q} - G$, then G is chromatically unique. This result extends both a theorem by Dong et al. [2] and the result in [4].

AMS (MOS) Subject Classification Codes: 05C15

Key Words: Chromatic Polynomial, Chromatically Unique, Chromatically Equivalent.

1. INTRODUCTION

All graphs considered here are simple graphs. For a graph G , let $V(G)$, $E(G)$, $\delta(G)$, $\Delta(G)$ and $P(G, \lambda)$ be the vertex set, edge set, minimum degree, maximum degree and the chromatic polynomial of G , respectively.

Two graphs G and H are said to be *chromatically equivalent* (or simply χ -equivalent), symbolically $G \sim H$, if $P(G, \lambda) = P(H, \lambda)$. The equivalence class determined by G under \sim is denoted by $[G]$. A graph G is *chromatically unique* (or simply χ -unique) if $H \cong G$ whenever $H \sim G$, i.e. $[G] = \{G\}$ up to isomorphism. For a set \mathcal{G} of graphs, if $[G] \subseteq \mathcal{G}$ for every $G \in \mathcal{G}$, then \mathcal{G} is said to be χ -closed. For two sets \mathcal{G}_1 and \mathcal{G}_2 of graphs, if $P(G_1, \lambda) \neq P(G_2, \lambda)$ for every $G_1 \in \mathcal{G}_1$ and $G_2 \in \mathcal{G}_2$, then \mathcal{G}_1 and \mathcal{G}_2 are said to be chromatically disjoint, or simply χ -disjoint.

For integers p, q, s with $p \geq q \geq 2$ and $s \geq 0$, let $\mathcal{K}^{-s}(p, q)$ (resp. $\mathcal{K}_2^{-s}(p, q)$) denote the set of connected (resp. 2-connected) bipartite graphs which can be obtained from $K_{p,q}$ by deleting a set of s edges.

For a bipartite graph $G = (A, B; E)$ with bipartition A and B and edge set E , let $G' = (A', B'; E')$ be the bipartite graph induced by the edge set $E' = \{xy \mid xy \notin E, x \in$

$A, y \in B \}$, where $A' \subseteq A$ and $B' \subseteq B$. We write $G' = K_{p,q} - G$, where $p = |A|$ and $q = |B|$. Let $\Delta(G')$ denote the maximum degree of G' .

Dong et al. [1] have shown that any $G \in \mathcal{K}_2^{-s}(p, q)$ with $p \geq q \geq 3$, is chromatically unique if one of the following conditions holds.

- (i): $5 \leq s \leq q - 1$ and if $\Delta(G') = s - 1$, or
- (ii): $7 \leq s \leq q - 1$ and if $\Delta(G') = s - 2$.

In [5], we proved that for any $G \in \mathcal{K}_2^{-s}(p, q)$ with $p \geq q \geq 3$, is chromatically unique if $9 \leq s \leq q - 1$ and if $\Delta(G') = s - 3$. In this paper, we give a similar result by examining the chromatic uniqueness of any $G \in \mathcal{K}_2^{-s}(p, q)$, where $11 \leq s \leq q - 1$ and if $\Delta(G') = s - 4$. Our result is similar to that of Dong et al. in [1].

2. PRELIMINARY RESULTS AND NOTATIONS

For a graph G and a positive integer k , a partition $\{A_1, A_2, \dots, A_k\}$ of $V(G)$ is called a k -independent partition in G if each A_i is a non-empty independent set of G . Let $\alpha(G, k)$ denote the number of k -independent partitions in G . For any graph G of order n , we have (see [3]):

$$P(G, \lambda) = \sum_{k=1}^n \alpha(G, k) \lambda(\lambda - 1) \cdots (\lambda - k + 1).$$

Thus, we have

Lemma 1. *If $G \sim H$, then $\alpha(G, k) = \alpha(H, k)$ for $k = 1, 2, \dots$*

Partition $\mathcal{K}^{-s}(p, q)$ into the following subsets:

$$\mathcal{D}_i(p, q, s) = \left\{ G \in \mathcal{K}^{-s}(p, q) \mid \Delta(G') = i \right\}, \quad i = 1, 2, \dots, s.$$

The following result was obtained in [1].

Theorem 2. *Let $p \geq q \geq 3$ and $1 \leq s \leq q - 1$.*

- (i): $\mathcal{D}_1(p, q, s)$ is χ -closed.
- (ii): $\cup_{2 \leq i \leq (s+3)/2} \mathcal{D}_i(p, q, s)$ is χ -closed for $s \geq 2$.
- (iii): $\mathcal{D}_i(p, q, s)$ is χ -closed for each i with $\lceil (s+3)/2 \rceil \leq i \leq \min\{s, q-2\}$.
- (iv): $\mathcal{D}_{q-1}(p, q, s) \cap \mathcal{K}_2^{-s}(p, q)$ is χ -closed for $s = q - 1$.

For any bipartite graph $G = (A, B; E)$ with bipartition A and B and edge set E , we have

$$\alpha'(G, 3) = \alpha(G, 3) - (2^{|A|-1} + 2^{|B|-1} - 2). \quad (2. 1)$$

For a bipartite graph $G = (A, B; E)$, let $\mathcal{I}(G)$ be the set of independent sets in G and let

$$\Omega(G) = \{ Q \in \mathcal{I}(G) \mid Q \cap A \neq \emptyset, Q \cap B \neq \emptyset \}.$$

The following result is then obtained.

Lemma 3. *(Dong et al. [2]) For $G \in \mathcal{K}^{-s}(p, q)$,*

$$\alpha'(G, 3) = |\Omega(G)| \geq 2^{\Delta(G')} + s - 1 - \Delta(G').$$

For a bipartite graph $G = (A, B; E)$, the number of 4-independent partitions $\{A_1, A_2, A_3, A_4\}$ in G with $A_i \subseteq A$ or $A_i \subseteq B$ for all $i = 1, 2, 3, 4$ is

$$\begin{aligned} & (2^{|A|-1} - 1)(2^{|B|-1} - 1) + \frac{1}{3!}(3^{|A|} - 3 \cdot 2^{|A|} + 3) + \frac{1}{3!}(3^{|B|} - 3 \cdot 2^{|B|} + 3) \\ & = (2^{|A|-1} - 2)(2^{|B|-1} - 2) + \frac{1}{2}(3^{|A|} + 3^{|B|}) - 2. \end{aligned}$$

Define

$$\alpha'(G, 4) = \alpha(G, 4) - \left\{ (2^{|A|-1} - 2)(2^{|B|-1} - 2) + \frac{1}{2}(3^{|A|} + 3^{|B|}) - 2 \right\}.$$

Observe that for $G, H \in \mathcal{K}^{-s}(p, q)$,

$$\alpha(G, 4) = \alpha(H, 4) \quad \text{if and only if} \quad \alpha'(G, 4) = \alpha'(H, 4).$$

The following lemmas will be used to prove our main result.

Lemma 4. (Dong et al. [3]) For $G = (A, B; E) \in \mathcal{K}^{-s}(p, q)$ with $|A| = p$ and $|B| = q$,

$$\begin{aligned} \alpha'(G, 4) = & \sum_{Q \in \Omega(G)} (2^{p-1-|Q \cap A|} + 2^{q-1-|Q \cap B|} - 2) \\ & + | \{ \{Q_1, Q_2\} \mid Q_1, Q_2 \in \Omega(G), Q_1 \cap Q_2 = \emptyset \} |. \end{aligned}$$

Lemma 5. (Dong et al. [3]) For a bipartite graph $G = (A, B; E)$, if uvw is a path in G' with $d_{G'}(u) = 1$ and $d_{G'}(v) = 2$, then for any $k \geq 2$,

$$\alpha(G, k) = \alpha(G + uv, k) + \alpha(G - \{u, v\}, k - 1) + \alpha(G - \{u, v, w\}, k - 1).$$

By using Lemma 5 we obtain the following lemma.

Lemma 6. (Roslan and Peng [5]) For a bipartite graph $G = (A, B; E)$, if uvw, uvw and wvy are three paths in G' with $d_{G'}(u) = 1$ and $d_{G'}(v) = 3$, then for any $k \geq 2$,

$$\begin{aligned} \alpha(G, k) = & \alpha(G + uv, k) + \alpha(G - \{u, v\}, k - 1) + \alpha(G - \{u, v, w\}, k - 1) + \\ & \alpha(G - \{u, v, y\}, k - 1) + \alpha(G - \{u, v, w, y\}, k - 1). \end{aligned}$$

By extending Lemmas 5 and 6, we obtain the following result.

Lemma 7. For a bipartite graph $G = (A, B; E)$, if uvw, uvw, wvt, wvy, wvt and yvt are six paths in G' with $d_{G'}(u) = 1$ and $d_{G'}(v) = 4$, then for any $k \geq 2$,

$$\begin{aligned} \alpha(G, k) = & \alpha(G + uv, k) + \alpha(G - \{u, v\}, k - 1) + \alpha(G - \{u, v, t\}, k - 1) + \\ & \alpha(G - \{u, v, y\}, k - 1) + \alpha(G - \{u, v, y, t\}, k - 1) + \\ & \alpha(G - \{u, v, w\}, k - 1) + \alpha(G - \{u, v, w, t\}, k - 1) + \\ & \alpha(G - \{u, v, w, y\}, k - 1) + \alpha(G - \{u, v, w, y, t\}, k - 1). \end{aligned}$$

Proof. Since $P(G, \lambda) = P(G + uv, \lambda) + P(G \cdot uv, \lambda)$, we have

$$\alpha(G, k) = \alpha(G + uv, k) + \alpha(G \cdot uv, k).$$

Let x be the vertex in $G \cdot uv$ produced by identifying u and v , and z the vertex in $G \cdot uv \cdot xw$ produced by identifying x and w , and s the vertex in $G \cdot uv \cdot xw \cdot zy$ produced by identifying z and y . Notice that x is adjacent to all vertices in $V(G \cdot uv \cdot xw) - \{x, w, y, t\}$, z is

adjacent to all vertices in $V(G \cdot uv \cdot xw) - \{z, y, t\}$ and s is adjacent to all vertices in $V(G \cdot uv \cdot xw \cdot zy) - \{s, t\}$. Thus

$$\begin{aligned}
 G \cdot uv + xw + xy + xt &= K_1 + (G - \{u, v\}), \\
 (G \cdot uv + xw + xy) \cdot xy &= K_1 + (G - \{u, v, t\}), \\
 (G \cdot uv + xw) \cdot xy + xt &= K_1 + (G - \{u, v, y\}), \\
 (G \cdot uv + xw) \cdot xy \cdot xt &= K_1 + (G - \{u, v, y, t\}), \\
 (G \cdot uv \cdot xw + zy + zt &= K_1 + (G - \{u, v, w\}), \\
 (G \cdot uv \cdot xw + zy) \cdot zt &= K_1 + (G - \{u, v, w, t\}), \\
 (G \cdot uv \cdot xw \cdot zy) + st &= K_1 + (G - \{u, v, w, y\}) \quad \text{and} \\
 G \cdot uv \cdot xw \cdot zy \cdot st &= K_1 + (G - \{u, v, w, y, t\}).
 \end{aligned}$$

We also observe that for any graph H , $\alpha(K_1 + H, k) = \alpha(H, k - 1)$, since $P(K_1 + H, \lambda) = \lambda P(H, \lambda - 1)$. Hence

$$\begin{aligned}
 \alpha(G \cdot uv, k) &= \alpha(G \cdot uv + xw, k) + \alpha(G \cdot uv \cdot xw, k) \\
 &= \alpha(G \cdot uv + xw + xy + xt, k) + \alpha((G \cdot uv + xw + xy) \cdot xt, k) + \\
 &\quad \alpha((G \cdot uv + xw) \cdot xy + xt, k) + \alpha((G \cdot uv + xw) \cdot xy \cdot xt, k) + \\
 &\quad \alpha(G \cdot uv \cdot xw + zy + zt, k) + \alpha((G \cdot uv \cdot xw + zy) \cdot zt, k) + \\
 &\quad \alpha((G \cdot uv \cdot xw \cdot zy) + st, k) + \alpha(G \cdot uv \cdot xw \cdot zy \cdot st, k) \\
 &= \alpha(K_1 + (G - \{u, v\}), k) + \alpha(K_1 + (G - \{u, v, t\}), k) + \\
 &\quad \alpha(K_1 + (G - \{u, v, y\}), k) + \alpha(K_1 + (G - \{u, v, y, t\}), k) + \\
 &\quad \alpha(K_1 + (G - \{u, v, w\}), k) + \alpha(K_1 + (G - \{u, v, w, t\}), k) + \\
 &\quad \alpha(K_1 + (G - \{u, v, w, y\}), k) + \alpha(K_1 + (G - \{u, v, w, y, t\}), k) \\
 &= \alpha(G - \{u, v\}, k - 1) + \alpha(G - \{u, v, t\}, k - 1) + \\
 &\quad \alpha(G - \{u, v, y\}, k - 1) + \alpha(G - \{u, v, y, t\}, k - 1) + \\
 &\quad \alpha(G - \{u, v, w\}, k - 1) + \alpha(G - \{u, v, w, t\}, k - 1) + \\
 &\quad \alpha(G - \{u, v, w, y\}, k - 1) + \alpha(G - \{u, v, w, y, t\}, k - 1).
 \end{aligned}$$

The lemma is then obtained. \square

3. MAIN RESULTS

In [2], Dong et al. proved that every 2-connected graph in $\mathcal{D}_s(p, q, s)$ is χ -unique. Then, Dong et al. in [1] also proved that G is χ -unique for every $G \in \mathcal{D}_{s-1}(p, q, s)$, where $s \geq 5$, and that G is χ -unique for every $G \in \mathcal{D}_{s-2}(p, q, s)$, where $s \geq 7$. In [5], we have shown that each graph G in $\mathcal{D}_{s-3}(p, q, s)$, where $s \geq 9$, then G is χ -unique. In this section, we shall prove that for each graph G in $\mathcal{D}_{s-4}(p, q, s)$, where $s \geq 11$, G is χ -unique. We first have the following lemma.

Lemma 8. *For any G in $\mathcal{D}_{s-4}(p, q, s)$, where $s \geq 9$, G' is one of the graphs in Figure 1 [8].*

We now present our main result in the following theorem.

Theorem 9. *For any $G \in \mathcal{K}_2^{-s}(p, q)$, with $p \geq q \geq s + 1 \geq 12$, if $\Delta(G') = s - 4$, then G is χ -unique.*

Proof. Since $s \geq 11$, $(s+3)/2 \geq s-3$ and thus by Theorem 2, $\mathcal{D}_{s-4}(p, q, s)$ is χ -closed. By Lemma 8, if G in $\mathcal{D}_{s-4}(p, q, s)$, then G' is one of the graphs in Figure 1 [8]. Thus $\mathcal{D}_{s-4}(p, q, s)$ contain 166 graphs, which are named as V_1, V_2, \dots, V_{166} (see table in [7]). We then group these graphs according to their $\alpha'(V_i, 3)$ which can be calculated by using Lemma 4.

$$\begin{aligned}
\mathcal{T}_1 &= \{ V_1, V_2 \} \\
\mathcal{T}_2 &= \{ V_3, V_4 \} \\
\mathcal{T}_3 &= \{ V_5, V_6 \} \\
\mathcal{T}_4 &= \{ V_7, V_8, V_9, V_{10} \} \\
\mathcal{T}_5 &= \{ V_{11}, V_{12}, V_{13}, V_{14} \} \\
\mathcal{T}_6 &= \{ V_{15}, V_{16}, V_{17}, V_{18}, V_{19}, V_{20} \} \\
\mathcal{T}_7 &= \{ V_{21}, V_{22}, V_{23}, V_{24}, V_{25}, V_{26}, V_{27}, V_{28} \} \\
\mathcal{T}_8 &= \{ V_{29}, V_{30}, V_{31}, V_{32}, V_{33}, V_{34}, V_{35}, V_{36} \} \\
\mathcal{T}_9 &= \{ V_{37}, V_{38}, \dots, V_{54} \} \\
\mathcal{T}_{10} &= \{ V_{55}, V_{56}, V_{57}, V_{58} \} \\
\mathcal{T}_{11} &= \{ V_{59}, V_{60}, \dots, V_{78} \} \\
\mathcal{T}_{12} &= \{ V_{79}, V_{80}, \dots, V_{104} \} \\
\mathcal{T}_{13} &= \{ V_{105}, V_{106}, \dots, V_{122} \} \\
\mathcal{T}_{14} &= \{ V_{123}, V_{124}, \dots, V_{142} \} \\
\mathcal{T}_{15} &= \{ V_{143}, V_{144}, \dots, V_{158} \} \\
\mathcal{T}_{16} &= \{ V_{159}, V_{160}, V_{161}, V_{162}, V_{163}, V_{164} \} \\
\mathcal{T}_{17} &= \{ V_{165}, V_{166} \}
\end{aligned}$$

Observe that for any i, j with $1 \leq i < j \leq 17$, $\alpha'(V_{i_1}, 3) > \alpha'(V_{j_1}, 3)$ if $V_{i_1} \in \mathcal{T}_i$ and $V_{j_1} \in \mathcal{T}_j$. Thus by Lemma 8 and Equation (2. 1), \mathcal{T}_i and \mathcal{T}_j ($1 \leq i < j \leq 17$) are χ -disjoint and since $\mathcal{D}_{s-4}(p, q, s)$ is χ -closed, each \mathcal{T}_i ($1 \leq i \leq 17$) is χ -closed. Hence, for each i , to show that all graphs in \mathcal{T}_i are χ -unique, it suffices to show that for any two graphs, $V_{i_1}, V_{i_2} \in \mathcal{T}_i$, if $V_{i_1} \not\cong V_{i_2}$, then either $\alpha'(V_{i_1}, 4) \neq \alpha'(V_{i_2}, 4)$ or $\alpha(V_{i_1}, 5) \neq \alpha(V_{i_2}, 5)$. The values of $\alpha'(V_i, 4)$ by using Lemma 4. We shall establish several inequalities of the form $\alpha'(V_i, 4) < \alpha'(V_j, 4)$ for some i, j . Since the method used to obtain these inequalities is standard, long and rather repetitive, we shall not discuss all here. In the following, we shall only show the examples of detailed comparisons. In the first example, we compare $\alpha'(V_1, 4)$ and $\alpha'(V_2, 4)$ when $p > q$, and in the second example, we compute $\alpha(V_{21}, 5) - \alpha(V_{23}, 5)$ when $p = q$. The reader may refer to [6, 7] for all graphs and other detailed comparisons.

(1) V_1 and V_2 when $p > q$

$$\begin{aligned}
& \alpha'(V_1, 4) - \alpha'(V_2, 4) \\
&= \left[\left(\sum_{i=1}^{s-4} \binom{s-4}{i} (2^{p-i-1} + 2^{q-2} - 2) \right) + 15 \cdot 2^{p-1} + 2^q + 15 \cdot 2^{q-3} \right. \\
&\quad \left. + 11 \cdot 2^{q-6} + 15 \cdot 2^{s-5} - 75 \right] - \left[\left(\sum_{i=1}^{s-4} \binom{s-4}{i} (2^{q-i-1} + 2^{p-2} - 2) \right) \right. \\
&\quad \left. + 15 \cdot 2^{q-1} + 2^p + 15 \cdot 2^{p-3} + 11 \cdot 2^{p-6} + 15 \cdot 2^{s-5} - 75 \right] \\
&= \left[\sum_{i=1}^{s-4} \binom{s-4}{i} (2^{p-i-1} - 2^{q-i-1})(1 - 2^{i-1}) \right] + 15(2^{p-1} - 2^{q-1}) - \\
&\quad (2^{p-2} - 2^{q-2}) - 15(2^{p-3} - 2^{q-3}) - 11(2^{p-6} - 2^{q-6}) \\
&< -15 \binom{s-4}{5} (2^{p-6} - 2^{q-6}) + 15 \cdot 2^5 (2^{p-6} - 2^{q-6}) \\
&\quad - 2^6 (2^{p-5} - 2^{q-5}) - 15 \cdot 2^3 (2^{p-5} - 2^{q-5}) - 11(2^{p-6} - 2^{q-6}) \\
&= (2^{p-6} - 2^{q-6}) \left[-15 \binom{s-4}{5} + 15 \cdot 32 - 64 - 15 \cdot 8 - 11 \right] \\
&\leq (2^{p-6} - 2^{q-6}) [-15 \cdot 21 + 285] \left[\text{since } \binom{s-4}{5} \geq \binom{7}{5} = 21 \right] \\
&= (2^{p-6} - 2^{q-5})(-30) < 0.
\end{aligned}$$

(2) V_{21} and V_{23} when $p = q$

When $p = q$, $\alpha'(V_{21}, 4) = \alpha'(V_{23}, 4)$. Thus we need to calculate $\alpha(V_{21}, 5) - \alpha(V_{23}, 5)$. Using Lemma 7, we have

$$\begin{aligned}
& \alpha(V_{21}, 5) - \alpha(V_{23}, 5) \\
&= \left[\alpha(V_{21} + a_1 b_1, 5) + \alpha(V_{21} - \{a_1, b_1\}, 4) + \alpha(V_{21} - \{a_1, b_1, e_1\}, 4) + \right. \\
&\quad \alpha(V_{21} - \{a_1, b_1, d_1\}, 4) + \alpha(V_{21} - \{a_1, b_1, d_1, e_1\}, 4) + \\
&\quad \alpha(V_{21} - \{a_1, b_1, c_1\}, 4) + \alpha(V_{21} - \{a_1, b_1, c_1, e_1\}, 4) + \\
&\quad \left. \alpha(V_{21} - \{a_1, b_1, c_1, d_1\}, 4) + \alpha(V_{21} - \{a_1, b_1, c_1, d_1, e_1\}, 4) \right] - \\
&\quad \left[\alpha(V_{23} + a_2 b_2, 5) + \alpha(V_{23} - \{a_2, b_2\}, 4) + \alpha(V_{23} - \{a_2, b_2, e_2\}, 4) + \right. \\
&\quad \alpha(V_{23} - \{a_2, b_2, d_2\}, 4) + \alpha(V_{23} - \{a_2, b_2, d_2, e_2\}, 4) + \\
&\quad \alpha(V_{23} - \{a_2, b_2, c_2\}, 4) + \alpha(V_{23} - \{a_2, b_2, c_2, e_2\}, 4) + \\
&\quad \left. \alpha(V_{23} - \{a_2, b_2, c_2, d_2\}, 4) + \alpha(V_{23} - \{a_2, b_2, c_2, d_2, e_2\}, 4) \right]
\end{aligned}$$

$$\begin{aligned}
&= \left(\alpha(V_{21} - \{a_1, b_1, e_1\}, 4) - \alpha(V_{23} - \{a_2, b_2, e_2\}, 4) \right) + \\
&\quad \left(\alpha(V_{21} - \{a_1, b_1, d_1\}, 4) - \alpha(V_{23} - \{a_2, b_2, d_2\}, 4) \right) + \\
&\quad \left(\alpha(V_{21} - \{a_1, b_1, d_1, e_1\}, 4) - \alpha(V_{23} - \{a_2, b_2, d_2, e_2\}, 4) \right) + \\
&\quad \left(\alpha(V_{21} - \{a_1, b_1, c_1\}, 4) - \alpha(V_{23} - \{a_2, b_2, c_2\}, 4) \right) + \\
&\quad \left(\alpha(V_{21} - \{a_1, b_1, c_1, e_1\}, 4) - \alpha(V_{23} - \{a_2, b_2, c_2, e_2\}, 4) \right) + \\
&\quad \left(\alpha(V_{21} - \{a_1, b_1, c_1, d_1\}, 4) - \alpha(V_{23} - \{a_2, b_2, c_2, d_2\}, 4) \right) + \\
&\quad \left(\alpha(V_{21} - \{a_1, b_1, c_1, d_1, e_1\}, 4) - \alpha(V_{23} - \{a_2, b_2, c_2, d_2, e_2\}, 4) \right) \\
&\text{since } V_{21} + a_1b_1 \cong V_{23} + a_2b_2, V_{21} - \{a_1, b_1\} \cong V_{23} - \{a_2, b_2\} \\
&= \left(\alpha'(V_{21} - \{a_1, b_1, e_1\}, 4) - \alpha'(V_{23} - \{a_2, b_2, e_2\}, 4) \right) + \\
&\quad \left(\alpha'(V_{21} - \{a_1, b_1, d_1\}, 4) - \alpha'(V_{23} - \{a_2, b_2, d_2\}, 4) \right) + \\
&\quad \left(\alpha'(V_{21} - \{a_1, b_1, d_1, e_1\}, 4) - \alpha'(V_{23} - \{a_2, b_2, d_2, e_2\}, 4) \right) + \\
&\quad \left(\alpha'(V_{21} - \{a_1, b_1, c_1\}, 4) - \alpha'(V_{23} - \{a_2, b_2, c_2\}, 4) \right) + \\
&\quad \left(\alpha'(V_{21} - \{a_1, b_1, c_1, e_1\}, 4) - \alpha'(V_{23} - \{a_2, b_2, c_2, e_2\}, 4) \right) + \\
&\quad \left(\alpha'(V_{21} - \{a_1, b_1, c_1, d_1\}, 4) - \alpha'(V_{23} - \{a_2, b_2, c_2, d_2\}, 4) \right) + \\
&\quad \left(\alpha'(V_{21} - \{a_1, b_1, c_1, d_1, e_1\}, 4) - \alpha'(V_{23} - \{a_2, b_2, c_2, d_2, e_2\}, 4) \right) \\
&= \left(\sum_{i=1}^{s-4} \binom{s-4}{i} (2^{p-3-i} + 2^{q-3} - 2) - \sum_{i=1}^{s-4} \binom{s-4}{i} (2^{p-2-i} + 2^{q-4} - 2) \right) \\
&\quad + \left(\sum_{i=1}^{s-4} \binom{s-4}{i} (2^{p-3-i} + 2^{q-3} - 2) - \sum_{i=1}^{s-4} \binom{s-4}{i} (2^{p-2-i} + 2^{q-4} - 2) \right)
\end{aligned}$$

$$\begin{aligned}
& + \left(\sum_{i=1}^{s-4} \binom{s-4}{i} (2^{p-4-i} + 2^{q-3} - 2) - \sum_{i=1}^{s-4} \binom{s-4}{i} (2^{p-2-i} + 2^{q-5} - 2) \right) \\
& + \left(\sum_{i=1}^{s-4} \binom{s-4}{i} (2^{p-3-i} + 2^{q-3} - 2) - \sum_{i=1}^{s-4} \binom{s-4}{i} (2^{p-2-i} + 2^{q-4} - 2) \right) \\
& + \left(\sum_{i=1}^{s-4} \binom{s-4}{i} (2^{p-4-i} + 2^{q-3} - 2) - \sum_{i=1}^{s-4} \binom{s-4}{i} (2^{p-2-i} + 2^{q-5} - 2) \right) \\
& + \left(\sum_{i=1}^{s-4} \binom{s-4}{i} (2^{p-4-i} + 2^{q-3} - 2) - \sum_{i=1}^{s-4} \binom{s-4}{i} (2^{p-2-i} + 2^{q-5} - 2) \right) \\
& + \left(\sum_{i=1}^{s-4} \binom{s-4}{i} (2^{p-5-i} + 2^{q-3} - 2) - \sum_{i=1}^{s-4} \binom{s-4}{i} (2^{p-2-i} + 2^{q-6} - 2) \right) \\
& = 37 \left\{ \binom{s-3}{1} (2^{p-6} - 2^{p-6}) + \binom{s-4}{2} (2^{p-6} - 2^{p-7}) + \right. \\
& \quad \left. \binom{s-4}{3} (2^{p-6} - 2^{p-8}) + \dots + \binom{s-4}{s-4} (2^{p-6} - 2^{p-s-1}) \right\} \text{ since } p = q \\
& > 0 \text{ since } s \geq 11.
\end{aligned}$$

Similarly, we can show that for any two graphs $V_{i_1}, V_{i_2} \in \mathcal{T}_i$, if $V_{i_1} \not\cong V_{i_2}$, then either $\alpha'(V_{i_1}, 4) \neq \alpha'(V_{i_2}, 4)$ or $\alpha(V_{i_1}, 5) \neq \alpha(V_{i_2}, 5)$ (see [6]). Hence the proof of the theorem is complete. \square

As conclusion of this paper, we give the following conjecture which is true for $t = 3, 4, 5$ and 6.

Conjecture. For any $G \in \mathcal{K}_2^{-s}(p, q)$, with $p \geq q \geq s + 1 \geq 2t$ ($t = 3, 4, 5, \dots$), if $\Delta(G') = s - t + 2$, then G is χ -unique.

Acknowledgement. The authors would like to thank the referees for their constructive and helpful comments.

REFERENCES

- [1] F.M. Dong, K.M. Koh, K.L. Teo, C.H.C. Little, M.D. Hendy, *An attempt to classify bipartite graphs by chromatic polynomials*, Discrete Math., **222** (2000), 73-88.
- [2] F.M. Dong, K.M. Koh, K.L. Teo, C.H.C. Little, M.D. Hendy, *Sharp bounds for the numbers of 3-partitions and the chromaticity of bipartite graphs*, J. Graph Theory, **37** (2001), 48-77.
- [3] F.M. Dong, K.M. Koh, K.L. Teo, C.H.C. Little, M.D. Hendy, *Chromatically unique bipartite graphs with low 3-independent partition numbers*, Discrete Math., **224** (2000), 107-124.
- [4] R.C. Read, W.T. Tutte, *Chromatic polynomials*, in: L.W. Beineke, R.J. Wilson (Eds.), Selected Topics in Graph Theory III, Academic Press, New York (1988), pp. 15-42.
- [5] H. Roslan and Y.H. Peng, *Chromatic uniqueness of complete bipartite graphs with certain edges deleted*, Ars Combinatoria, **98** (2011), 203-213.
- [6] H. Roslan and Y.H. Peng, *Chromatic uniqueness of complete bipartite graphs with certain edges deleted II*, Research Report, **9/2003**, Institute for Mathematical Research, Universiti Putra Malaysia (2003).
- [7] <http://www.fsas.upm.edu.my/yhpeng/publish/table1.pdf>
- [8] <http://www.fsas.upm.edu.my/yhpeng/publish/figure1.pdf>

Newton-like Methods with At least Quadratic Order of Convergence for the Computation of Fixed Points

Ioannis K. Argyros
Cameron University
Department of Mathematics Sciences
Lawton, OK 73505, USA
Email: iargyros@cameron.edu

Abstract. The well known contraction mapping principle or Banach's fixed point theorem asserts: The method for successive substitutions converges only linearly to a fixed point of an operator equation in a Banach space setting [5], [7]. In practice, if Newton's method is used one ignores the additional information about the contraction mapping information. Werner in [9] provided a local analysis for a Newton-like method of at least Q -order 3 which uses this information. Here we provide a finer local convergence analysis for the same method under weaker hypotheses which do not necessarily imply the contraction property of the mapping. A numerical example is provided to show that our results compare favorably with the ones in [9]. The semilocal convergence of the method not considered in [9] is also examined.

AMS (MOS) Subject Classification Codes: 65G99, 65H10, 47H17, 49M15

Key Words: Contraction mapping principle, fixed point, Banach's fixed point Theorem, Newton-like methods, Lipschitz conditions, radius of convergence, ratio of convergence.

1. INTRODUCTION

In this study we are concerned with the problem of approximating a locally unique fixed point x^* of a Fréchet-differentiable operator F which is defined on a convex subset D of a Banach space X with values in X .

The contraction mapping principle or Banach's fixed point theorem [5], [7] asserts that if

$$\|F'(x)\| < 1 \text{ for all } x \in X \quad (1.1)$$

then there exists a unique fixed x^* of operator F on X . The method of successive substitutions or Picard's iteration

$$y_{n+1} = F(y_n) \quad (y_0 \in X) \quad (n \geq 0) \quad (1.2)$$

converges only linearly to x^* (the definition of Q order for an iterative method is well known and can be found in [8, Definition 9.1.5, p. 284]). In order to increase the speed of convergence to Q order at least two, and also use the contraction mapping property of

operator F Werner in [9] introduced the Newton-like method

$$x_{n+1} = x_n - M_n^{-1}(x_n - F(x_n)) \quad (x_0 \in D), \quad (x \geq 0), \quad \gamma \in [0, 1] \quad (1.3)$$

where, $M_n \in L(X)$ ($n \geq 0$) the space of bounded linear operators on X , is given by

$$M_n = I - F'(\gamma x_n + (1 - \gamma)F(x_n)) \quad (n \geq 0). \quad (1.4)$$

If $\gamma = 1$, we obtain Newton's method [4], [5]-[9], whereas if $\gamma = 0$ we obtain Stirling's method [1]-[3], [5]. Other choices are also possible [9]. Note that method (1.3) (as Newton's method does) requires one function evaluation and one evaluation of the Fréchet derivative F' of F per step independent of γ .

The motivation for introducing method (1.3) is due to the fact that if (1.1) holds, then $F(x_n)$ is a better approximation to x^* than x_n . Then, we can write:

$$x_n - F(x_n) = x^* - F(x^*) + \int_0^1 [I - F'(x^* + t(x_n - x^*))] dt (x_n - x^*) \quad (1.5)$$

or

$$x^* = x_n - \left\{ \int_0^1 [I - F'(x^* + t(x_n - x^*))] dt \right\}^{-1} (x_n - F(x_n)). \quad (1.6)$$

Werner noted that the choice $\gamma = \frac{1}{2}$ is the most appropriate choice of the free parameter γ in (1.3) leading to the midpoint rule. Werner provided a local convergence analysis for method (1.3) (see Proposition 1 in [9]) under hypothesis (1.1) when $D = X$.

Here we refine Werner's result by providing a local convergence analysis under weaker hypotheses with the following advantages: finer error estimates on $\|x_n - x^*\|$ ($n \geq 0$), and a larger radius of convergence allowing for a wider choice of initial guesses x_0 . We then provide a numerical example where our results compare favorably with the ones by Werner in [9]. Finally the semilocal convergence of method (1.3) not considered in [9] is studied.

2. LOCAL CONVERGENCE ANALYSIS OF NEWTON-LIKE METHOD (1.3)

We can show the main local convergence theorem for Newton-like method (1.3):

Theorem 1. *Let x^* be a fixed point of operator F such that $\|F'(x^*)\| < 1$. Assume there exist parameters $\alpha_0 \in [0, 1]$ and $L_0 \geq 0$ such that*

$$\|F(x) - F(x^*)\| \leq \alpha_0 \|x - x^*\|, \quad (2.1)$$

$$\begin{aligned} & \| [I - F'(x^*)]^{-1} [F'(F(x) + \delta(x - F(x))) - F'(x^*)] \| \leq \\ & \leq L_0 \|F(x + \delta(x - F(x))) - x^*\| \end{aligned} \quad (2.2)$$

for all $x \in D$, $\delta \in [0, 1]$ and

$$\bar{U}(x^*, r) = \{x \in X : \|x - x^*\| \leq r\} \subseteq D, \quad (2.3)$$

where,

$$r = \frac{1}{c}, \quad (2.4)$$

$$c = a + b,$$

$$a = L_0 \left[\frac{1}{2} + \alpha_0(1 - \gamma) + 3\gamma \right],$$

and

$$b = L_0 [(1 - \gamma)\alpha_0 + \gamma].$$

Then sequence $\{x_n\}$ generated by Newton-like method (1.3) is well-defined, remains in $U(x^*, r)$ and converges to x^* provided that $x_0 \in U(x^*, r)$. Moreover the following error bounds hold for all $n \geq 0$:

$$\|x_{n+1} - x^*\| \leq \frac{\alpha \|x_n - x^*\|^2}{1 - b \|x_n - x^*\|}. \quad (2.5)$$

Furthermore if $\alpha_0 \in [0, 1)$, x^* is the unique fixed point of F in $\bar{U}(x^*, r)$.

Proof. Let $x \in U(x^*, r)$. Then by (2.1) we have

$$\|F(x) - x^*\| = \|F(x) - F(x^*)\| \leq \alpha_0 \|x - x^*\| \leq \|x - x^*\| < r,$$

which implies that $F(x) \in U(x^*, r)$. Note also that $F(x) + \gamma(x - F(x)) \in U(x^*, r)$, since

$$\begin{aligned} \|F(x) + \gamma(x - F(x)) - x^*\| &\leq (1 - \gamma) \|F(x) - F(x^*)\| + \gamma \|x - x^*\| \\ &\leq [(1 - \gamma)\alpha_0 + \gamma] \|x - x^*\| \\ &\leq \|x - x^*\| < r. \end{aligned}$$

By hypothesis $x_0 \in U(x^*, r)$. Let us assume $x_k \in U(x^*, r)$ for all $k = 0, 1, \dots, n$. In view of (2.1)-(2.4) we obtain in turn

$$\begin{aligned} &\| [I - F'(F(x^*) + \gamma(x^* - F(x^*)))]^{-1} \cdot [I - F'(F(x^*) + \gamma(x^* - F(x^*))) \\ &\quad - (I - F'(F(x_k) + \gamma(x_k - F(x_k))))] \| \leq \\ &\leq L_0 \| [I - F'(x^*)]^{-1} [F(x_k) + \gamma(x_k - F(x_k)) - F(x^*) - \gamma(x^* - F(x^*))] \| \\ &\leq L_0 \| [I - F'(x^*)]^{-1} [(1 - \gamma)(F(x_k) - F(x^*)) + \gamma(x_k - x^*)] \| \\ &\leq L_0 [(1 - \gamma)\alpha_0 + \gamma] \|x_k - x^*\| \leq br < 1. \end{aligned} \quad (2.6)$$

It follows from (2.6) and the Banach Lemma on invertible operators [7] that $[I - F'(F(x_k) + \gamma(x_k - F(x_k)))]^{-1}$ exists, and

$$\begin{aligned} &\| [I - F'(F(x_k) + \gamma(x_k - F(x_k)))]^{-1} [I - F'(x^*)] \| \\ &\leq [1 - b \|x_k - x^*\|]^{-1} \leq [1 - br]^{-1}. \end{aligned} \quad (2.7)$$

We need the following estimates:

$$\begin{aligned} &\left\| [I - F'(x^*)]^{-1} \int_0^1 [F'(x^* + t(x_k - x^*)) - F'(x^* + \gamma(x_k - x^*))] dt \right\| \\ &\leq \left\| [I - F'(x^*)]^{-1} \int_0^1 [F'(x^* + t(x_k - x^*)) - F'(x^*)] dt \right\| \\ &\quad + \| [I - F'(x^*)]^{-1} [F'(x^*) - F'(x^* + \gamma(x_k - x^*))] \| \\ &\leq L_0 \left\{ \int_0^1 \|x^* + t(x_k - x^*) - x^*\| dt + \|x^* - x^* - \gamma(x_k - x^*)\| \right\} \\ &\leq L_0 \left(\frac{1}{2} + \gamma \right) \|x_k - x^*\|, \end{aligned} \quad (2.8)$$

and

$$\begin{aligned}
& \left\| [I - F'(x^*)]^{-1} [F'(x^* + \gamma(x_k - x^*)) - F'(F(x_k) + \gamma(x_k - F(x_k)))] \right\| \quad (2.9) \\
& \leq \left\| [I - F'(x^*)]^{-1} [F'(x^* + \gamma(x_k - x^*)) - F'(x^*)] \right\| \\
& + \left\| [I - F'(x^*)]^{-1} [F'(x^*) - F'(F(x_k) + \gamma(x_k - F(x_k)))] \right\| \\
& \leq L_0 \{ \|x^* - x^* - \gamma(x_k - x^*)\| + \\
& \|F(x_k) + \gamma(x_k - F(x_k)) - F(x^*) - \gamma(x^* - F(x^*))\| \} \\
& \leq L_0 [\gamma + \alpha_0(1 - \gamma) + \gamma] \|x_k - x^*\|.
\end{aligned}$$

Let us define, $A_k(t) = F'(x^* + t(x_k - x^*))$ and $B_k(t) = F'(F(x_k) + t(x_k - F(x_k)))$, $t \in [0, 1]$. In view of (1.3) we get

$$\begin{aligned}
x_{k+1} - x^* &= [I - B_k(\gamma)]^{-1} [I - F'(x^*)] [I - F'(x^*)]^{-1} \quad (2.10) \\
& \quad \cdot \{F(x_k) - F(x^*) - B_k(\gamma)(x_k - x^*)\}.
\end{aligned}$$

Using (2.1), (2.2), (2.8) and (2.9) we get

$$\begin{aligned}
& \left\| [I - F'(x^*)]^{-1} [F(x_k) - F(x^*) - B_k(\gamma)(x_k - x^*)] \right\| \quad (2.11) \\
& = \left\| [I - F'(x^*)]^{-1} \int_0^1 (A_k(t) - B_k(\gamma))(x_k - x^*) dt \right\| \\
& \leq \left\| [I - F'(x^*)]^{-1} \int_0^1 (A_k(t) - A_k(\gamma))(x_k - x^*) dt \right\| \\
& + \left\| [I - F'(x^*)]^{-1} (A_k(\gamma) - B_k(\gamma))(x_k - x^*) \right\| \\
& \leq a \|x_k - x^*\|^2.
\end{aligned}$$

By (2.8), (2.10) and (2.11) we obtain (2.5). It follows by (2.5) and the definition of r that

$$\|x_{k+1} - x^*\| < \|x_k - x^*\| < r,$$

which shows that $x_{k+1} \in U(x^*, r)$ and $\lim_{k \rightarrow \infty} x_k = x^*$. To show uniqueness, let y^* be a fixed point of F in $\bar{U}(x^*, r)$ with $x^* \neq y^*$. Using (2.1) we get

$$\|x^* - y^*\| = \|F(x^*) - F(y^*)\| \leq \alpha_0 \|x^* - y^*\| < \|x^* - y^*\|,$$

which contradicts $x^* \neq y^*$. That completes the proof of the theorem. \square

Remark 2. The conclusions of the theorem hold under the stronger conditions

$$\begin{aligned}
& \left\| [I - F'(x^*)]^{-1} [F'(x^* + t(x - x^*)) - F'(x^* + \gamma(x - x^*))] \right\| \quad (2.12) \\
& \leq L_1 |t - \gamma| \|x - x^*\|
\end{aligned}$$

and

$$\begin{aligned}
& \left\| [I - F'(x^*)]^{-1} [F'(x^* + \gamma(x - x^*)) - F'(F(x) + \gamma(x - F(x)))] \right\| \quad (2.13) \\
& \leq L_2(1 - \gamma) \|x - x^*\|
\end{aligned}$$

for all $x \in D$ (together with (2.2) and (2.3)). It follows from the proof of Theorem 1 that the conclusions hold provided that a is replaced by \bar{a} given by

$$\bar{a} = L_1 \left(\gamma^2 - \gamma + \frac{1}{2} \right) + L_2 \alpha_0 (1 - \gamma). \quad (2.14)$$

Werner in [9] used the stronger conditions (1.1) and

$$\left\| [I - F'(x^*)]^{-1} (F'(x) - F'(y)) \right\| \leq L \|x - y\| \quad (2.15)$$

for all $x, y \in D$. To arrive at (2.5) with a, b being replaced by \bar{a}, b given by

$$\bar{a} = \frac{L}{1-\alpha} \left[\frac{1}{2} + \alpha - (1+\alpha)\gamma + \gamma^2 \right] \text{ and } 0, \tag{2.16}$$

respectively.

Clearly

$$L_0 \leq L, \alpha_0 \leq \alpha \tag{2.17}$$

hold in general, and $\frac{L}{L_0}, \frac{\alpha}{\alpha_0}$ can be arbitrarily large [4], [5]. Hence the error bounds are finer, and the radius of convergence larger under our (weaker) conditions. Note also that condition (2.2) can be replaced by

$$\| [I - F'(x^*)]^{-1} [F'(x) - F'(x^*)] \| \leq L'_0 \|x - x^*\| \tag{2.18}$$

for all $x \in D$.

Note also that

$$L'_0 \leq L \tag{2.19}$$

holds in general and $\frac{L}{L'_0}$ can be arbitrarily large [4], [5].

Let us provide a numerical example, where our results compare favorably with the ones given by Werner in [9].

Example 1. Let $X = C[0, 1]$, the space of continuous functions defined on interval $[0, 1]$, equipped with the max-norm and let $D = \bar{U}(0, 1)$.

Define function F on D by

$$F(x)(s) = A x(s) + B s \int_0^1 \theta x^3(\theta) d\theta \tag{2.20}$$

for some given real constants $A \neq 1$ and B . Then the Fréchet-derivative F' of function F is given by

$$F'(x(w))s = A I w(s) + 3 B s \int_0^1 \theta x^2(\theta) w(\theta) d\theta \text{ for all } w \in D. \tag{2.21}$$

We have $x^* = x^*(s) = 0$ is a fixed point of function F . Using (2.20) and (2.21), we can set

$$\alpha_0 = |A| + \frac{1}{2} |B|, \quad \alpha = |A| + \frac{3}{2} |B|,$$

$$L_0 = \frac{3}{2} |B(1-A)^{-1}| \quad \text{and} \quad L = 3 |B(1-A)^{-1}|.$$

Let $\delta = \gamma = 1$.

Case 1: $A = B = \frac{1}{2}$. We get

$$\alpha_0 = \frac{3}{4} < 1, \quad L_0 = L'_0 = \frac{3}{2}, \quad L = 3 \quad \text{and} \quad \alpha = \frac{5}{4} > 1.$$

Hence, contraction hypothesis (1.1) used by Werner in [9] is violated. That is, there is no guarantee that sequence $\{x_n\}$ converges to $x^*(s) = 0$.

However, by Theorem 1, we have

$$a = \frac{21}{4}, \quad b = \frac{3}{2}, \quad r = \frac{4}{27} \quad \text{and}$$

sequence $\{x_n\}$ converges to $x^*(s)$ provided that $x_0 = x_0(s) \in \bar{U}(0, r)$.

Case 2: $A = \frac{1}{2}$ and $B = \frac{1}{4}$. This time, we have

$$\alpha_0 = \frac{5}{6}, \quad L_0 = L'_0 = \frac{3}{4}, \quad L = \frac{3}{2}, \quad \alpha = \frac{7}{8},$$

$$a = \frac{21}{8}, \quad b = \frac{3}{4}, \quad \bar{a} = 6$$

and

$$r_W = \frac{1}{6} < r_A = \frac{8}{27}.$$

That is our radius of convergence is larger which allows a wider choice of initial guesses x_0 . Moreover, our error bounds (2.5) are tighter, since $a \leq \bar{a}$.

3. SEMILOCAL CONVERGENCE ANALYSIS OF NEWTON-LIKE METHOD (1.3)

We can show the following semilocal convergence result for Newton-like method (1.3):

Theorem 3. Let F be a Fréchet-differentiable operator defined on a convex subset D of a Banach space X with values in X . Assume: there exist positive parameters p_0 , p , l_0 and l such that for some $x_0 \in D$, $\gamma \in [0, 1]$ $M_0^{-1} \in L(X)$ and for all $x, y \in D$:

$$\|F(x) - F(x_0)\| \leq p_0 \|x - x_0\| \quad (3.1)$$

$$\|M_0^{-1}F'(x)\| \leq p, \quad (3.2)$$

$$\|M_0^{-1}[F'(z) - F'(w)]\| \leq l_0 \|z - w\| \quad (3.3)$$

for $z = z(\gamma, x) = \gamma x + (1 - \gamma)F(x)$, $w = w(\gamma) = \gamma x_0 + (1 - \gamma)F(x_0)$,

$$\|M_0^{-1}[F'(z) - F'(v)]\| \leq l \|z - v\| \quad (3.4)$$

for $v = v(t) = x + t(y - x)$ for all $t \in [0, 1]$; for r_0, r_1, r_2 , and r_3 given by

$$r_0 = \frac{\|x_0 - F(x_0)\|}{1 - p_0}, \quad r_1 = \frac{1 - (p_0 + p) + \sqrt{D_1}}{2q_0},$$

$$r_2 = \frac{1 - l(1 - \gamma)\|x_0 - F(x_0)\| + \sqrt{D_2}}{2[q_0 + l(p_0(1 - \gamma) + \gamma^2 - \gamma + \frac{1}{2})]},$$

$$D_1 = [1 - (p_0 + p)] - 4q_0 \|x_0 - F(x_0)\|,$$

$$r_3 = \frac{1}{q_0} \left[1 - \sqrt[3]{q \|x_0 - F(x_0)\|} \right],$$

where, $q_0 = l_0[\gamma + (1 - \gamma)p_0]$,

$$q_1 = l(\gamma^2 - \gamma + \frac{1}{2}), \quad q_2 = l(1 - \gamma), \quad q = q_1 + q_2 p$$

the following hold:

$$r_0 < \min\{r_1, r_3\}, \quad (3.5)$$

$$\|x_0 - F(x_0)\| \leq \frac{1}{q}, \quad \|M_0^{-1}[x_0 - F(x_0)]\| < \frac{[1 - (p_0 + p)]^2}{4q_0}, \quad 0 \leq p_0 + p < 1 \quad (3.6)$$

or

$$r_0 < \min\{r_2, r_3\}, \quad (3.7)$$

$$\|x_0 - F(x_0)\| \leq \frac{1}{q}, \quad \|M_0^{-1}[x_0 - F(x_0)]\| < \min\left\{\frac{1}{\ell(1 - \gamma)}, r_4\right\} \quad (3.8)$$

where, r_4 is the smallest root of equation

$$c_2 r^2 + c_1 r + c_0 = 0, \quad (3.9)$$

$$c_2 = \ell^2(1 - \gamma)^2, \quad c_1 = -2[1 - \gamma + 2(q_0 + \ell(p_0(1 - \gamma) + \gamma^2 - \gamma + \frac{1}{2}))],$$

$$c_0 = 1,$$

$$c_1^2 \geq 4c_0c_1; \quad (3.10)$$

and

$$\bar{U}(x_0, r) \subseteq D \quad (3.11)$$

for some $\{r \in [r_0, \min\{r_1, r_3\}]\}$ if (3.5) and (3.6) hold or $r \in [r_0, \min\{r_2, r_3\}]\}$ if (3.7)-(3.10) hold.

Then sequence $\{x_n\}$ generated by Newton-like method (1.3) is well defined, remains in $\bar{U}(x_0, r)$ for all $n \geq 0$ and converges to a fixed point $x^* \in \bar{U}(x_0, r)$ of operator F . Moreover the following estimates hold:

$$\|x_{n+1} - F(x_{n+1})\| \leq \frac{[q_1 \|x_{n+1} - x_n\| + q_2 \|x_{n+1} - F(x_n)\|] \|x_{n+1} - x_n\|}{1 - q_0 \|x_{n+1} - x_0\|} \quad (3.12)$$

$$\leq \varepsilon_n \|x_n - F(x_n)\|^2, \quad (n \geq 0)$$

and

$$\|x_{n+1} - x_n\| \leq \bar{\varepsilon}_n \|x_{n-1} - F(x_{n-1})\|^2 \quad (n \geq 1), \quad (3.13)$$

where,

$$\varepsilon_n = \frac{q}{(1 - q_0 \|x_n - x_0\|)^2(1 - q_0 \|x_{n+1} - x_0\|)} \quad (n \geq 0),$$

and

$$\bar{\varepsilon}_n = \frac{\varepsilon_{n-1}}{1 - q_0 \|x_n - x_0\|} \quad (n \geq 1).$$

Furthermore if

$$r \in [r_0, r_4], \quad (3.14)$$

where,

$$r_4 = \left\{ q_0 + \ell \left[\gamma^2 - \gamma + \frac{1}{2} + (1 - \gamma)p_0 \right] \right\}^{-1},$$

then the fixed point x^* is unique in $\bar{U}(x_0, r)$. Finally the following estimate holds:

$$\|x_{n+1} - x^*\| \leq \frac{\ell \left[\gamma^2 - \gamma + \frac{1}{2} + (1 - \gamma)p_0 \right]}{1 - q_0 \|x_n - x_0\|} \|x_n - y^*\|^2 \quad (n \geq 0). \quad (3.15)$$

Proof. We shall first show that for all $\gamma \in [0, 1]$, $x \in \bar{U}(x_0, r)$ and $\gamma x + (1 - \gamma)F(x) \in \bar{U}(x_0, r)$.

We can have

$$\begin{aligned} \gamma x + (1 - \gamma)F(x) - x_0 &= \gamma(x - x_0) + (1 - \gamma)(F(x) - F(x_0)) \\ &\quad + (1 - \gamma)(F(x_0) - x_0). \end{aligned} \quad (3.16)$$

In view of (3.1), (3.16) and the choice of $r \geq r_0$ we get

$$\begin{aligned} \|\gamma x + (1 - \gamma)F(x) - x_0\| &\leq \gamma \|x - x_0\| + (1 - \gamma) \|F(x) - F(x_0)\| \\ &\quad + (1 - \gamma) \|F(x_0) - x_0\| \\ &\leq [\gamma + (1 - \gamma)p_0] r + (1 - \gamma) \|F(x_0) - x_0\| \leq r, \end{aligned} \quad (3.17)$$

which implies $\gamma x + (1 - \gamma)F(x)$ is in $\bar{U}(x_0, r)$.

We shall next show $M(x)^{-1} \in L(X)$ for all $x \in \bar{U}(x_0, r)$. Using (3.1), (3.3) and the choice of $r \leq r_3$ we get in turn

$$\begin{aligned} & \|M(0)^{-1} [M(0) - M(x)]\| & (3.18) \\ & \leq \|M_0^{-1} [F'(\gamma x + (1 - \gamma)F(x)) - F'(\gamma x_0 + (1 - \gamma)F(x_0))]\| \\ & \leq \ell_0 \|\gamma x - \gamma x_0 + (1 - \gamma)(F(x) - F(x_0))\| \\ & \leq \ell_0 [\gamma \|x - x_0\| + (1 - \gamma)p_0 \|x - x_0\|] \\ & = q_0 \|x - x_0\| \leq q_0 r < 1. \end{aligned}$$

It follows from (3.18), and the Banach Lemma on invertible operators that $M(x)^{-1} \in L(X)$ with

$$\|M(x)^{-1} M(0)\| \leq \frac{1}{1 - q_0 \|x - x_0\|}. \quad (3.19)$$

Let us assume $x_k \in \bar{U}(x_0, r)$ for $k = 0, 1, \dots, n$. We shall show (3.12), (3.13) and $x_{k+1} \in \bar{U}(x_0, r)$ hold true.

Using (1.3) we get the identity

$$\begin{aligned} x_{k+1} - F(x_{k+1}) &= & (3.20) \\ &= x_{k+1} - F(x_{n+1}) - M_k(x_{k+1} - x_k) - (x_k - F(x_k)) \\ &= F(x_k) - F(x_{k+1}) + F'(\gamma x_k + (1 - \gamma)F(x_k))(x_{k+1} - x_k) \\ &= \int_0^1 [F'(x_{k+1} + t(x_k - x_{k+1})) - F'(\gamma x_k + (1 - \gamma)F(x_k))] (x_k - x_{k+1}) dt \end{aligned}$$

By (1.3), (3.4) and (3.19) (for $x = x_{n+1}$) and (3.20) we obtain in turn:

$$\begin{aligned} & \|x_{k+1} - F(x_{k+1})\| & (3.21) \\ & \leq \frac{\ell \int_0^1 \|x_{k+1} + t(x_k - x_{k+1}) - \gamma x_k - (1 - \gamma)F(x_k)\| \|x_{k+1} - x_k\| dt}{1 - q_0 \|x_{k+1} - x_0\|} \\ & \leq \frac{\ell \left[\int_0^1 |t - \gamma| \|x_{k+1} - x_k\| dt + (1 - \gamma) \|x_{k+1} - F(x_k)\| \right] \|x_{k+1} - x_k\|}{1 - q_0 \|x_{k+1} - x_0\|} \\ & \leq \frac{[q_1 \|x_{k+1} - x_k\| + q_2 \|x_{k+1} - F(x_k)\|] \|x_{k+1} - x_k\|}{1 - q_0 \|x_{k+1} - x_0\|}. \end{aligned}$$

We need an upper bound on the $\|x_{k+1} - F(x_k)\|$. In view of (1.3) we obtain the identity

$$\begin{aligned} x_{k+1} - F(x_k) &= & (3.22) \\ &= x_k - F(x_k) - M_k^{-1}(x_k - F(x_k)) \\ &= M_k^{-1} \{ [I - F'(\gamma x_k + (1 - \gamma)F(x_k))](x_k - F(x_k)) - (x_k - F(x_k)) \} \\ &= [M_k^{-1} M_0] [M_0^{-1} F'(\gamma x_k + (1 - \gamma)F(x_k))](x_k - F(x_k)). \end{aligned}$$

Using (3.2), (3.19) (for $x = x_k$) and (3.21) we obtain

$$\|x_{k+1} - F(x_k)\| \leq \frac{p \|x_k - F(x_k)\|}{1 - q_0 \|x_k - x_0\|}. \quad (3.23)$$

In view of (1.3) we get

$$\|x_{k+1} - x_k\| \leq \frac{\|x_k - F(x_k)\|}{1 - q_0 \|x_k - x_0\|}. \quad (3.24)$$

By combining (3.23) and (3.24) in (3.21) we obtain (3.12) and (3.13).

We must show $\|x_n - F(x_n)\| \rightarrow 0$ as $n \rightarrow \infty$, which will then imply that $\|x_{n+1} - x_n\| \rightarrow 0$ and $\|x_n - x^*\| \rightarrow 0$ as $n \rightarrow \infty$. By (3.12) it suffices to show

$$\varepsilon_n \|x_n - F(x_n)\| < 1 \tag{3.25}$$

or

$$\frac{q \|x_0 - F(x_0)\|}{(1 - q_0 r)^3} < 1 \tag{3.26}$$

which is true by the choice of $r \leq r_3$ and the choice of $\|x_0 - F(x_0)\| < \frac{1}{q}$. We must also show $x_{k+1} \in \bar{U}(x_0, r)$. Two estimates for $\|x_{k+1} - x_0\|$ will be given.

Estimate 1. Using (3.1), (3.2), (3.5), (3.6), and (3.19). By (1.3) we get in turn

$$\begin{aligned} x_{k+1} - x_0 & \tag{3.27} \\ &= x_k - x_0 - M_k^{-1}(x_k - F(x_k)) \\ &= [M_k^{-1}M_0]M_0^{-1}[F(x_k) - F(x_0) - F'(\gamma(x_k + (1 - \gamma)F(x_k)))(x_k - x_0) \\ & \quad + (F(x_0) - F(x_0))] \end{aligned}$$

and

$$\|x_{k+1} - x_0\| \leq \frac{\|F(x_0) - x_0\| + (p_0 + p)r}{1 - q_0 r} \leq r, \tag{3.28}$$

by the choice of $r \leq 1$ and the choice of

$$\|M_0^{-1}[x_0 - F(x_0)]\| \leq \frac{[10p_0 + p]^2}{4q_0}, \quad 0 \leq p_0 + p < 1.$$

Estimate 2. Using (3.1), (3.4), (3.19) and (3.27). We obtain that the expression inside the bracket in (3.27) composed by M_0^{-1} is bounded above (in norm) by

$$\begin{aligned} & \left\| M_0^{-1} \int_0^1 F'(x_0 + t(x_k - x_0)) - F'(\gamma x_k + (1 - \gamma)F(x_k)) \right\| \|x_k - x_0\| dt \tag{3.29} \\ & + \|M_0^{-1}(F(x_0) - x_0)\| \\ & \leq \int_0^1 \ell \|x_0 + t(x_k - x_0) - \gamma x_k - (1 - \gamma)F(x_k)\| \|x_k - x_0\| dt \\ & + \|M_0^{-1}(F(x_0) - x_0)\| \\ & \leq (\|x_0 - F(x_0)\| (1 - \gamma) + p_0(1 - \gamma) \|x_k - x_0\| + (\gamma^2 - \gamma + \frac{1}{2}) \\ & \|x_k - x_0\|) \cdot \|x_k - x_0\| + \|M_0^{-1}(x_0 - F(x_0))\| \end{aligned}$$

That is it suffices to show

$$\begin{aligned} & \|x_{k+1} - x_0\| \tag{3.30} \\ & \leq \frac{\ell \|x_0 - F(x_0)\| (1 - \gamma)r + \ell [\gamma^2 - \gamma + \frac{1}{2} + p_0(1 - \gamma)]r^2 + \|M_0^{-1}(x_0 - F(x_0))\|}{1 - q_0 r} \\ & \leq r, \end{aligned}$$

which is true by the choice of $r \leq r_2$ and the choice of

$$\|M_0^{-1}(x_0 - F(x_0))\| \leq \min \left\{ \frac{1}{\ell(1 - \gamma)}, r_4 \right\}.$$

Finally to show uniqueness, let us assume $y^* \in \bar{U}(x_0, r)$ is a fixed point of F . Using (1.3) we obtain the identity

$$\begin{aligned} x_{k+1} - y^* & & (3.31) \\ &= x_k - y^* - M_k^{-1}(x_k - F(x_k)) \\ &= M_k^{-1} [(I - F'(\gamma x_k + (1 - \gamma)F(x_k)))] (x_k - y^* - (x_k - F(x_k))) \\ &= [M_k^{-1} M_0] M_0^{-1} \int_0^1 [F'(y^* + t(x_k - y^*)) - F'(\gamma x_k + (1 - \gamma)F(x_k))](x_k - y^*) dt. \end{aligned}$$

Using (3.4), (3.19), (3.31) and the choice of $r \in [r_0, r_4)$ we obtain in turn

$$\begin{aligned} & \|x_{k+1} - y^*\| & (3.32) \\ & \leq \frac{\ell \left[\int_0^1 |t - \gamma| \|x_k - y^*\| dt + (1 - \gamma)(F(x_k) - F(y^*)) \|x_k - y^*\| \right]}{1 - q_0 r} \\ & \leq \frac{\ell \left[\gamma^2 - \gamma + \frac{1}{2} + (1 - \gamma)p_0 \right] \|x_k - y^*\|^2}{1 - q_0 r} \\ & < \|x_k - y^*\|, \end{aligned}$$

which shows (3.15), and $\lim_{k \rightarrow \infty} x_k = y^*$. However, we showed $\lim_{k \rightarrow \infty} x_k = x^*$. Hence, we deduce

$$x^* = y^*. \quad (3.33)$$

That completes the proof of the theorem. \square

Remark 4. It follows from theorem 3 that the Q -order of convergence for Newton-like method (1.3) is at least quadratic. Conditions (3.3) and (3.4) can be replaced by the usual stronger Lipschitz conditions where z and v are simply in D . Note also that

$$p_0 \leq p \text{ and } \ell_0 \leq \ell, \quad (3.34)$$

hold in general, and $\frac{p}{p_0}, \frac{\ell}{\ell_0}$ can be arbitrarily large [4], [5].

REFERENCES

- [1] S. Amat, S. Busquier, *Convergence and numerical analysis of a family of two-step Steffensen's methods*, Comput. and math. with Appl., **49** (2005), 13–22.
- [2] I.K. Argyros, *On Stirling's method*, Tamkang J. Math., **27** (1995), 37–52.
- [3] I.K. Argyros, *Stirling's method and fixed points of nonlinear operator equations in Banach space*, Publ. Inst. Math. Acad. Sin., **23** (1995), 13–20.
- [4] I.K. Argyros, *A unifying local-semilocal convergence analysis and applications for two-point Newton-like methods in Banach spaces*, J. Math. Anal. Appl., **298** (2004), 374–397.
- [5] I.K. Argyros, *Approximate solution of nonlinear operator equations with applications*, World Scientific Publ. Co. NJ, U.S.A., 2005.
- [6] J.M. Gutiérrez, M.A. Hernández, M.A. Salanova, *Accessibility of solutions by Newton's method*, Intern. J. Comput. Math., **57** (1995), 239–247.
- [7] L.V. Kantorovich, G.P. Akilov, *Functional Analysis in Normed Spaces*, Pergamon Press, Oxford, 1982.
- [8] J.M. Ortega, W.C. Rheinboldt, *Iterative Solution of Nonlinear Equations in Several Variables*, Academic press, New York, 1970.
- [9] W. Werner, *Newton-like method for the computation of fixed points*, Comput. and Math. with Appl., **10** (1984), 77–84.

On the Semilocal Convergence of Werner's Method for Solving Equations Using Recurrent Functions

Ioannis K. Argyros
Cameron University
Department of Mathematics Sciences
Lawton, OK 73505, USA
Email: iargyros@cameron.edu

Saïd Hilout
Poitiers University
Laboratoire de Mathématiques et Applications
Bd. Pierre et Marie Curie, Téléport 2, B.P. 30179
86962 Futuroscope Chasseneuil Cedex, France
Email: said.hilout@math.univ-poitiers.fr

Abstract. We prove semilocal convergence of Werner's method for approximating locally unique solution of nonlinear equation in a Banach space setting. Using our new idea of recurrent functions, we provide estimates on the distances involved and information on the location of the solution. A numerical example shows that our results can apply to solve equations but the Kantorovich's sufficient convergence condition is unapplicable [7].

AMS (MOS) Subject Classification Codes: 65H10, 65G99, 65J15, 47H17, 49M15

Key Words: Werner's method, Banach space, recurrent functions, local/semilocal convergence, Fréchet-derivative, Newton-Kantorovich hypothesis.

1. INTRODUCTION

In this study we are concerned with the problem of approximating a locally unique solution x^* of equation

$$F(x) = 0, \quad (1.1)$$

where F is a twice Fréchet-differentiable operator defined on a convex subset \mathcal{D} of a Banach space \mathcal{X} with values in a Banach space \mathcal{Y} .

A large number of problems in applied mathematics and also in engineering are solved by finding the solutions of certain equations. For example, dynamic systems are mathematically modeled by difference or differential equations and their solutions usually represent the states of the systems. For the sake of simplicity, assume that a time-invariant system is driven by the equation $\dot{x} = T(x)$, for some suitable operator T , where x is the state. Then the equilibrium states are determined by solving equation (1.1). Similar equations are used in the case of discrete systems. The unknowns of engineering equations can be functions (difference, differential and integral equations), vectors (systems of linear

or nonlinear algebraic equations), or real or complex numbers (single algebraic equations with single unknowns). Except in special cases, the most commonly used solution methods are iterative—when starting from one or several initial approximations a sequence is constructed that converges to a solution of the equation. Iteration methods are also applied for solving optimization problems. In such cases, the iteration sequences converge to an optimal solution of the problem at hand. Since all of these methods have the same recursive structure, they can be introduced and discussed in a general framework.

We revisit Werner's method [9], [10]:

$$x_{n+1} = x_n - A_n^{-1} F(x_n), \quad A_n = F' \left(\frac{x_n + y_n}{2} \right) \quad (1.2)$$

$$y_{n+1} = x_{n+1} - A_n^{-1} F(x_{n+1}), \quad (n \geq 0), \quad (x_0, y_0 \in \mathcal{D}).$$

The local convergence of Werner's method (1.2) was given in [9], [10] under Lipschitz conditions on the first and second Fréchet-derivatives given in non-affine invariant form (see (2.52) and (2.53)). The order of convergence of Werner's method (1.2) is $1 + \sqrt{2}$. The derivation of this method and its importance has well been explained in [9], [10] (see also [3]). The two-step method uses one inverse and two function evaluations. Note that if $x_0 = y_0$, then (1.2) becomes Newton's method [1]–[11].

We provide a semilocal convergence analysis using our new idea of recurrent functions. Our Lipschitz hypotheses are provided in affine invariant form. As far as we know the semilocal analysis of Werner's method has not been studied in this setting. We are mostly interested in finding weak sufficient convergence conditions, so as to extend the applicability of the method.

Our new approach can also be used on other one-step or two-step iterative methods [1], [3], [4]–[11].

The semilocal convergence is examined in Section 2 and a numerical example is given in Section 3.

2. SEMILOCAL CONVERGENCE ANALYSIS OF WERNER'S METHOD

It is convenient for us to define some auxiliary functions appearing in connection to majorizing sequences for Werner's method (1.2).

Let $\ell_0 > 0$, $\ell > 0$, $\alpha \geq 0$, $\eta > 0$, $\bar{\eta} \geq \eta$ and $\beta = 1 + \alpha$ be given constants. It is convenient for us to define function \bar{f}_1 on $[0, +\infty)$ by

$$\bar{f}_1(t) = \ell t^\beta + 4 \ell_0 t - 2. \quad (2.1)$$

We have:

$$\bar{f}_1(0) = -2 < 0. \quad (2.2)$$

There exists sufficiently large $u > 0$, such that:

$$\bar{f}_1(t) > 0, \quad t > u. \quad (2.3)$$

It follows from (2.2), (2.3) and the intermediate value theorem that there exists $v \in (0, u)$, such that

$$\bar{f}_1(v) = 0. \quad (2.4)$$

The number v is the unique positive zero in $(0, +\infty)$ of function \bar{f}_1 , since

$$\bar{f}'_1(t) = \ell \beta t^\alpha + 4 \ell_0 > 0 \quad (t \geq 0). \quad (2.5)$$

That is function \bar{f}_1 is increasing and as such it crosses the positive axis only once.

Moreover, define function g on $[0, +\infty)$ by

$$g(t) = 2 \ell_0 t^3 + 2 \ell_0 t^2 + \ell \eta^\alpha t - \ell \eta^\alpha. \tag{2.6}$$

We have as above:

$$g(0) = -\ell \eta^\alpha < 0 \tag{2.7}$$

and

$$g(t) > 0 \quad (t > \zeta) \tag{2.8}$$

for sufficiently large $\zeta > 0$.

Hence, as above there exists $\delta_+ \in (0, \zeta)$, such that:

$$g(\delta_+) = 0. \tag{2.9}$$

The number δ_+ is the unique positive zero of function g on $(0, +\infty)$, since

$$g'(t) = 6 \ell_0 t^2 + 4 \ell_0 t + \ell \eta^\alpha > 0 \quad (t \geq 0). \tag{2.10}$$

Set

$$\delta_0 = \frac{\ell \eta^\beta}{1 - \ell_0 (\eta + \bar{\eta})}, \quad \ell_0 (\eta + \bar{\eta}) \neq 1, \tag{2.11}$$

$$v_\infty = 1 - 2 \ell_0 \eta \tag{2.12}$$

and

$$\delta_1 = \max \left\{ \frac{\delta_0}{2}, \delta_+ \right\}. \tag{2.13}$$

We can show the following result on majorizing sequences for Werner's method (1.2):

Lemma 1. *Let $\ell_0 > 0$, $\ell > 0$, $\alpha \geq 0$, $\eta > 0$, $\bar{\eta} \geq \eta$ and $\beta = 1 + \alpha$ be given constants.*

Assume:

$$\ell_0 (\eta + \bar{\eta}) < 1, \quad \eta \leq v \tag{2.14}$$

and

$$\delta_1 \leq v_\infty, \tag{2.15}$$

where, v , δ_1 , δ_+ , v_∞ were defined by (2.4), (2.13), (2.9) and (2.12), respectively.

Choose:

$$\delta \in [\delta_1, v_\infty]. \tag{2.16}$$

Then, sequence $\{t_n\}$ ($n \geq 0$), generated by

$$t_0 = 0, \quad t_1 = \eta, \quad t_{n+2} = t_{n+1} + \frac{\ell (t_{n+1} - t_n)^{1+\beta}}{2 (1 - \ell_0 (t_{n+1} + s_{n+1}))}, \tag{2.17}$$

with,

$$s_0 = 0, \quad s_1 = \bar{\eta}, \quad s_{n+2} = t_{n+2} + \frac{\ell (t_{n+2} - t_{n+1})^{1+\beta}}{2 (1 - \ell_0 (t_{n+1} + s_{n+1}))}, \tag{2.18}$$

is non-decreasing, bounded above by:

$$t^{**} = \frac{2 \eta}{2 - \delta} \tag{2.19}$$

and converges to its unique least upper bound t^ with*

$$t^* \in [0, t^{**}]. \tag{2.20}$$

Moreover the following estimates hold for all $n \geq 0$:

$$t_n \leq s_n, \tag{2.21}$$

$$0 < t_{n+2} - t_{n+1} \leq \frac{\delta}{2} (t_{n+1} - t_n) \leq \left(\frac{\delta}{2}\right)^{n+1} \eta \tag{2.22}$$

and

$$0 < s_{n+2} - t_{n+2} \leq \frac{\delta}{2} (s_{n+1} - t_{n+1}) \leq \left(\frac{\delta}{2}\right)^{n+2} \eta. \quad (2.23)$$

Proof. We shall show using induction on m :

$$\begin{aligned} 0 \leq t_{m+2} - t_{m+1} &= \frac{\ell (t_{m+1} - t_m)^\beta}{2 (1 - \ell_0 (t_{m+1} + s_{m+1}))} (t_{m+1} - t_m) \\ &\leq \frac{\delta}{2} (t_{m+1} - t_m), \end{aligned} \quad (2.24)$$

$$\begin{aligned} 0 \leq s_{m+2} - t_{m+2} &= \frac{\ell (t_{m+2} - t_{m+1})^\beta}{2 (1 - \ell_0 (t_{m+1} + s_{m+1}))} (t_{m+2} - t_{m+1}) \\ &\leq \frac{\delta}{2} (t_{m+2} - t_{m+1}) \end{aligned} \quad (2.25)$$

and

$$\ell_0 (t_{m+1} + s_{m+1}) < 1. \quad (2.26)$$

Estimates (2.24)–(2.26) for $m = 0$ will hold if:

$$\frac{\ell (t_1 - t_0)^\beta}{1 - \ell_0 (t_1 + s_1)} = \frac{\ell \eta^\beta}{1 - \ell_0 (\eta + \bar{\eta})} = \delta_0 \leq \delta, \quad (2.27)$$

$$\frac{\ell (t_2 - t_1)^\beta}{1 - \ell_0 (t_1 + s_1)} \leq \frac{\ell \left(\frac{\delta}{2} \eta\right)^\beta}{1 - \ell_0 (\eta + \bar{\eta})} = \bar{\delta}_0 \leq \delta_0 \leq \delta \quad (2.28)$$

and

$$\ell_0 (t_1 + s_1) = \ell_0 (\eta + \bar{\eta}) < 1, \quad (2.29)$$

respectively, which are true by (2.16) and (2.14). Let us assume (2.21)–(2.26) hold for all $n \leq m + 1$.

Then, we get from (2.24) and (2.25):

$$t_{m+2} \leq \frac{1 - \left(\frac{\delta}{2}\right)^{m+2}}{1 - \frac{\delta}{2}} \eta < \frac{2\eta}{2 - \eta} = t^{**} \quad (2.30)$$

and

$$s_{m+2} \leq t_{m+2} + \left(\frac{\delta}{2}\right)^{m+2} \eta \leq \left\{ \frac{1 - \left(\frac{\delta}{2}\right)^{m+2}}{1 - \frac{\delta}{2}} + \left(\frac{\delta}{2}\right)^{m+2} \right\} \eta. \quad (2.31)$$

We shall only show (2.24), since (2.25), will then follows (as (2.28) follows from (2.27)). Using the induction hypotheses, (2.24) certainly holds if:

$$\ell (t_{m+1} - t_m)^\beta + \ell_0 \delta (t_{m+1} + s_{m+1}) - \delta \leq 0$$

or,

$$\ell \left\{ \left(\frac{\delta}{2}\right)^m \eta \right\}^\beta + \ell_0 \delta \left\{ \frac{1 - \left(\frac{\delta}{2}\right)^{m+1}}{1 - \frac{\delta}{2}} + \frac{1 - \left(\frac{\delta}{2}\right)^{m+1}}{1 - \frac{\delta}{2}} + \left(\frac{\delta}{2}\right)^{m+1} \right\} \eta - \delta \leq 0,$$

or, since $\beta \geq 1$

$$\ell \left(\frac{\delta}{2}\right)^m \eta^\beta + \ell_0 \delta \left\{ 2 \frac{1 - \left(\frac{\delta}{2}\right)^{m+1}}{1 - \frac{\delta}{2}} + \left(\frac{\delta}{2}\right)^{m+1} \right\} \eta - \delta \leq 0. \tag{2.32}$$

We are motivated from (2.32) to define functions f_m ($m \geq 1$) on $[0, +\infty)$, for $v = \frac{\delta}{2}$ and show instead of (2.32):

$$f_m(v) = \ell v^{m-1} \eta^\beta + 2 \ell_0 (2(1 + v + \dots + v^m) + v^{m+1}) \eta - 2 \leq 0. \tag{2.33}$$

We need a relationship between two consecutive functions f_m :

$$\begin{aligned} f_{m+1}(v) &= \ell v^m \eta^\beta + 2 \ell_0 (2(1 + v + \dots + v^{m+1}) + v^{m+2}) \eta - 2 \\ &= \ell v^m \eta^\beta + \ell v^{m-1} \eta^\beta - \ell v^{m-1} \eta^\beta + \\ &\quad 2 \ell_0 (2(1 + v + \dots + v^m) + v^{m+1} + v^{m+1} + v^{m+2}) \eta - 2 \\ &= f_m(v) + \ell v^m \eta^\beta - \ell v^{m-1} \eta^\beta + 2 \ell_0 (v^{m+1} + v^{m+2}) \eta \\ &= f_m(v) + g(v) v^{m-1} \eta, \end{aligned} \tag{2.34}$$

where, function g is given by (2.6).

We have by (2.33):

$$f_1(0) = \ell \eta^\beta + 4 \ell_0 \eta - 2 < 0, \tag{2.35}$$

$$f_m(0) = 4 \ell_0 \eta - 2 < 0 \quad (m > 1) \tag{2.36}$$

and for sufficiently large $v > 0$:

$$f_m(v) > 0. \tag{2.37}$$

It follows from (2.35)–(2.37), and the intermediate value theorem that there exists $v_m > 0$, such that $f_m(v_m) = 0$. Moreover, each v_m is the unique positive zero of f_m , since $f'_m(v) > 0$ for $v \in [0, +\infty)$.

We shall show

$$f_m(v) \leq 0 \quad \text{for all } v \in [0, v_m] \quad (m \geq 1). \tag{2.38}$$

If there exists $m \geq 0$, such that $v_{m+1} \geq \frac{\delta}{2}$, then, using (2.6) and (2.34), we get:

$$f_{m+1}(v_{m+1}) = f_m(v_{m+1}) + g(v_{m+1}) v_{m+1}^{m-1} \eta$$

or

$$f_m(v_{m+1}) \leq 0,$$

since $f_{m+1}(v_{m+1}) = 0$ and $g(v_{m+1}) v_{m+1}^{m-1} \eta \geq 0$, which imply $v_{m+1} \leq v_m$.

We can certainly choose the last of the v_m 's denoted by v_∞ (obtained from (2.32) by letting $m \rightarrow \infty$ and given in (2.12)), to be v_{m+1} .

It then follows sequence $\{v_m\}$ is non-increasing, bounded below by zero and as such it converges to its unique maximum lowest bound v^* satisfying $v^* \geq v_\infty$.

Then estimate (2.38) certainly holds, if

$$\frac{\delta}{2} \leq v_\infty,$$

which is true by hypothesis (2.15).

Finally, sequences $\{t_n\}$, $\{s_n\}$ are non-decreasing, bounded above by t^{**} , given by (2.20). Hence, they converge to their common, and unique least upper bound t^* satisfying (2.20).

That also completes the proof of Lemma 1. □

We can also provide a second majorizing result.

Let us define function h_m ($m \geq 1$) as f_m by:

$$h_m(s) = \ell s^{m-1} \eta^\beta + 4 \ell_0 (1 + s + \dots + s^m) \eta - 2, \quad (2.39)$$

$$\bar{\delta}_+ = \frac{-\ell \eta^\beta + \sqrt{\ell^2 \eta^{2\alpha} + 16 \ell_0 \ell \eta^\alpha}}{8 \ell_0}, \quad (2.40)$$

$$\bar{\delta}_0 = \frac{\ell \eta^\beta}{1 - \ell_0 (\eta + \bar{\eta})}, \quad \ell_0 (\eta + \bar{\eta}) \neq 1, \quad (2.41)$$

$$\bar{\delta}_1 = \max \left\{ \frac{\bar{\delta}_0}{2}, \bar{\delta}_+ \right\} \quad (2.42)$$

and

$$\bar{v}_\infty = v_\infty. \quad (2.43)$$

Then, with the above changes and simply following the proof of Lemma 1, we can provide another result on majorizing sequences for Werner's method (1.2), using a different approach than in Lemma 1:

Lemma 2. Let $\ell_0 > 0$, $\ell > 0$, $\alpha \geq 0$, $\eta > 0$, $0 < \bar{\eta} \leq \eta$ and $\beta = 1 + \alpha$ be given constants. Assume:

$$\ell_0 (\eta + \bar{\eta}) < 1 \quad (2.44)$$

and

$$\bar{\delta}_1 \leq \bar{v}_\infty, \quad (2.45)$$

where $\bar{\delta}_1$, \bar{v}_∞ , $\bar{\delta}_+$ are given by (2.42), (2.43) and (2.40), respectively.

Choose

$$\delta \in [\bar{\delta}_1, \bar{v}_\infty]. \quad (2.46)$$

Then, scalar sequence $\{v_n\}$ ($n \geq 0$), given by

$$v_0 = 0, \quad v_1 = \eta, \quad v_{n+2} = v_{n+1} + \frac{\ell (v_{n+1} - v_n)^{1+\beta}}{2 (1 - \ell_0 (v_{n+1} + \bar{s}_{n+1}))}, \quad (2.47)$$

with,

$$\bar{s}_0 = 0, \quad \bar{s}_1 = \bar{\eta}, \quad \bar{s}_{n+2} = v_{n+2} + \frac{\ell (v_{n+2} - v_{n+1})^{1+\beta}}{2 (1 - \ell_0 (v_{n+1} + \bar{s}_{n+1}))}, \quad (2.48)$$

is non-decreasing, bounded above by t^{**} and converges to its unique least upper bound t^* with $t^* \in [0, t^{**}]$, where t^{**} is given by (2.19).

Moreover, the following estimates hold for all $n \geq 0$:

$$\bar{s}_n \leq v_n, \quad (2.49)$$

$$0 < v_{n+2} - v_{n+1} \leq \frac{\delta}{2} (v_{n+1} - v_n) \leq \left(\frac{\delta}{2}\right)^{n+1} \eta \quad (2.50)$$

and

$$0 < v_{n+2} - \bar{s}_{n+2} \leq \frac{\delta}{2} (v_{n+1} - \bar{s}_{n+1}) \leq \left(\frac{\delta}{2}\right)^{n+2} \eta. \quad (2.51)$$

We also need a lemma due to Werner [9, Lemma 1, p. 335]:

Lemma 3. Let $G : \mathcal{D} \subseteq \mathcal{X} \rightarrow \mathcal{Y}$ be a twice Fréchet differentiable operator. Assume that there exist a positive constants $L_1, L_{2,\alpha}$ and $\alpha \in [0, 1]$, such that:

$$\| G'(x) - G'(y) \| \leq L_1 \| x - y \| \quad (2.52)$$

and

$$\| G''(x) - G''(y) \| \leq L_{2,\alpha} \| x - y \|^\alpha \quad (2.53)$$

for all $x, y \in \mathcal{D}$.

Then, the following estimates hold:

$$\| G(x) - G(y) - G'(z)(x - y) \| \leq L_1 \int_0^1 \| (1-t)y + tx - z \| dt \| x - y \|$$

for all $x, y, z \in \mathcal{D}$

(2.54)

and

for $\theta \in [0, 1]$, $x, y \in \mathcal{D}$, $z_\theta = \theta x + (1 - \theta)y$:

$$\| G(x) - G(y) - G'(z_\theta)(x - y) \| \leq \left(\frac{1}{4} + \left(\theta - \frac{1}{2} \right)^2 \right) \frac{L_{2,\alpha} \| x - y \|^{2+\alpha}}{(\alpha + 1)(\alpha + 2)} + L_1 \left| \theta - \frac{1}{2} \right| \| x - y \|^2.$$

(2.55)

We can show the following semilocal convergence result for Werner's method (1.2):

Theorem 4. Let $F : \mathcal{D} \subseteq \mathcal{X} \rightarrow \mathcal{Y}$ be a twice Fréchet differentiable operator.

Assume:

There exist points $x_0, y_0 \in \mathcal{D}$, $L_0 > 0$, $\alpha \in [0, 1]$ and $L_{2,\alpha} > 0$, such that for all $x, y \in \mathcal{D}$:

$$A_0^{-1} \in \mathcal{L}(\mathcal{Y}, \mathcal{X}), \quad (2.56)$$

$$\| A_0^{-1} [F'(x) - F'(\frac{x_0 + y_0}{2})] \| \leq L_0 \| x - \frac{x_0 + y_0}{2} \|, \quad (2.57)$$

$$\| A_0^{-1} [F''(x) - F''(y)] \| \leq L_{2,\alpha} \| x - y \|^\alpha, \quad (2.58)$$

$$y_0 \in \overline{U}(x_0, t^*) = \{x \in \mathcal{X}, \| x - x_0 \| \leq t^*\} \subseteq \mathcal{D}, \quad (2.59)$$

$$\| A_0^{-1} F(x_0) \| \leq \eta, \quad (2.60)$$

$$\| A_0^{-1} F(x_1) \| \leq \bar{\eta}, \quad (2.61)$$

where,

$$x_1 = x_0 - F'(\frac{x_0 + y_0}{2})^{-1} F(x_0) \quad (2.62)$$

and

Conditions of Lemma 1 hold, with

$$\ell_0 = \frac{L_0}{2}, \quad \ell = \frac{L_{2,\alpha}}{2\beta(1+\beta)}. \quad (2.63)$$

Then sequence $\{x_n\}$ defined by Werner's method (1.2) is well defined, remains in $\overline{U}(x_0, t^*)$ for all $n \geq 0$ and converges to a unique solution x^* of equation $F(x) = 0$ in $U(x_0, t^*)$.

Moreover the following estimate holds for all $n \geq 0$:

$$\| x_n - x^* \| \leq t^* - t_n, \quad (2.64)$$

where, sequence $\{t_n\}$ ($n \geq 0$) is given in Lemma 1.

Proof. We shall show using induction on the integer m :

$$\|x_{m+1} - x_m\| \leq t_{m+1} - t_m \quad (2.65)$$

and

$$\|y_{m+1} - x_{m+1}\| \leq s_{m+1} - t_{m+1}. \quad (2.66)$$

Estimates (2.65) and (2.66) hold for $m = 0$ by the initial conditions.

Let us assume (2.65), (2.66) hold true and $x_n, y_n \in \bar{U}(x_0, t^*)$ for all $n \leq m + 1$.

Using (2.58), we obtain:

$$\begin{aligned} \|A_0^{-1}(A_0 - A_n)\| &\leq L_0 \left\| \frac{x_n + y_n}{2} - \frac{x_0 + y_0}{2} \right\| \\ &\leq \frac{L_0}{2} \left(\|x_n - x_0\| + \|y_n - y_0\| \right) \\ &\leq \frac{L_0}{2} \left((t_n - t_0) + (s_n - t_0) \right) \\ &= \ell_0 (t_n + s_n) < 1 \quad (\text{by (2.26)}). \end{aligned} \quad (2.67)$$

It follows from (2.67) and the Banach lemma of invertible operators [4], [7], that A_n^{-1} exists so that

$$\|A_n^{-1} A_0\| \leq \frac{1}{1 - \ell_0 (t_n + s_n)}. \quad (2.68)$$

In view of (1.2), we obtain the approximations:

$$F(x_{m+1}) = F(x_{m+1}) - F(x_m) - F'\left(\frac{x_m + y_m}{2}\right)(x_{m+1} - x_m) \quad (2.69)$$

$$F(x_{m+2}) = F(x_{m+2}) - F(x_{m+1}) - F'\left(\frac{x_m + y_m}{2}\right)(y_{m+1} - x_{m+1}). \quad (2.70)$$

By composing both sides of (2.69), (2.70) by A_0^{-1} , using Lemma 3 for $\theta = \frac{1}{2}$, $G = A_0^{-1} F$, we obtain:

$$\|A_0^{-1} F(x_{m+1})\| \leq \frac{L_{2,\alpha}}{4(\alpha+1)(\alpha+2)} \|x_{m+1} - x_m\|^{2+\alpha} \leq \ell (t_{m+1} - t_m)^{1+\beta} \quad (2.71)$$

and

$$\|A_0^{-1} F(x_{m+2})\| \leq \frac{L_{2,\alpha}}{4(\alpha+1)(\alpha+2)} \|x_{m+2} - x_{m+1}\|^{2+\alpha} \leq \ell (t_{m+2} - t_{m+1})^{1+\beta}, \quad (2.72)$$

respectively.

Using (1.2), (2.68), (2.17), (2.18), (2.71) and (2.72), we obtain:

$$\begin{aligned} \|x_{m+2} - x_{m+1}\| &\leq \|A_{m+1}^{-1} A_0\| \|A_0^{-1} F(x_{m+1})\| \\ &\leq \frac{\ell (t_{m+1} - t_m)^{1+\beta}}{2(1 - \ell_0 (t_{m+1} + s_{m+1}))} \\ &= t_{m+2} - t_{m+1} \end{aligned}$$

and

$$\begin{aligned} \|y_{m+2} - x_{m+2}\| &\leq \|A_{m+1}^{-1} A_0\| \|A_0^{-1} F(x_{m+2})\| \\ &\leq \frac{\ell (t_{m+2} - t_{m+1})^{1+\beta}}{2(1 - \ell_0 (t_{m+1} + s_{m+1}))} \\ &= s_{m+2} - t_{m+2}, \end{aligned}$$

which complete the induction for (2.65) and (2.66).

By Lemma 1, (2.65) and (2.66), sequence $\{x_n\}$ ($n \geq 0$) is Cauchy sequence in a Banach space \mathcal{X} and as such it converges to some $x^* \in \overline{U}(x_0, t^*)$ (since $\overline{U}(x_0, t^*)$ is a closed set). By letting $m \rightarrow \infty$ in (2.71), we obtain $F(x^*) = 0$.

Finally to show uniqueness, let $y^* \in U(x_0, t^*)$ be a solution of equation $F(x) = 0$.

Let:

$$\mathcal{M} = \int_0^1 F'(x^* + t(y^* - x^*)) dt. \tag{2.73}$$

Using (2.58), we obtain in turn:

$$\begin{aligned} \|A_0^{-1}(A_0 - \mathcal{M})\| &\leq L_0 \int_0^1 \left\| \frac{x_0 + y_0}{2} - (x^* + t(y^* - x^*)) \right\| dt \\ &\leq L_0 \int_0^1 \left((1-t) \left\| \frac{(x_0 - x^*) + (y_0 - x^*)}{2} \right\| + \right. \\ &\quad \left. t \left\| \frac{(y_0 - y^*) + (x_0 - y^*)}{2} \right\| \right) dt \\ &\leq \frac{L_0}{4} \left(\|x_0 - x^*\| + \|y_0 - x^*\| + \|y^* - x_0\| + \right. \\ &\quad \left. \|y^* - y_0\| \right) \\ &< \frac{L_0}{4} 4 t^* = L_0 t^* \leq 1 \quad (\text{by (2.26)}). \end{aligned} \tag{2.74}$$

In view of (2.74) and the Banach lemma on invertible operators, \mathcal{M}^{-1} exists.

It follows from the identity:

$$0 = F(x^*) - F(y^*) = \mathcal{M}(x^* - y^*),$$

that

$$x^* = y^*.$$

That completes the proof of Theorem 4. □

Remark 5. (a) The most appropriate choices for δ in Lemmas 1 and 2 seem to be $\delta = \delta_1$ and $\delta = \bar{\delta}_1$, respectively.

(b) Note that the conclusions of Theorem 4 hold if Lemma 1 is replaced by Lemma 2 and (2.18) by (2.48).

(c) The limit point t^* (see Theorem 4) can be replaced by t^{**} given in closed form by (2.19).

3. APPLICATIONS

Let us provided a numerical example.

Example 1. Let $\mathcal{X} = \mathcal{Y} = \mathbb{R}$, $x_0 = 1$, $\mathcal{D} = \{x : |x - x_0| \leq 1 - \gamma\}$, $\gamma \in \left[0, \frac{1}{2}\right)$, and define function F on U_0 by

$$F(x) = x^3 - \gamma. \tag{3.1}$$

The Kantorovich hypotheses for Newton's method are [4], [7]:

$$\|F'(x_0)^{-1}(F'(x) - F'(y))\| \leq K \|x - y\|, \quad \text{for all } x, y \in \mathcal{D} \tag{3.2}$$

and

$$h_K = 2 K \eta \leq 1. \tag{3.3}$$

Using (3.1) and (2.60) (for $x_0 = y_0 = 1$), we obtain

$$\eta = \frac{1}{3} (1 - \gamma) \quad \text{and} \quad K = 2 (2 - \gamma). \quad (3.4)$$

The Kantorovich condition is violated since:

$$\frac{4}{3} (1 - \gamma) (2 - \gamma) > 1 \quad \text{for all} \quad \gamma \in \left[0, \frac{1}{2}\right).$$

Hence, there is no guarantee that Newton's method starting at $x_0 = 1$ converges to $x^* = \sqrt[3]{\gamma}$.

However, the condition of our Theorem 4 under the conditions of Lemma 2 are satisfied, say for $\gamma = .49$.

Indeed, using (2.1), (2.40)–(2.43), (2.60), (2.61) and (3.1), we obtain:

$$\begin{aligned} v &= 2.749087577, \\ \bar{\delta}_+ &= .0723581, \quad \bar{\delta}_0 = .008401651, \\ \bar{\delta}_1 &= \bar{\delta}_+, \quad v_\infty = \bar{v}_\infty = .5733, \quad \text{and} \quad \delta = \delta_0. \end{aligned}$$

Then all hypotheses of Theorem 4 hold. Hence, Werner's method (1.2) converges to $x^* = \sqrt[3]{.49} = .788373516$.

CONCLUSION

We provided a semilocal convergence analysis for Werner's method in order to approximate a locally unique solution of an equation in a Banach space.

Using recurrent functions, a combination of Hölder condition on the second derivative and center-Lipschitz condition on the first derivative, instead of only Hölder and Lipschitz conditions [9], [10], we provided an analysis with the following advantages over the work in [9], [10]: weaker sufficient convergence conditions and larger convergence domain.

A numerical example further validating the results is also provided in this study.

REFERENCES

- [1] I.K. Argyros, *On the convergence of two-step methods generated by point-to-point operators*, Appl. Math. Comput., **82** (1997), 85–96.
- [2] I.K. Argyros, *A new semilocal convergence theorem for Newton's method in Banach space using hypotheses on the second Fréchet-derivative*, J. Comput. Appl. Math., **130** (2001), 369–373.
- [3] I.K. Argyros, *A unifying local-semilocal convergence analysis and applications for two-point Newton-like methods in Banach space*, J. Math. Anal. Appl., **298** (2004), 374–397.
- [4] I.K. Argyros, *Convergence and applications of Newton-type iterations*, Springer-Verlag Publ., New York, 2008.
- [5] J.E. Dennis, *Toward a unified convergence theory for Newton-like methods*, in Nonlinear Functional Analysis and Applications (L.B. Rall, ed.), Academic Press, New York, (1971), 425–472.
- [6] P. Deuffhard, G. Heindl, *Affine invariant convergence theorems for Newton's method and extensions to related methods*, SIAM J. Numer. Anal., **16** (1979), 1–10.
- [7] L.V. Kantorovich, G.P. Akilov, *Functional Analysis*, Pergamon Press, Oxford, 1982.
- [8] F.A. Potra, *Sharp error bounds for a class of Newton-like methods*, Libertas Mathematica, **5** (1985), 71–84.
- [9] W. Werner, *Über ein Verfahren der Ordnung $1 + \sqrt{2}$ zur Nullstellenbestimmung*, Numer. Math., **32** (1979), 333–342.
- [10] W. Werner, *Some supplementary results on the $1 + \sqrt{2}$ order method for the solution of equations*, Numer. Math., **38** (1982), 383–392.
- [11] T. Yamamoto, *A convergence theorem for Newton-like methods in Banach spaces*, Numer. Math., **51** (1987), 545–557.

Simulation of Rotational Flows in Cylindrical Vessel with Double Rotating Stirrers; Part-A: Analysis of Flow Structure and Pressure Differentials

R. A. Memon

Centre for Advance Studies in Pure and Applied Mathematics,
Bahauddin Zakria University,
Multan, Punjab, Pakistan.
Email: ra-memon1@yahoo.com

M. A. Solangi

Department of Basic Sciences and Related Studies,
Mehran University of Engineering and Technology,
Jamshoro, Sindh, Pakistan.
Email: manwarsolangi@yahoo.com

A. Baloch

Department of Basic Sciences and Related Studies,
Mehran University of Engineering and Technology,
Jamshoro, Sindh, Pakistan.
Email: csbaloch@yahoo.com

Abstract. In this article incompressible rotating mixing flows of Newtonian fluid inside the cylindrical vessel are investigated. The numerical simulations are combination of stationary and rotating double stirrer cases. The influence of rotational speed and rotational direction of stirrers have been observed on the predictions of the flow structure in the dissolution rotating vessel with fixed and rotating stirrers. The problem is relevant to the food industry, of mixing fluid within a cylindrical vessel, where stirrers are located on the lid of the vessel eccentrically configured with fixed and rotating stirrers. Here, the motion is premeditated as driven by the rotation of the outer vessel wall, with various rotational speeds and rotational directions of stirrers. A time-stepping finite element method is employed to foresee the numerical solutions. The numerical technique adopted is based on a semi-implicit Taylor-Galerkin/ pressure-correction scheme, posed in a two-dimensional cylindrical polar coordinate system. Variation with increasing speed of vessel, change in speed of stirrers and change in rotational direction of stirrers in mixer geometry are investigated, with respect to the re-circulating flow pressure isobars. The ultimate objective is to envisage and adjust the design of dough mixers, so that the optimal dough processing may be achieved markedly, with reference to work input on the dough.

Key Words: Numerical Simulation, Finite Element Method, Newtonian Fluids, Rotational Mixing Flows, Co-rotating Stirrer, Contra-rotating Stirrer and Mix-rotating Stirrer.

1. INTRODUCTION

In mixing industries the analysis of complex mixing of fluids remains a persistent challenge for engineers. In order to improve design of the mixing components and ensure safety and satisfactory operating performance, precise knowledge of their transient response is required. In a first modelling step, design engineers must identify the meaningful physical phenomena in their particular geometry. Generally, industrial problems are demanding to treat with, mainly in the field of chemical process applications, such as mixing of dough in a food processing industry [1–5], granular mixing, powder mixing processes [6], mixing of paper pulp in paper industry and many other industrial processes. The case of a circular cylinder confined in cylindrical fluid domains has already attracted a great attention due to its recurrence in the design of mixing components. Flow between a rotating cylindrical vessel and rotating cylindrical stirrers is perhaps the most popular candidate in experimental and numerical studies of rotational flows. Very few experimental/numerical investigations have been reported in the literature on such type of flows.

Similar type of problems in the literature are as oscillating cylinders in cross or stationary flow frequently observed in offshore structures and power cables with fluidstructure interactions [2]. Building on the understanding of flow over a single stationary cylinder, many researchers have recently focused attention on multiple stationary or oscillating cylinders. Flow around two oscillating cylinders has characteristics of both an oscillating cylinder and multiple cylinders [1, 6 and 7].

In many mixing processes the complicating factors are the use of agitators with stirrer in fact that the agitator may be operated in the transitional regime, the use of the fluids which exhibits very complex rheological behaviour and the rotational speed and rotational direction of stirrers. Previous investigations of identical phenomenon also explored by number of researcher, such complex problem is still persist a challenge [8–11].

The fully three-dimensional incompressible mixing flows had been simulated to obtain the numerical solution for non-Newtonian fluids using generalised Navier-Stokes equation [5] in finite vessel. Whilst, for modelling the dough kneading problem the two-dimensional non-Newtonian mixing flows was investigated with different number and shapes of stirrers [3–6]. Subsequently, the parallel version of this finite element scheme is also developed [1–4].

The motivation for this work is to advance fundamental technology in modelling of the dough kneading with the ultimate aim to forecast the optimal design of dough mixers themselves, hence, leading to efficient dough mixing processing. The present work is one of these forms, expressed as the flow between a rotating cylindrical vessel and two stationary as well rotating cylindrical stirrers in co-rotating, contra-rotating and mix-rotating directions against the direction of rotational cylindrical vessel. Stirrers are located on the mixing vessel lid, and placed in an eccentrically. In two-dimension, similar problem was also investigated with different number and shapes of stirrers [4–6].

In the present work a semi-implicit Taylor-Galerkin/Pressure-Correction (TGPC) time-marching scheme adopted, which has been developed and refined over the last couple

of decades. The flow is modelled as incompressible via so-called TGPC finite element scheme posed in a two-dimensional cylindrical polar coordinate system which applies a temporal discretisation in a Taylor series prior to a Galerkin spatial discretisation. A semi-implicit treatment for diffusion is employed to address linear stability constraints. An inelastic model with shear rate dependent viscosity is considered [5]. This scheme, firstly conceived in chronological form, is appropriate for the simulation of various types of incompressible Newtonian flows [1].

In Section 2, the complete problem is specified and the governing equations and numerical method are described in Section 3. Numerical results and discussions are presented in Section 4 and conclusions are drawn in Section 5.

2. PROBLEM SPECIFICATION

The problem addressed in this article is a cylindrical vessel with a couple of rotating cylindrical stirrers located eccentrically cingured in the side of the vessel. The fluid is driven by the outer vessel wall and two rotating cylindrical stirrers fixed at the top of the vessel. Fixed and rotating stirrers are adopted. initially, the flow analyse between two stationary stirrers and rotating cylindrical vessel, to validate the finite element predications in this cylindrical polar co-ordinate system to compare the present numerical predictions against numerical results obtained in previous investigations [3–6]. Subsequently, three alternative rotational directions (Co-rotating, Contra-rotating and Mix-rotating) and three rotational speeds (half, same and double against the speed of cylindrical vessel) of stirrers are investigated.

Rotational Direction are shown in figure–1 (a), (b) and (c) for Co-rotating, Contra-rotating and Mix-rotating directions of stirrers respectively. Computational domain and finite element mesh for the study involved is shown in figure–2. For the finite element mesh, triangular elements are selected in the current research work. Total numbers of elements are 8960, nodes and degrees-of-freedom, are 18223 and 40057 respectively. Details on mesh convergence, initial and boundary conditions reader is referred to our pervious investigations [1–6]. In this study, solution fields of interest are presented of flow structure and pressure differential through contour plots of streamlines and isobars respectively [1].

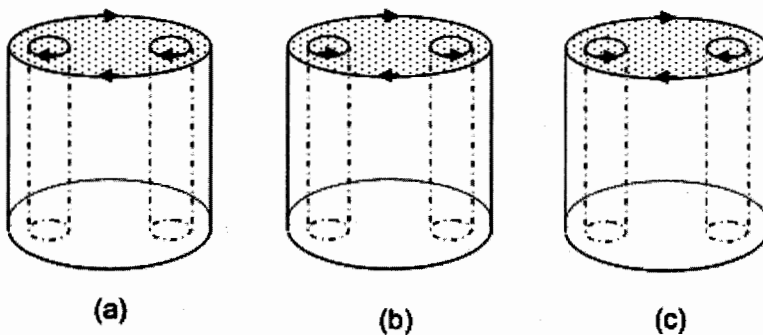


FIGURE 1. Rotational direction of eccentric rotating cylindrical flow, with double stationary and rotating stirrers.

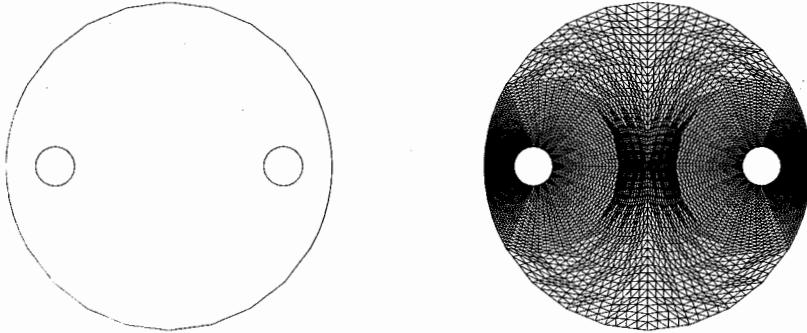


FIGURE 2. Computational domain and finite element mesh of eccentric rotating cylindrical flow, with double stationary and rotating stirrers.

To provide a well-posed specification for each flow problem, it is necessary to prescribe appropriate initial and boundary conditions. Simulations commence from a quiescent initial state. Boundary conditions are taken as follows. For stationary stirrer the fluid may stick to the solid surfaces, so that the components of velocity vanish on the solid inner stirrer sections of the boundary ($v_r = 0$ and $v_\theta = 0$). For non-stationary stirrer, fixed constant velocity boundary conditions are applied. For co-rotating stirrer, vanishing radial velocity component ($v_r = 0$) is fixed and for azimuthal velocity component is fixed with three different non-dimensional speeds ($v_\theta = 0.5, 1$ and 2 unit). Similarly, for contra-rotating stirrer only azimuthal velocity component is changed and fixed in reverse direction (i.e., $v_\theta = -0.5, -1$ and -2 unit). On the outer rotating cylinder vessel a fixed constant velocity boundary condition is applied ($v_r = 0$ and $v_\theta = 1$ unit), and a pressure level is specified as zero for both co-, contra- and mix-rotating stirrers on vessel wall. For stream function, outer cylinder is fixed zero and at inner stirrer is left unconstrained, being solutions on closed streamlines.

3. GOVERNING SYSTEM OF EQUATIONS AND NUMERICAL SCHEME

Incompressible rotational flows of isothermal Newtonian fluid in two-dimensions can be modelled through a system comprising of the generalised momentum transport and conservation of mass equations. The coordinate reference frame is a two-dimensional cylindrical coordinate system taken over domain Ω in two-dimensional system. In the absence of body forces, the system of equations can be represented through the conservation of mass equation, as,

$$\nabla \cdot \mathbf{u} = 0, \quad (3.1)$$

the conservation of momentum transport equation, as,

$$\frac{\partial \mathbf{u}}{\partial t} = \frac{1}{Re} \nabla^2 \mathbf{u} - \mathbf{u} \cdot \nabla \mathbf{u} - \nabla p, \quad (3. 2)$$

where, \mathbf{u} is the fluid velocity vector field, p is the isotropic fluid pressure (per unit density), t represents time and ∇ is the spatial differential operator.

Relevant non-dimensional Reynolds number is defined as:

$$Re = \frac{\rho V R}{\mu}, \quad (3. 3)$$

The characteristic velocity V is taken to be the rotational speed of the vessel, the characteristic length scale is the radius, R , of a stirrer and ρ is the fluid density and the characteristic viscosity μ is the zero shear-rate viscosity.

Appropriate scaling in each variable takes the form. At a characteristic rotational speed 50 rpm and zero shear viscosity of 105 Pa s, scaling yields dimensional variables $p = 2444 p^*$. To compute numerical solutions through a semi-implicit Taylor-Galerkin/pressure-correction scheme in this study, a time-marching finite element algorithm is employed, based on a fractional-step formulation. Briefly, this involves discretisation, first in the temporal domain, obtain through Taylor series expansion and a pressure-correction operator-split technique, to build a second-order time-stepping scheme. Spatial discretisation is achieved via Galerkin approximation for the momentum equations. The finite element basis functions employed are quadratic (ϕ_j) for velocities, and linear (ψ_k) for pressure. A detail on numerical algorithm, fully discrete system and definition of matrices is described can be found [9–12].

4. NUMERICAL RESULTS AND DISCUSSIONS

Two different directions are employed to analysed the predicted solutions: firstly, change in rotational direction (co-rotating, contra-rotating and mix-rotating) and second, rotational speed ($v_\theta = \frac{1}{2}, 1, 2$; half, same and double respectively) of the stirrer against to the speed of vessel. This leads to testing with respect to increasing viscosity levels (decrease of Reynolds number) for Newtonian fluid and comparison of flow structure and pressure variation across problem instances. The predicted solutions are displayed for Newtonian fluid through contours plots of streamlines, and pressure isobars and these are plotted from minimum value to maximum value, over a range (in all figures Maximum values indicated with SQUARE shape and Minimum Value indicated with OVAL shape).

The Reynolds numbers of $Re = 8.0$, $Re = 0.8$ and $Re = 0.08$, the corresponding zero shear viscosities are $\mu = 1.05$ Pa s, $\mu = 10.5$ Pa s and $\mu = 105.0$ Pa s. Of these levels, a range of material properties is covered from those for model fluids, to model dough, to actual dough, respectively.

4.1. Flow patterns and pressure differential for stationary stirrers with increasing inertia. Computations are carried out at $Re = 0.08$, $Re = 0.8$ and $Re = 8$. The effect of increasing Reynolds number upon streamline patterns on left and pressure differential on right isobars are represented in contour plots for stationary stirrers in figure–3. At a low level of inertia, $Re = 0.08$, an intense recirculating region forms in the centre of the vessel,

parallel to the stirrers and symmetrically intersecting the diameter that passes through the centres of the vessel and stirrers. Flow structure remains unaffected as Reynolds number rises to values of $O(1)$; hence the solution field has been suppressed. However, upon increasing Reynolds number up to eight, so $O(10)$, inertia takes hold and the recirculation region twist and shifts towards the upper-half plane, vortex intensity wanes and the vortex eye is pushed towards the vessel wall. The flow becomes asymmetric as a consequence of the shift in vortex core upwards. The diminishing trend in vortex intensity is tabulated in Table 1.

Table-1: Vortex intensity for Newtonian fluids ($\mu_c = 105, 10.5$ and 1.05 Pas)

Problem	Speed of stirrer	Re = 0.08		Re = 0.8		Re = 8.0	
		Min	Max	Min	Max	Min	Max
Stationary stirrer	Zero	0	3.7613	0	3.75964	0	3.61976
Co-rotating stirrer	Half	0	5.68479	0	5.68248	0	5.57629
	Same	0	7.75524	0	7.76814	0	7.99449
	Double	0	11.9254	0	12.0221	0	13.4436
Contra-rotating stirrer	Half	0	2.66273	0	2.66225	0	2.62743
	Same	-0.93386	2.02191	-0.9386	2.01946	-1.49938	1.81904
	Double	-5.019	1.58694	-5.0849	1.58592	-7.41413	1.71834
Mix-rotating stirrer	Half	0	4.25444	0	4.25387	0	4.19542
	Same	0	5.42041	0	5.42056	0	5.42893
	Double	-1.997	7.84833	-1.98886	7.85385	-1.6173	8.11336

Comparable symmetry influence relate across the geometry variants in pressure differential, at $Re = 0.08$, symmetric pressure isobars appear with equal magnitude in non-dimensional positive and negative extrema on the two sides (upper and lower) of the stirrers in the narrow-gap. As inertia increases from $Re = 0.8$ to $Re = 8$, asymmetric isobars are observed, with positive maximum on the top of the stirrer and negative minimum at the outer stirrer tip (near the narrow-gap), numerical results are tabulated in Table 2.

Asymmetrical flow structure is observed in all variables and transversely all occurrence as inertia increase from $Re = 0.08$ to $Re = 8.0$, recirculating flow-rate decrease by just five percent. In non-dimensional terms above $Re = 0.08$ (noting scale differences), there is increase in pressure-differential rise by as much as twenty-two percent, at $Re = 8.0$, although pressure differential increase on the lower part of the stirrers. For Newtonian fluid, the extrema of recirculating region along with vortex intensity and pressure differential, are tabulated for completeness in tables 1 and 2.

4.2. Flow patterns and pressure differential for co-rotating stirrers with increasing inertia. With increasing Reynolds number from $Re = 0.08$ to $Re = 8.0$, equivalent field kinematic data for co-rotating stirrers is presented in figure-4 and -5, to make direct comparisons across all instances for Newtonian fluids, with rigorous reference to localised vortex intensity and pressure drops are tabulated in tables 1 and 2.

Stream lines are shown for increasing rotational speed of the stirrer (from left to right), double speed, same speed and half speed ($v_\theta = 0.5, 1.0$ and 2.0 respectively) for co-rotating case, only single vortex is formed, shown in figure-3. At Reynolds number 0.08, half

speed of the stirrers the vortex is formed at the centre of the stirrers and is of the elliptical shape in the horizontal direction and smooth in formation, but as the speed of the stirrers is increased to double speed the vortex changes the direction from horizontal to vertical and its size is large as compare to half speed of the stirrers also showing an increase space between the centre of vortex and diameter of secondary streamline. Streamlines tend to increase in density at the edges of the stirrers. At Reynolds number 0.8, half speed of the stirrers the vortex changes the direction from horizontal to vertical and change noted at the same speed is vice-versa, but at the double speed of the stirrers is the vortex twist to the stirrers in rotational direction of the vessel. At $Re = 8.0$, half speed the diameter of the vortex increases and the shape of the vortex is changed in circular shape similarly at same speed, the diameter of the vortex decreases at the double speed and vortex centre amplifies in the size. Consequently, the fluid recirculates at the centre of the vessel and create vacuum in the centre of the vessel.

In figure-5, illustrates the pressure differential at all comparable parameter values for co-rotating instances, The speed of stirrer is half virtually small change in the pressure differential is observed and remain unaltered for all Reynolds numbers values, the pressure differentials is very low and remain in order of two for all inertial values when increasing the speed of stirrers from same to double speed, consequently, the pressure differentials are noted high and is about seven times in negative extrema compare to stationary stirrer, at $Re = 8$ and small change is observed in positive maxima. See Table-2.

Table-2: Pressure drop for Newtonian fluids ($\mu_c = 105, 10.5$ and 1.05 Pas)

Problem	Speed of stirrer	Re = 0.08		Re = 0.8		Re = 8.0	
		Min	Max	Min	Max	Min	Max
Stationary stirrer	Zero	-3.35114	3.33577	-3.42489	3.27096	-4.51328	3.29584
Co-rotating stirrer	Half	-1.45201	1.4338	-1.53811	1.356	-3.59659	0.94539
	Same	-1.31591	1.2375	-1.66359	0.87996	-8.18721	0.51811
	Double	-4.51104	4.35319	-5.35531	3.79051	-27.334	2.90016
Contra-rotating stirrer	Half	-5.26616	5.24019	-5.38462	5.14477	-6.71983	4.5179
	Same	-7.18218	7.13253	-7.40446	6.92244	-10.0362	4.98229
	Double	-11.0943	10.9296	-11.8754	10.2863	-24.6213	6.93863
Mix-rotating stirrer	Half	-5.69415	5.67199	-5.81121	5.58275	-8.45116	5.11985
	Same	-8.10922	8.04915	-8.42092	7.76947	-13.7993	5.92129
	Double	-12.9865	12.757	-14.064	11.7682	-29.6726	8.50339

4.3. Flow patterns and pressure differential for contra-rotating stirrers with increasing inertia. Corresponding field kinematics data for contra-rotating stirrers situation with increasing Reynolds number at $Re = (0.08, 0.8$ and $8.0)$ the streamline contours and pressure differentials are presented in figure-7 respectively. In figure-6, for contra-rotating case, streamlines are demonstrate for increasing speed of the stirrers from half (left) to double (right) against the speed of vessel the six vortices arises, and symmetric behaviour around the stirrer. At the half speed of stirrers and $Re = 0.08$ there is embro vertices appear in the narrow-gap of both stirrers, and in narrow gap as well in middle of the vessel, two vortices are noted in the upper and lower region of vessel away from stirrer close to vessel

wall. In the narrow gap, where stirrers spins in oppose direction of the vessel rotation, a small vortex appear with low vortex intensity, as the speed of stirrers increase these vortices strength up to fifty percent high at low $Re = 0.08$.

In table 1, minima and maxima of vortex intensity is tabulated when the vortex intensity is observed with increase in inertia. As inertia takes hold in the central region of recirculation, centres of vortices shift towards the upper and lower half plane in the direction of rotation of the both stirrers against to the vessel. For all Reynolds number values, at double speed of stirrers, the central vortices rotate in counter directions against two other vortices. These recirculation regions have different rotational direction which is very important phenomena in homogenisation of the fluid.

For all three instances, comparable equilibrium influence apply across the geometry variants in pressure differential, at $Re = 0.08$ and double rotational speed of stirrer, symmetric pressure isobars appear with equal magnitude in non-dimensional positive and negative extrema on both sides (upper and lower) of the stirrer in the narrow-gap as shown in figure-7. The associated values of pressure differentials are tabulated in table 2. As inertia increase from $Re = 0.8$ to $Re = 8$, asymmetric isobars are observed, with positive maxima on the top of the stirrer and negative minima at the outer stirrer tip (near the narrow-gap), see also Table 2. For the contra-rotating instance, in contrast to co-rotating case, the pressure differentials are somewhat symmetrical in geometry at maxima and minima at twice the speed of stirrer and at half the speed of stirrer for both inertial values $Re = 0.08$ and $Re = 0.8$. However, upon increasing Reynolds number up to eight, thus $O(10)$, inertia takes hold the pressure differentials are observed asymmetrical, increasing the speed of the stirrer to double increases the pressure differentials more than twice in negative minima and in contrast it decrease up to thirty five percent in positive maxima. Comparing against co-rotating case at same double speed of stirrer increase in minima is merely eight percent and increase in maxima is about thirty percent.

4.4. Flow patterns and pressure differential for mix-rotating stirrers with increasing inertia. For mix-rotating stirrers, the field kinematics data with increasing Reynolds number from 0.08 to 8.0 the streamline contours are shown in figure-8 and in figure-9 pressure differentials. For mix-rotating case, three vortices arise, one in right of the stirrer rotate in same direction of vessel and in right and left of the stirrer rotate in opposite direction of vessel. At the $Re = 0.08$ and the $Re = 0.8$ note the same behaviour for half to double speed of stirrers respectively. There is two in the vicinity of both stirrers, and in narrow gap as well in middle of the vessel, two vortices are noted in the upper and lower region of vessel away from stirrer close to vessel wall. In the narrow gap, where stirrers spins in oppose direction of the vessel rotation, a small vortex appear with low vortex intensity, as the speed of stirrers increase these vortices strength up to fifty percent high at low $Re = 0.08$. The growth in minima of vortex intensity is examine with increase in inertia, however, it dominate in maxima of vortex intensity. As inertia takes hold in the central region of recirculation centres of vortices shift towards the upper and lower half plane in the direction of rotation of the both stirrers against to the vessel. For all Reynolds number values at double speed of stirrer, the central vortices rotate in counter directions against two other vortices. These recirculation regions have different rotational direction which is very important phenomena in homogenisation of the fluid.

5. CONCLUSIONS

Computational results of cylindrical rotating vessel with couple of cylindrical rotating stirrers present certain characteristics of symmetry, the rotation of the double stirrer case against stationary stirrer case in co-rotating, contra-rotating, and mix-rotating directions are being investigated with increasing inertia. It is confirmed that, fluid flow structure lose its symmetry and recirculating region move upwards in the direction of vessel motion with increasing inertia and non-dimensional pressure differential increases for stationary stirrer case. For co-rotating stirrer case, single recirculating region develops in the centre of the stirrers and fluid suppressed in direction of rotation of the vessel with increasing inertia and speed of stirrer. Whilst at twice the speed of stirrer pressure differentials are higher and lower at lower speed of stirrer and for the case mix-rotating stirrer different position has been analysed, a re-circulating region develops in the right of the stirrers rotating in direction of vessel and left and right of the stirrer rotating in anti-direction of vessel and fluid suppressed in direction of rotation of the vessel with increasing inertia and speed of stirrer. Whilst at twice the speed of stirrer pressure differentials are higher and lower at lower speed of stirrer.

Contra-rotating case flow structure and pressure differential illustrates completely different picture in contrast to above cases. There is six recirculating regions have been examined with different position of vortex centres. The pressure differentials are generally higher, and similar balance in extrema is noted to those flows. However, the position, in those negative maxima exceeds to positive minima by about four times and in the mix-rotating the narrow gap appears where stirrers spins in oppose direction of the vessel rotation, a small vortex appear with low vortex intensity.

We have productively demonstrated the use of two-dimensional numerical simulations for this complex mixing process using Newtonian fluid flow solver for the industrial flow of dough mixing. Promising future directions of this work are investigation of rotation of two stirrers case in co-rotating, contra-rotating and mixed rotating directions, changing material properties using non-Newtonian fluids and introducing agitator in concentric configured stirrer. Through the calculative capability generated, we shall be able to relate this to mixer design that will ultimately impact upon the processing of dough products.

Acknowledgement: The authors are greatly acknowledged to the Mehran University of Engineering and Technology, Jamshoro, for providing computational facility and financial grant of Higher Education Commission of Pakistan.

REFERENCES

- [1] A. Baloch, R. A. Memon, and M. A. Solangi, *Prediction of Power Consumption of Rotational Flow in Cylindrical Vessel*, , Mehran University Research Journal of Engg and Tech, **28**(3), (2009) 329–342,.
- [2] A. Baloch, G. Q. Memon, and M. A. Solangi, *Simulation of Rotational Flows in Cylindrical Vessel with Rotating Single Stirrer*, *Punjab University Journal of Mathematics*, **40**, (2008) 83–96.
- [3] A. Baloch, and M. F. Webster, M. F., *Distributed Parallel Computation for Complex Rotating Flows of Non-Newtonian Fluids*, *Int. J. Numer. Meth. Fluids*, **43**, (2003) 1301–1328.
- [4] A. Baloch, P. W. Grant and M. F. Webster, M. F., *Parallel Computation of Two-Dimensional Rotational Flows of the Viscoelastic Fluids in Cylindrical Vessel*, *Int. J. Comp. Aided Eng. and Software, Eng. Comput.*, **19**(7), (2002) 820–853.
- [5] K. S. Sujatha., D. Ding, M. F. Webster, *Modelling of free surface in two and three dimensions*, in: C. A. Brebbia, B. Sarlen (Eds.), *Sixth International Conference on Computational Modelling of Free and Moving Boundary Problems - 2001*, WIT, Lemnos, Greece, (2001) 102–111.

- [6] K. S. Sujatha,, D. Ding, M. F. Webster, *Modelling three-dimensions mixing flows in cylindrical-shaped vessels*, in: *ECCOMAS CFD - 2001, Swansea, UK*, (2001) 1–10.
- [7] D. Ding, M. F. Webster, *Three-dimensional numerical simulation of dough kneading*, in: *D. Binding, N. Hudson, J. Mewis, J.-M. Piau, C. Petrie, P. Townsend, M. Wagner, K. Walters (Eds.), XIII Int. Cong. on Rheol., Vol. 2, British Society of Rheology, Cambridge, UK*, (2000) 318–320.
- [8] P. M. Portillo, F. J. Muzzio and M. G. Ierapetritou, *Hybrid DEM-Compartment Modelling Approach for Granular Mixing*, *AIChE Journal*, **53**(1), (2007) 119–128.
- [9] N. Phan-Thien, M. Newberry and R. I. Tanner, *Non-linear oscillatory flow of a solid-like viscoelastic material*, *J. Non-Newtonian Fluid Mech.*, **92**, (2000) 67–80.
- [10] K. S. Sujatha, M. F. Webster, D. M. Binding, M. A. Couch, *Modelling and experimental studies of rotating flows in part-filled vessels: wetting and peeling*, *J. Foods Eng.*, **57**, (2002), 67–79.
- [11] D. M. Binding, M. A. Couch, K. S. Sujatha, M. F. Webster, *Experimental and numerical simulation of dough kneading in filled geometries*, *J. Foods Eng.* **57**, (2002) 1–13.
- [12] P. Townsend and M. F. Webster, *An algorithm for the three-dimensional transient simulation of non-Newtonian fluid flows*, in: *G. Pande, J. Middleton (Eds.), Proc. Int. Conf. Num. Meth. Eng.: Theory and Applications, NUMETA, Nijhoff, Dordrecht*, **T12** (1987) 1–11.

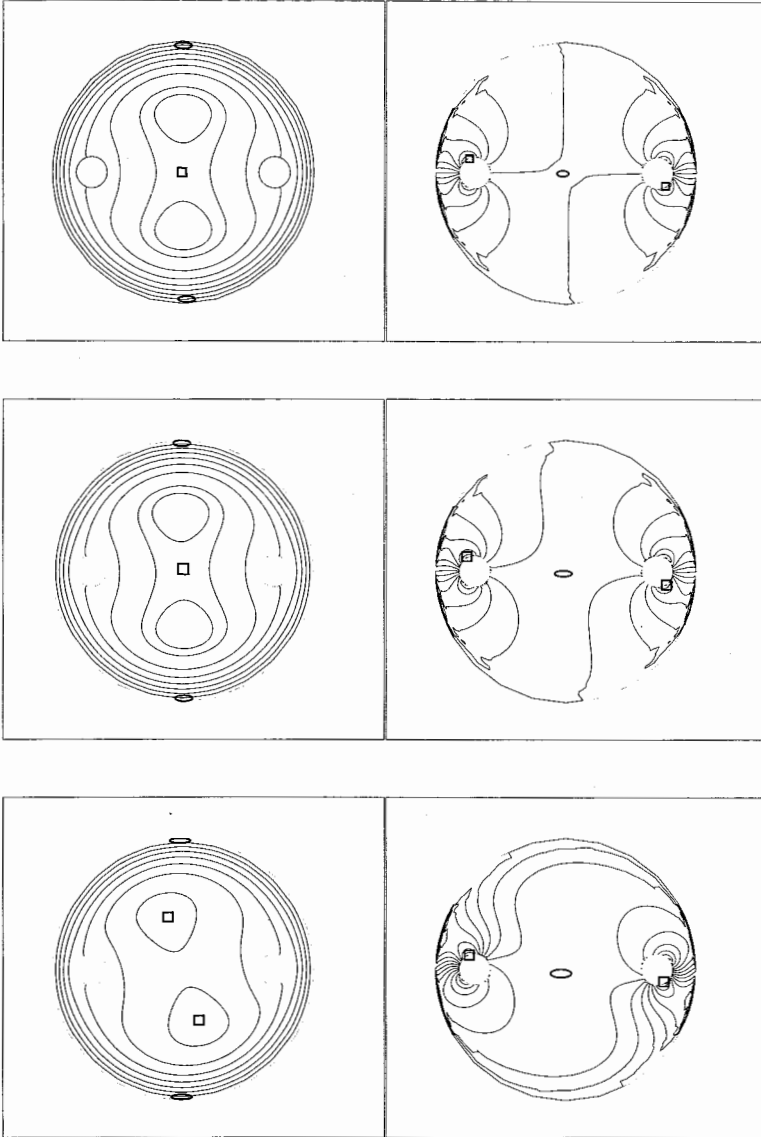


FIGURE 3. Streamline contours and Pressure isobars of stationary stirrers ($v_{\theta} = 0.0$), with increasing Reynolds number ($Re = 0.08, 0.8$ and 8.0) from top to bottom.

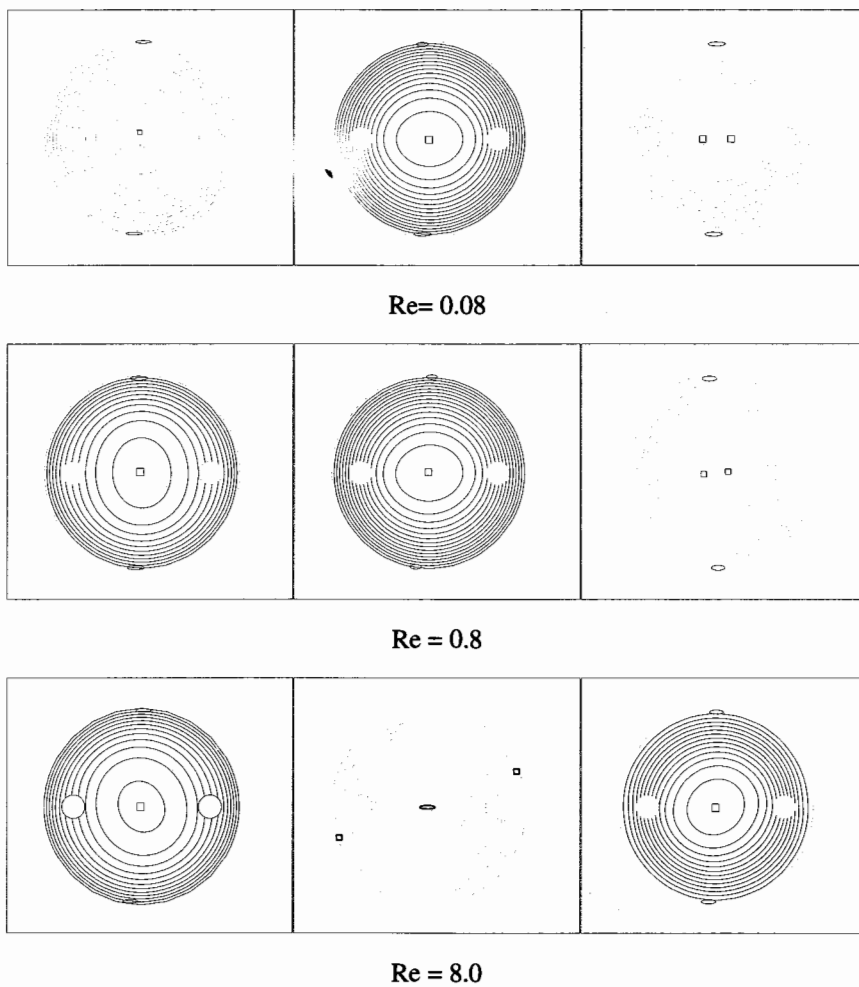


FIGURE 4. Streamline contours for co-rotating stirrers with increasing speed of the stirrers ($v_\theta = 0.5, 1.0$ and 2.0) from left to right against the speed of the vessel and increasing Reynolds number.

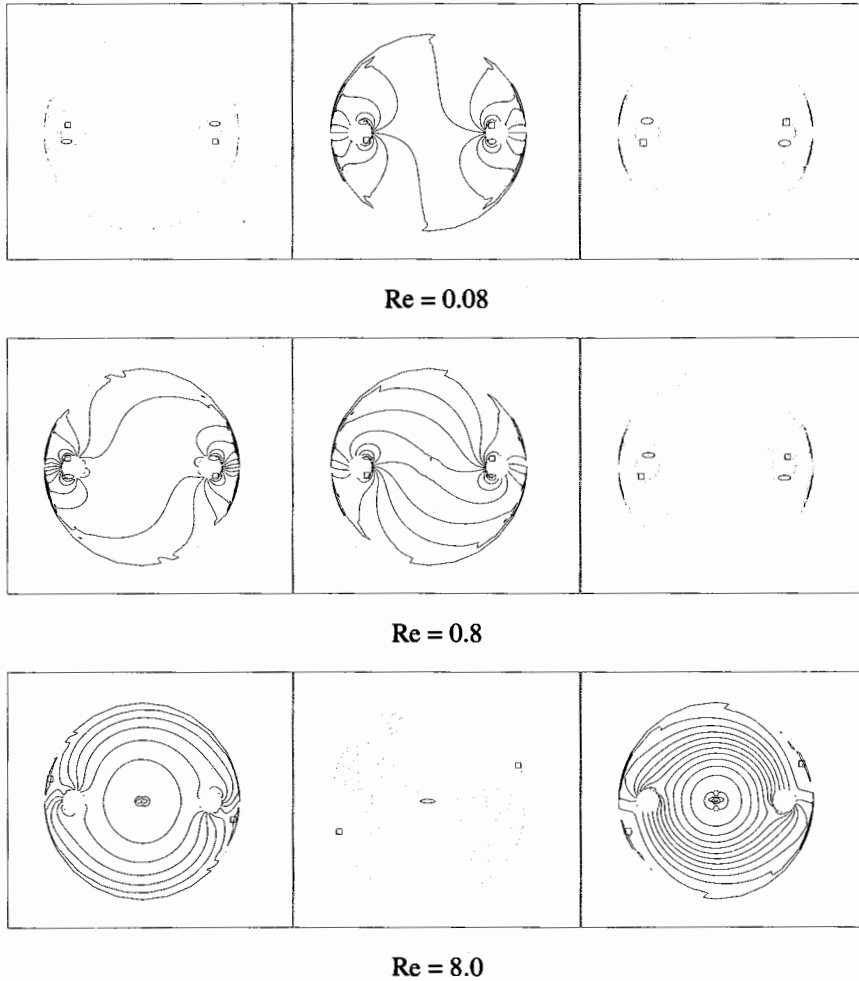


FIGURE 5. Pressure isobars for co-rotating stirrers with increasing speed of the stirrers ($v_\theta = 0.5, 1.0$ and 2.0) from left to right against the speed of the vessel and increasing Reynolds number.

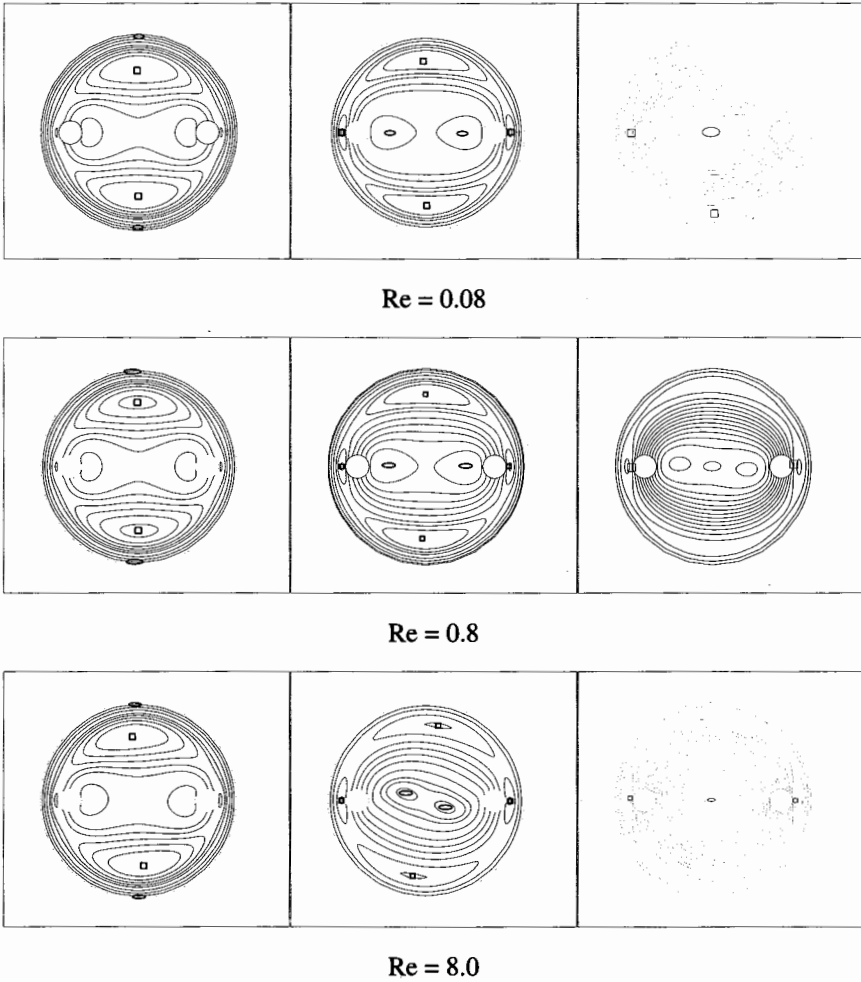


FIGURE 6. Streamline contours for contra-rotating stirrers with increasing speed of the stirrers ($v_\theta = 0.5, 1.0$ and 2.0) from left to right against the speed of the vessel and increasing Reynolds number.

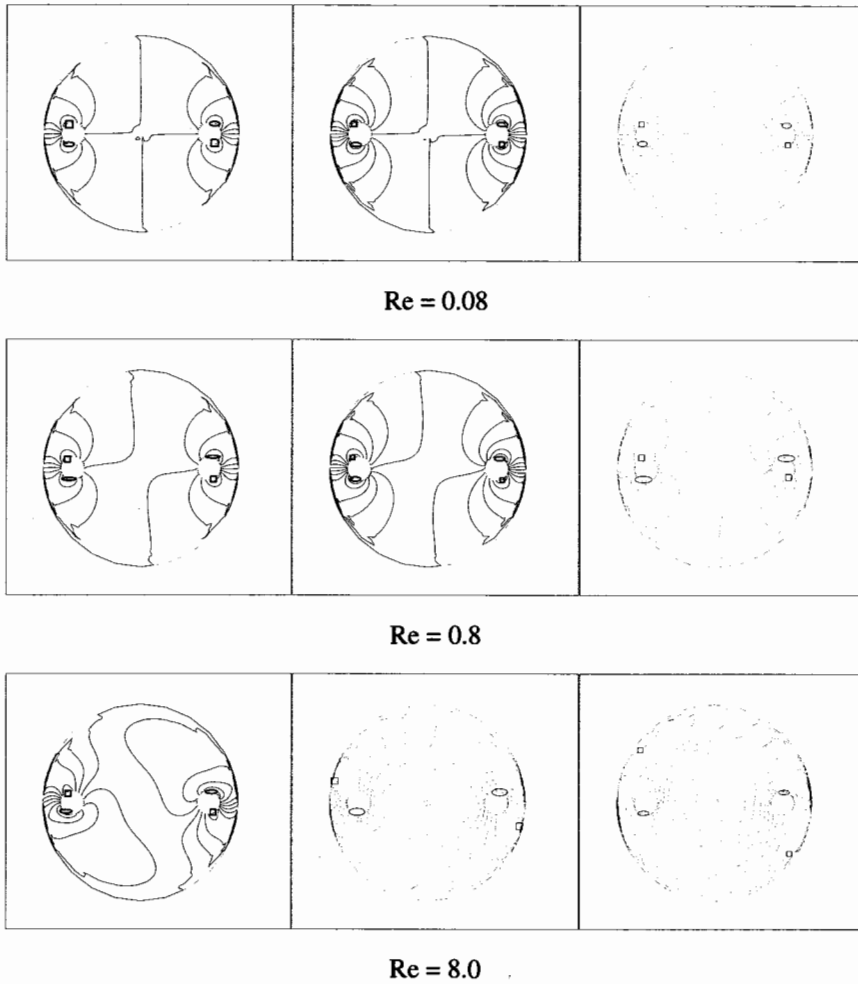


FIGURE 7. Pressure isobars for contra-rotating stirrers with increasing speed of the stirrers ($v_\theta = 0.5, 1.0$ and 2.0) from left to right against the speed of the vessel and increasing Reynolds number.

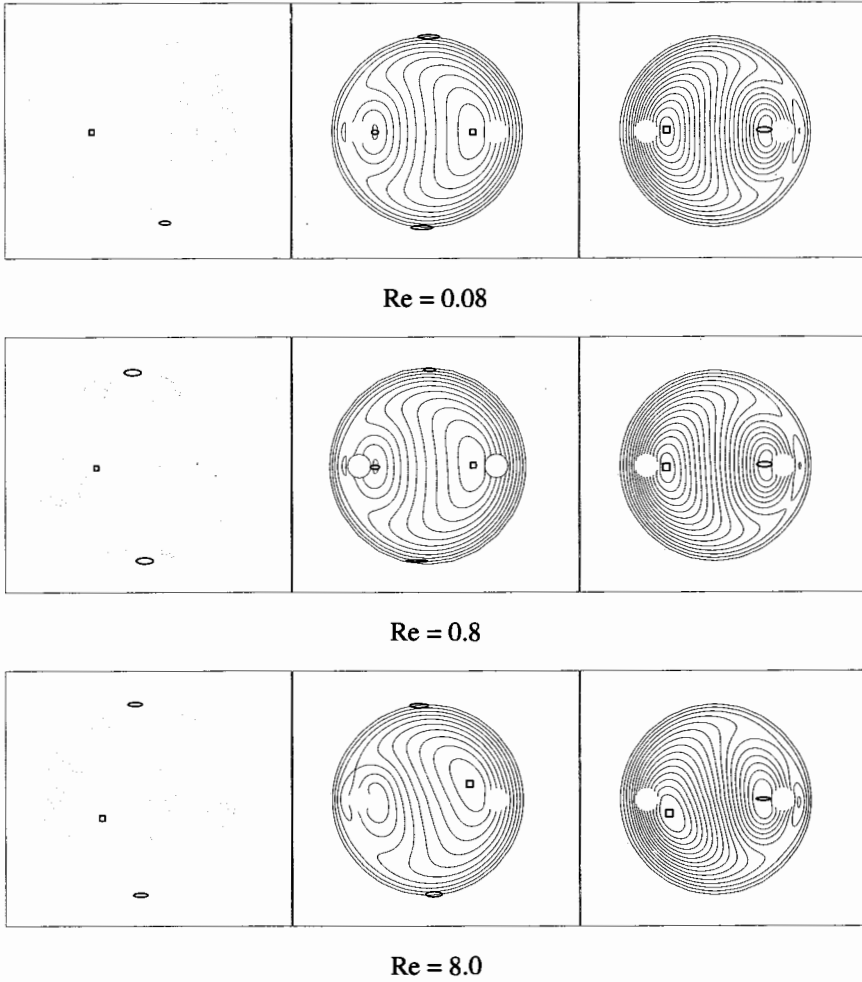


FIGURE 8. Streamline contours for Mix-rotating stirrers with increasing speed of the stirrers ($v_\theta = 0.5, 1.0$ and 2.0) from left to right against the speed of the vessel and increasing Reynolds number.

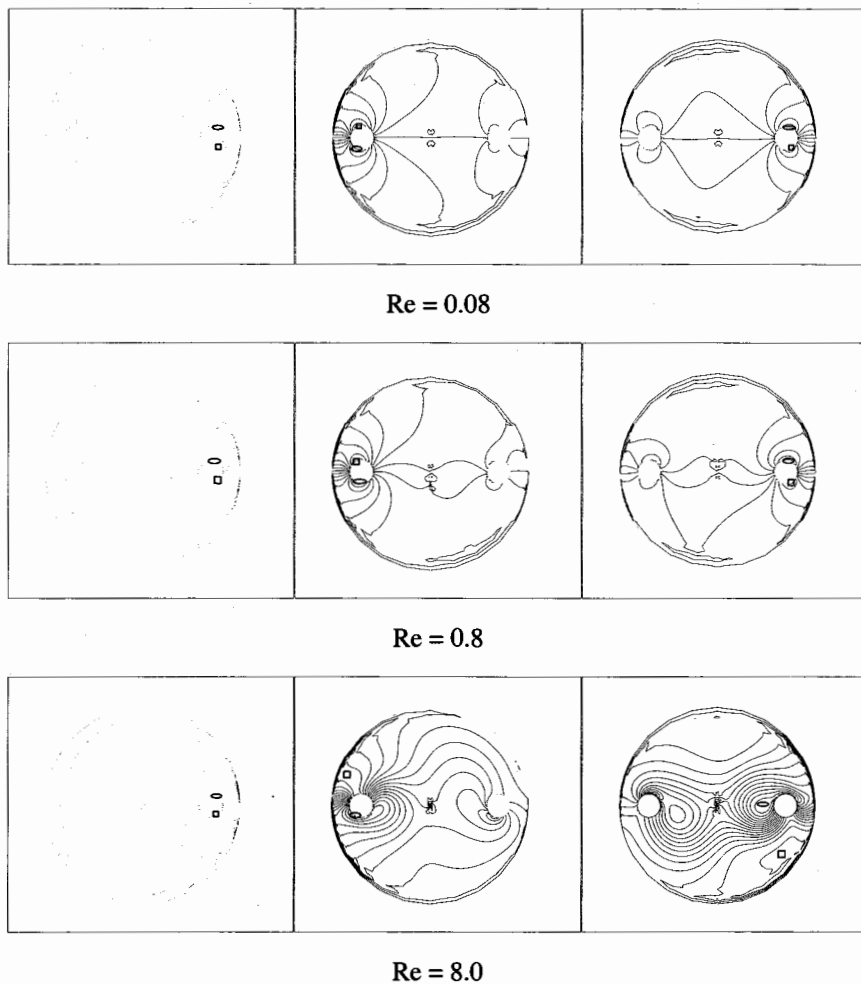


FIGURE 9. Pressure isobars for Mix-rotating stirrers with increasing speed of the stirrers ($v_\theta = 0.5, 1.0$ and 2.0) from left to right against the speed of the vessel and increasing Reynolds number.

Analysis of Stresses and Power Consumption of Mixing Flow in Cylindrical Container

R. A. Memon

Centre for Advance Studies in Pure and Applied Mathematics,
Bahauddin Zakria University,
Multan, Punjab, Pakistan.
Email: ra-memon1@yahoo.com

M. A. Solangi

Department of Basic Sciences and Related Studies,
Mehran University of Engineering and Technology,
Jamshoro, Sindh, Pakistan.
Email: manwarsolangi@yahoo.com

A. Baloch

Department of Basic Sciences and Related Studies,
Mehran University of Engineering and Technology,
Jamshoro, Sindh, Pakistan.
Email: csbaloch@yahoo.com

Abstract: This research article addresses the mixing flow of Newtonian fluid in a cylindrical vessel and investigates the rotational speeds and rotational directions of double stirrer cases on the predictions of the power consumption in the dissolution rotating vessel configured with fixed and rotating stirrers. The numerical simulations are sought for incompressible rotating mixing flows of Newtonian fluid. The context is one, relevant to the food industry, of mixing fluid within a cylindrical vessel, where stirrers are located on the lid of the vessel eccentrically. Here, the motion is considered as driven by the rotation of the outer vessel wall, with various rotational speeds of vessel and stirrers. A time-stepping finite element method is employed to predict the solutions. The numerical technique adopted is based on a semi-implicit TGPC scheme, posed in a two-dimensional cylindrical polar coordinate system. In mixer geometry, with respect to the velocity gradient, shear-rate, shear stress and power consumption are analysed.

AMS (MOS) Subject Classification Codes: 65N30, 65M60, 74S05, 68Q05, 76D05, 35Q30, 76U05

Key Words: Numerical Simulation, Finite Element Method, Rotational Mixing Flows, Newtonian Fluids, Double Stirrers, Co-rotation, Contra-rotation, Mix-rotation, Power Consumption.

1. INTRODUCTION

Mixing flows within the cylindrical vessel are investigated in this article, and is the extension of the previous work to achieve the solution of industrial challenging problems in mixing processing, the design of the mixer with rotational mixing in a stirred vessel to predict power consumption, generally industrial problems are challenging to deal with, particularly in the field of chemical process applications, such as mixing of dough in a food processing industry [1, 2, 3, 4, 5], granular mixing, powder mixing processes [6], mixing of paper pulp in paper industry and many other industrial processes. The present problem is one of these forms, expressed as the flow between an outer rotating cylindrical vessel and double stationary and rotating cylindrical stirrers rotate in three different rotational directions (co-rotating, contra-rotating and mix-rotating directions) and three different speeds (half, same and double) of the stirrers against the speed of the cylindrical vessel.

Stirrers are located on the mixing vessel lid. Under two-dimensional assumptions, the vessel essentially is considered to have infinite height. Elsewhere, the finite vessel problem in three-dimensions [6, 7] has been analysed. In two-dimension, similar problem is also investigated with different number and shapes of stirrers [8, 9, 10]. The motivation for this work is to advance fundamental technology in modelling of the dough kneading with the ultimate aim to predict the optimal design of dough mixers themselves, hence, leading to efficient dough processing.

The simulation procedure addresses the numerical solution of the two-dimension Navier-Stokes equations for incompressible flow in cylindrical frame of reference. This involves a so-called Taylor-Galerkin finite element formulation, which applies a temporal discretisation in a Taylor series prior to a Galerkin spatial discretisation. A semi-implicit treatment for diffusion is employed to address linear stability constraints. The flow is modelled as incompressible via a pressure-correction scheme [8, 9, 10, 11]. The present study adopts a semi-implicit Taylor-Galerkin/Pressure-Correction (TGPC) time-marching scheme, which has been developed and refined over the last couple of decades. This scheme, initially conceived in sequential form, is appropriate for the simulation of incompressible Newtonian flows [11].

The object is to comprehensively examine the influence of speed of stirrers and variation in inertia, assessing how this imposes upon the flow structure, rate-of-work done generated and power consumption. The corresponding applications of dough kneading are the target through build-up of the material structure, achieved by maximizing the local rate-of-work done per unit power. Computations are performed for Newtonian fluid.

In Section 2, the complete problem is specified and the governing equations and numerical scheme are described in Section 3. This is followed, in Section 4, by Simulation results for all cases are presented and our conclusions are drawn in Section 5.

2. PROBLEM SPECIFICATION

The two-dimensional mixing flows of Newtonian fluids are investigated, relevance to the food industry. In reality, within the industrial process, fluid is driven by the rotation of the lid of the vessel would rotate with stirrers attached. For simulations, the mixing is performed through the rotation of cylindrical-shaped vessel and the stirrers are held in place by being attached to the lid of the vessel. A fixed and rotating double stirrer in

an eccentric configuration is adopted. Initially, the problem is analysed for rotating flow between stationary stirrers and rotating cylindrical vessel, to validate the finite element predications in this cylindrical polar co-ordinate system to compare the numerical results against results obtained in previous investigations [8, 9]. Subsequently, different rotational directions with three setting options (co-rotation, contra-rotation and mix-rotation) of stirrers are also investigated against stationary stirrers in a rotating cylindrical vessel.

In this study, solution fields of interest are presented through contour plots of velocity gradients (∇u), shear-rate ($\dot{\gamma}$), shear-stress ($\tau_{r\theta}$), hoop and radial stress difference ($N_1 = \tau_{\theta\theta} - \tau_{rr}$) and power (P). Power may be equated to the spatial integral of the rate-of-work done where I_2 is the second invariant of rate-of-deformation tensor and w is rate of work done over total time t_n , v_r and v_θ are velocity components in radial 'r' and azimuthal ' θ ' direction respectively and ω is domain of interest in two dimensional polar coordinate.

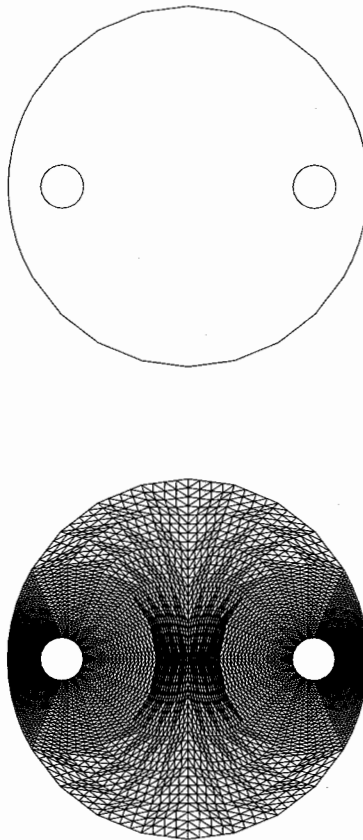


FIGURE 1. Computational domain and finite element mesh of eccentric rotating cylindrical flow, with double stationary and rotating stirrers.

Domain and finite element mesh for the problem involved is shown in figure-1. Total number of elements, nodes and degrees-of-freedom are 8960, 18223 and 40057 respectively. Details on mesh convergence, initial and boundary conditions reader is referred to our pervious investigations [7, 8, 9]. In this study, solution fields of interest are presented through contour plots of velocity gradients, shear-rate, shear-stress and power. Power may be equated to the spatial integral of the rate-of-work done [8, 9].

3. GOVERNING SYSTEM OF EQUATIONS AND NUMERICAL SCHEME

Two-dimensional incompressible rotational flows of isothermal Newtonian fluids can be modelled through the continuity and generalised momentum transport equations in a cylindrical polar coordinate system. In the absence of body forces, after applying appropriate scaling in each variable ($\mathbf{u} = V\mathbf{u}^*$, $p = V^2 p^*$, $t = R t^*/V$, where R and V are characteristic radius and velocity of vessel respectively and the time divided by the characteristic time) takes the form of the non-dimensional system of equations can be represented through the conservation of mass equation, as,

$$\nabla \cdot \mathbf{u} = 0, \quad (3.1)$$

the conservation of momentum transport equation, as,

$$\frac{\partial \mathbf{u}}{\partial t} = \frac{1}{Re} \nabla^2 \mathbf{u} - \mathbf{u} \cdot \nabla \mathbf{u} - \nabla p, \quad (3.2)$$

where, \mathbf{u} is the fluid velocity vector field, p is the isotropic fluid pressure (per unit density), \mathbf{d} is the rate of deformation tensor, t represents time and ∇ is the spatial differential operator. For Newtonian fluid case, μ_0 is the corresponding constant fluid viscosity at zero shear-rate. Relevant non-dimensional Reynolds number is

$$Re = \frac{\rho V R}{\mu_0} \quad (3.3)$$

The characteristic velocity V is taken to be the rotational speed of the vessel, the characteristic length scale is the radius, R , of a stirrer and is the fluid density. A detail on numerical algorithm, fully discrete system and definition of matrices is described and can be found in [8, 9, 11, 12].

4. NUMERICAL RESULTS AND DISCUSSIONS

The predicted solutions are analysed in two different directions: change in rotational direction (co-rotating, contra-rotating and mix-rotating) and speed of the stirrers. This leads to testing with respect to increasing viscosity levels for Newtonian fluid, comparison of contour plots of velocity gradient, shear-rate, shearstress and power consumption across problem instances. Contours are plotted from minimum value to maximum value,

over a range. Numerical solutions are also analysed through graph of work done over time interval and power consumption. Comparative diagnostics may be derived accordingly.

Various increasing levels of zero-shear viscosities μ_0 are considered, from which Reynolds numbers are computed, as defined above. For Reynolds numbers $Re = 8.0$, $Re = 0.8$ and $Re = 0.08$, the corresponding zero shear viscosities are $\mu_0 = 1.05 \text{ Pa s}$, $\mu_0 = 10.5 \text{ Pa s}$ and $\mu_0 = 105.0 \text{ Pa s}$, respectively. Of these levels, a range of material properties is covered from those for model fluids, to model dough, to actual dough, respectively. In this study there is no major difference found between model fluids and model dough so for $Re = 0.8$ not discussed for model dough, maximum attention has been given on model fluids and actual dough in this paper but results are given for model dough i.e., $Re = 0.8$ in tables.

4.1. Effects of increasing inertia on velocity gradient, shear-rate, shear stress and power consumption for stationary stirrers: For $Re = 0.08$ and $Re = 8$ computations are carried out to demonstrate the effect of increasing inertia upon velocity gradient, shear-rate, shear stress and power consumption. In figure–2, contour plots for stationary stirrers are presented. At a low level of inertia, $Re = 0.08$, contours of all variables demonstrate symmetric formations in the central region of the vessel, parallel to the stirrers and symmetrically intersecting the diameter that passes through the centres of the vessel and stirrers. Flow remains unaffected as Reynolds number rises to values of $O(1)$, i.e., $Re = 0.8$; hence this data has been suppressed. However, upon increasing Reynolds number up to eight, so $O(10)$, i.e., $Re = 8.0$; inertia takes hold and the contour region twist in the direction of rotation of the vessel and shifts towards the upper and lower-half plane, symmetry breakups in velocity gradient, shear-rate and shear stress and the material is pushed towards the vessel wall. The flow becomes asymmetric as a consequence of the shift in core of material upwards. The trend of rise in maxima and drop in minima is observed and the values are tabulated in Table–1.

Similar symmetry arguments apply across the geometry variants in all variables, at $Re = 0.08$, symmetric isobars for velocity gradient, shear-rate, shear stress and power consumption appear with unequal magnitude in non-dimensional positive extrema and negative minima on the two sides (upper and lower) of the stirrers in the narrow-gap. As inertia increases from $Re = 0.8$ to $Re = 8$, asymmetric contours are observed in all variables and across all instances, with positive maximum on the top of the stirrers and negative minimum at the outer stirrers tip (near the narrow-gap), see also Table–1. In non-dimensional terms above $Re = 0.08$ (noting scale differences), there is increase in velocity gradient, shear-rate and shear stress rise by as much as two percent in positive maxima, at $Re = 8.0$. However, in-contrast, the first stress difference decrease in same order approximately is observed. Whilst in power consumption and work-done which is about ten percent increase in maxima is observed with increasing inertia. The graph of work-done and power consumption is plotted in figure–3 against non-dimensional time step variants. Initially, work-done and power consumption is very high to drive the flow in the vessel. Subsequently, this high value for power consumption decreases gradually and reaches at some plateau for steady-state solution. Whilst, sum of work-done increase in same fashion up to steady-state.

4.2. Effects of increasing inertia on velocity gradient, shear-rate, shear stress and power consumption for co-rotating stirrers: Contours of all variables velocity gradient, shear-rate, shear stress and power consumption with increasing Reynolds number 0.08 to

TABLE 1. Various variables for stationary stirrers with Newtonian fluids ($\mu_0 = 105, 10.5$ and 1.05 Pas);

Variables	Re = 0.08		Re = 0.8		Re = 8.0	
	Minima	Maxima	Minima	Maxima	Minima	Maxima
Velocity gradient	-1.14461	-1.14461	-1.14293	4.46645	-1.15125	4.68969
Shear rate	0.00	4.4631	0.002	4.46645	0.00	4.68969
Shear stress	-1.03394	2.23155	-1.05805	2.23322	-1.33561	2.41851
Stress Difference	-6.03566	6.0248	-6.08941	5.98074	-6.90787	5.79796
Power	0	19.9192	0	19.9491	0	21.9932

8.0 and increasing rotational speed of the stirrers for half, same and double presents in figure -4, -6 and -8 respectively, in the same direction of the rotation of the vessel for co-rotating stirrers.

As inertia increase from $Re = 0.08$ to $Re = 8$, asymmetric contours are observed, with positive maxima on the top of the both stirrers and negative minima at the outer stirrers tip, numerical results are shown in the Table-2. In the narrow gap, where stirrers rotates in the same direction of the vessel rotation, small values in minima and maxima appear for all variable instances and these values further decrease as the speed of stirrers decrease at low value of $Re = 0.08$. The increase in minima and maxima is observed and strengthen approximately from double to four times with increase in inertia at $Re = 8.0$.

For all instances, comparable equilibrium influence apply across the geometry variants in minima and maxima of velocity gradient, shear-rate and shear-stress, at $Re = 0.08$ and double rotational speed of stirrers, symmetric contours appear with equal magnitude in non-dimensional positive and negative extrema on both sides (upper and lower) of both stirrers in the narrow-gap as shown in figure-8.

The associated values of all variables are tabulated in Table-2 with increasing the speed of stirrers against the speed of vessel from half to double. As speed of stirrers increase, increase in the minima and maxima are noted for all cases at both inertial values. The velocity gradients are somewhat symmetrical in geometry at maxima and minima at twice the speed of stirrers and at half the speed of stirrers for both inertial values $Re = 0.08$ and $Re = 0.8$. However, upon increasing Reynolds number up to eight, thus $O(10)$, inertia takes hold the tabulated variables are observed asymmetrical and the maxima and minima are also increase. Increasing the speed of the stirrers to double increases the power consumption remains same in minima and in contrast it increase up to twenty five percent in positive maxima.

In figure-5, -7 and -9, the graph of work-done and power consumption is shown against non-dimensional time step variants. Initially, work-done and power consumption is very high to drive the flow in the vessel. Subsequently, this high value for power consumption decreases fastely at a stage and reaches at some plateau for steady-state solution for co-rotating stirrers at the half and same speed but for double speed this passion is changed and decreases gradually. Whilst, work-done increase in same fashion up to steady-state.

TABLE 2. Various variables for co-rotating stirrers with Newtonian fluids ($\mu_0 = 105, 10.5$ and 1.05 Pas);

Variables	Speed	Re = 0.08		Re = 0.8		Re = 8.0	
		Minima	Maxima	Minima	Maxima	Minima	Maxima
Velocity gradient	Half	-0.11208	2.00842	-0.13028	2.01165	-0.28207	2.18178
	Same	-0.45398	1.69145	-0.45478	1.68572	-0.53672	1.9848
	Double	-5.37553	4.54706	-5.41958	4.57853	-7.24099	6.49085
Shear rate	Half	0.00083	1.87109	1.87432	1.87432	0.00173	4.34502
	Same	0.00051	1.30313	1.29741	1.29741	0.00142	9.89532
	Double	0.02125	5.92486	5.96891	5.96891	0.00394	33.1876
Shear stress	Half	-0.39279	1.00421	-0.4102	1.00583	-0.5839	1.79271
	Same	-0.44277	0.84572	-0.5126	0.84286	-1.1181	0.94252
	Double	-2.68777	2.27353	-3.1924	2.28926	-7.473	4.65567
Stress difference	Half	-2.69669	2.6867	-2.74653	2.64657	-3.5136	2.44376
	Same	-2.12539	2.45995	-1.96852	2.3089	-1.3368	3.62055
	Double	-7.31813	7.38789	-7.07431	7.85733	-5.74278	16.7961
Power	Half	0	3.50097	0	3.51308	0	4.17976
	Same	0	1.69814	0	1.70324	0	2.24019
	Double	0	35.104	0	35.6279	0	35.6742

4.3. Effects of increasing inertia on velocity gradient, shear-rate, shear stress and power consumption for contra-rotating stirrers: Increasing Reynolds number from $Re = 0.08$ to $Re = 8.0$ for contra-rotating double stirrers, equivalent field kinematic data in all variables is presented in figure–10 for half speed, figure–12 for same speed and figure–14 for double speed of the stirrers against the speed of the vessel, to make direct comparisons across all occurrences for Newtonian fluids, with particular reference to localised velocity gradient, shear-rate, shear stress and power consumption.

Isobars are shown for increasing speed of the stirrers from half speed to double speed display symmetry patterns at low inertial value $Re = 0.08$ and asymmetric configuration at higher value of inertia $Re = 8.0$ is shaped. In compare to the stationary stirrer case where formation of Newtonian stresses and other parameters are symmetric for all instances and at the same parameters asymmetric formation is observed, see figures–10, –12 and –14. At $Re = 0.08$, when increases the speed of stirrers for half, same and double respectively, no symmetry break-up is observed but at $Re = 8$, introducing the motion of stirrers from half speed to double speed of the stirrers effective changes has been observed in the stresses and other variables.

The graph illustrates the work-done over time interval and power consumption at all comparable parameter values for contra-rotating instances in figure–11, 13 and 15 for half

speed, same speed and double speed of stirrers respectively. The behaviour for all instances is same, however, for both Reynolds numbers the comparable values are much higher and is almost ten times from half speed to double speed of the stirrers.

The tabulated values are in Table-3, minima and maxima for various variables. For velocity gradient, shear-rate, shear-stress and first stress difference between azimuthal and radial stresses, increase in the speed of stirrers from half to double, increase in the minima is observed. At low inertial value, $Re = 0.08$, this increase is almost double, however, at higher value of inertial, $Re = 8$, is approximately double to four times increase is noted. Whilst for power consumption is about five times approximately.

TABLE 3. Various variables for contra-rotating stirrers with Newtonian fluids ($\mu_0 = 105, 10.5$ and 1.05 Pas);

Variable	Speed	Re=0.08		Re=0.8		Re=8.0	
		Minima	Maxima	Minima	Maxima	Minima	Maxima
Velocity gradient	Half	-2.58992	6.92803	-2.58798	6.92932	-2.43719	7.02753
	Same	-4.01149	9.38669	-4.01449	9.38694	-5.59621	9.5513
	Double	-6.8582	14.306	-6.90486	14.3229	-11.4476	16.8857
Shear rate	Half	0.00089	7.06537	0.00218	7.06665	0.00806	7.16486
	Same	0.00514	9.66136	0.00502	9.66161	0.00408	6.82598
	Double	0.01690	14.8553	0.011238	14.8423	0.00481	22.4677
Shear stress	Half	-1.67833	3.46402	-1.68435	3.46468	-1.74401	3.51377
	Same	-2.3286	4.69335	-2.40102	4.69347	-3.21727	8.90697
	Double	-3.64196	7.153	-3.96812	7.16147	-8.93301	20.743
Stress difference	Half	-9.38309	9.38414	-9.38008	9.39063	-9.46162	9.56863
	Same	-2.7151	12.741	-12.6002	2.8584	-11.7256	15.1497
	Double	-19.3628	19.4766	-8.8845	20.0245	-16.9897	36.4228
Power	Half	0	49.9194	0	49.9376	0	51.3353
	Same	0	93.3419	0	93.3466	0	96.5495
	Double	0	220.681	0	221.184	0	289.588

4.4. Effects of increasing inertia on velocity gradient, shear-rate, shear stress and power consumption for mix-rotating stirrers: For mix-rotating stirrers, the field kinematics data with increasing Reynolds number from 0.08 to 8.0 with particular reference to localised velocity gradient, shear-rate, shear stress and power consumption are shown in figure -16, -18 and -20 for half, same and double speed of stirrers respectively to make direct comparisons across all instances for Newtonian fluids. For this case, interested phenomena arise. In the case of half speed at low inertial value $Re = 0.08$, isobars are noted in around of the stirrer rotate in same direction of vessel and in right and left of the stirrer rotate in opposite direction of vessel with symmetric pattern in upper and lower region of vessel. When inertia increase upto $Re = 8.0$ isobars twist towards the upper region in the direction of rotation of the vessel. Whenever, situation examines vice-versa in the case of same speed of the stirrers.

Isobars are shown for double speed of the stirrers demonstrates symmetry patterns at low value of Reynolds number $Re = 0.08$ is formed in upper and lower region of the vessel.

TABLE 4. Various variables for mix-rotating stirrers with Newtonian fluids ($\mu_0 = 105, 10.5$ and 1.05 Pas);

Variable	Speed	Re=0.08		Re=0.8		Re=8.0	
		Minima	Maxima	Minima	Maxima	Minima	Maxima
Velocity gradient	Half	-0.11208	2.00842	-0.13028	2.01165	-0.28207	2.18178
	Same	-0.45398	1.69145	-0.45478	1.68572	-0.53672	1.9848
	Double	-5.37553	4.54706	-5.41958	4.57853	-7.24099	6.49085
Shear rate	Half	0.004395	4.70657	0.004183	7.41495	0.00363	8.02225
	Same	0.003052	10.3516	0.002647	10.368	0.00142	11.6491
	Double	0.026373	16.2418	0.026461	14.2848	0.02993	21.8123
Shear stress	Half	-2.04905	3.63462	-2.04643	3.63881	-2.11429	3.94246
	Same	-4.05551	5.03848	-4.05503	5.04669	-5.24735	5.68721
	Double	-8.46209	8.15661	-8.48911	8.19283	-21.4674	10.9102
Stress difference	Half	-9.87923	9.8799	-9.88829	9.89485	-10.742	10.7666
	Same	-3.6366	13.6632	-13.5415	13.807	-14.1731	18.239
	Double	-2.3713	21.4936	-20.8918	22.1177	-20.7601	45.2794
Power	Half	0	54.8573	0	54.9815	0	64.3564
	Same	0	107.156	0	107.496	0	135.701
	Double	0	263.796	0	265.196	0	405.861

In contrast to the half and same speed of mix-rotating stirrers case where formation of Newtonian stresses and other parameters are symmetric for all instances, see figures – 20. At $Re = 0.08$ and for double speed of stirrers, no symmetry break-up is observed. However, at $Re = 8$, effective has been observed in the stresses and other variables and isobars twist towards the upper and lower region in the rotational direction of the vessel.

In figure –17, –19 and 21, for mix-rotating instances, graphs illustrate the work-done over time interval and power consumption at all comparable parameter values. The behaviour for all instances is same, however, for both Reynolds numbers the comparable values are much higher and is almost ten times from half speed to double speed of the stirrers.

Minima and maxima for velocity gradient, shear-rate, shear-stress, first stress difference and power consumption are tabulated in the Table4, increase in the speed of stirrers from half to double, increase in the minima is observed. At low inertial value, $Re = 0.08$, this increase is almost double, however, at higher value of inertial, $Re = 8$, is approximately three times. Whilst for is about eight times.

5. CONCLUSIONS

The use of a numerical flow simulator as a prediction tool for this industrial flow problem has been successfully demonstrated. For this complex mixing process, using Newtonian fluid, physically realistic simulations have been provided.

Addressing the rotation of the double stirrer case with stationary stirrers against the three cases of rotating stirrers in co-rotating, contra-rotating and mix-rotating directions are investigated with increasing inertia form $Re = 0.08$ to $Re = 8.0$. For stationary stirrers case, it is clearly demonstrated contours of all variables demonstrate symmetric formations in

the central region of the vessel, parallel to the stirrers at $Re = 0.08$ and asymmetric when inertia reaches at $Re = 8.0$ and material moves in the direction vessel rotation.

The associated values of all variables for the case of co-rotating stirrers as speed of stirrers increase, increase in the minima and maxima are noted for all cases at both inertial values. The velocity gradients are somewhat symmetrical in geometry at maxima and minima at twice the speed of stirrers and at half the speed of stirrers for both inertial values variables are observed asymmetrical and the maxima and minima are also increase. Increasing the speed of the stirrers to double increases the power consumption remains same in minima.

In the case of contra-rotating Isobars are shown for half speed to double speed display symmetry patterns at low inertial value and asymmetric configuration at higher value of inertia. When increases the speed of stirrers from half to double, no symmetry break-up is observed but at higher inertia, introducing the motion of stirrers from half speed to double speed of the stirrers effective changes has been observed in the stresses and other variables.

Minima and maxima for velocity gradient, shear-rate, shear-stress, first stress difference and power consumption in the case of mix-rotating stirrers, increase in the speed of stirrers from half to double, increase in the minima is observed. At low inertial value, $Re = 0.08$, this increase is almost double, however, at higher value of inertial, $Re = 8$, is approximately three times.

Through the predictive capability generated, we shall be able to relate this to mixer design that will ultimately impact upon the processing of dough products. Promising future directions of this work are investigation of rotation of two stirrers case in co-rotating, contra-rotating and mix-rotating directions, changing material properties using non-Newtonian fluids and further introducing agitator in concentric configured stirrers in future.

Acknowledgement

The authors are greatly acknowledged to the Mehran University of Engineering and Technology, Jamshoro, for providing computational facility and financial grant of Higher Education Commission of Pakistan.

REFERENCES

- [1] K. S. Sujatha, M. F. Webster, D. M. Binding, M. A. Couch, *Modelling and experimental studies of rotating flows in part-filled vessels: wetting and peeling*, *J. Foods Eng.*, **57**, (2002), 67–79.
- [2] D. M. Binding, M. A. Couch, K. S. Sujatha, M. F. Webster, *Experimental and numerical simulation of dough kneading in filled geometries*, *J. Foods Eng.*, **57**, (2002) 1–13.
- [3] K. S. Sujatha,, D. Ding, M. F. Webster, *Modelling three-dimensions mixing flows in cylindrical-shaped vessels*, in: *ECCOMAS CFD - 2001, Swansea, UK*, (2001) 1–10.
- [4] K. S. Sujatha,, D. Ding, M. F. Webster, *Modelling of free surface in two and three dimensions*, in: *C. A. Brebbia, B. Sarlen (Eds.), Sixth International Conference on Computational Modelling of Free and Moving Boundary Problems - 2001, WIT, Lemnos, Greece*, (2001) 102–111.
- [5] D. Ding, M. F. Webster, *Three-dimensional numerical simulation of dough kneading*, in: *D. Binding, N. Hudson, J. Mewis, J.-M. Piau, C. Petrie, P. Townsend, M. Wagner, K. Walters (Eds.), XIII Int. Cong. on Rheol., Vol. 2, British Society of Rheology, Cambridge, UK*, (2000) 318–320.
- [6] N. Phan-Thien, M. Newberry and R. I. Tanner, *Non-linear oscillatory flow of a solid-like viscoelastic material*, *J. Non-Newtonian Fluid Mech.*, **92**, (2000) 67–80.
- [7] P. M. Portillo, F. J. Muzzio and M. G. Ierapetritou, *Hybrid DEM-Compartment Modelling Approach for Granular Mixing*, *AIChE Journal*, **53**(1), (2007) 119–128.

- [8] A. Baloch, P. W. Grant and M. F. Webster, M. F., *Parallel Computation of Two-Dimensional Rotational Flows of the Viscoelastic Fluids in Cylindrical Vessel*, *Int. J. Comp. Aided Eng. and Software, Eng. Comput.*, **19(7)**, (2002) 820–853.
- [9] A. Baloch, G. Q. Memon, and M. A. Solangi, *Simulation of Rotational Flows in Cylindrical Vessel with Rotating Single Stirrer*, *Punjab University Journal of Mathematics*, **40**, (2008) 83–96.
- [10] A. Baloch, and M. F. Webster, M. F., *Distributed Parallel Computation for Complex Rotating Flows of Non-Newtonian Fluids*, *Int. J. Numer. Meth. Fluids*, **43**, (2003) 1301–1328.
- [11] P. Townsend and M. F. Webster, *An algorithm for the three-dimensional transient simulation of non-Newtonian fluid flows*, in: G. Pande, J. Middleton (Eds.), *Proc. Int. Conf. Num. Meth. Eng.: Theory and Applications*, NUMETA, Nijhoff, Dordrecht, **T12** (1987) 1–11.
- [12] D. M. Hawken, H. R. Tamaddon-Jahromi, P. Townsend, M. F. Webster, *A Taylor-Galerkin-based algorithm for viscous incompressible flow*, *Int. J. Num. Meth. Fluids*, **10**, (1990) 327–351.

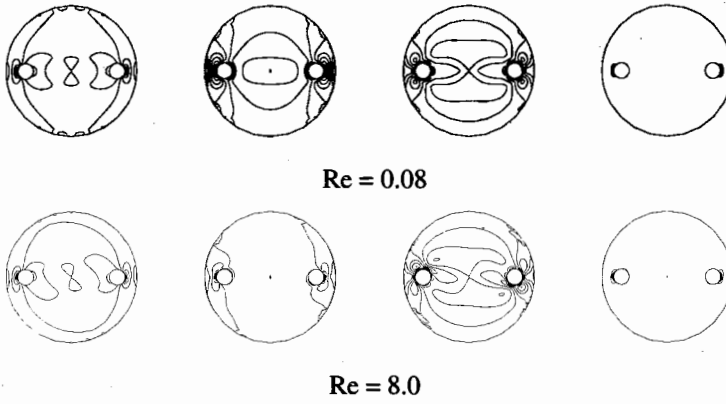


FIGURE 2. Contour plots of Velocity gradient, Shear-rate, Shear stress and Power for stationary stirrers for Newtonian fluid with increasing Reynolds number.

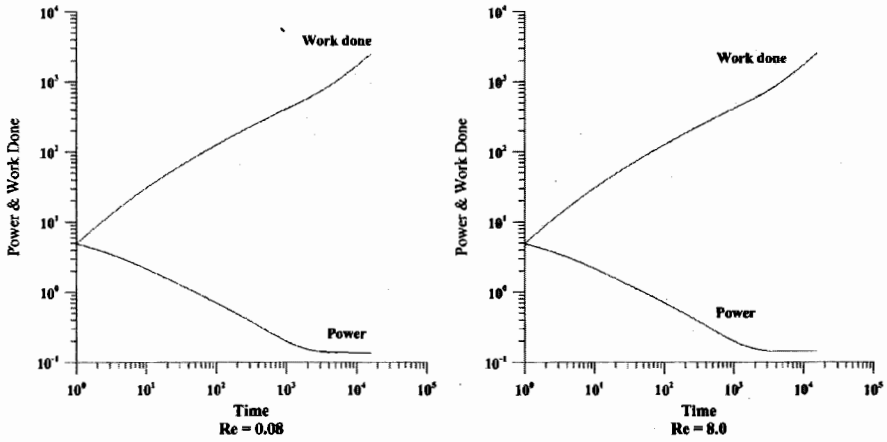


FIGURE 3. Graphs of power and work done for stationary stirrers for Newtonian fluid with increasing Reynolds number.

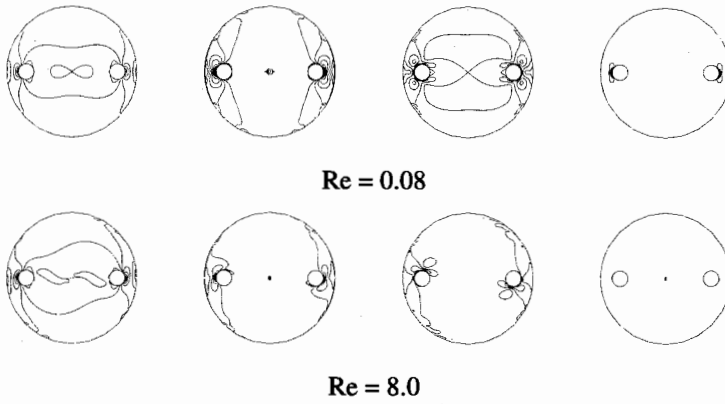


FIGURE 4. Contour plots of Velocity gradient, Shear-rate, Shear stress and Power for co-rotating stirrers with half speed for Newtonian fluid with increasing Reynolds number.

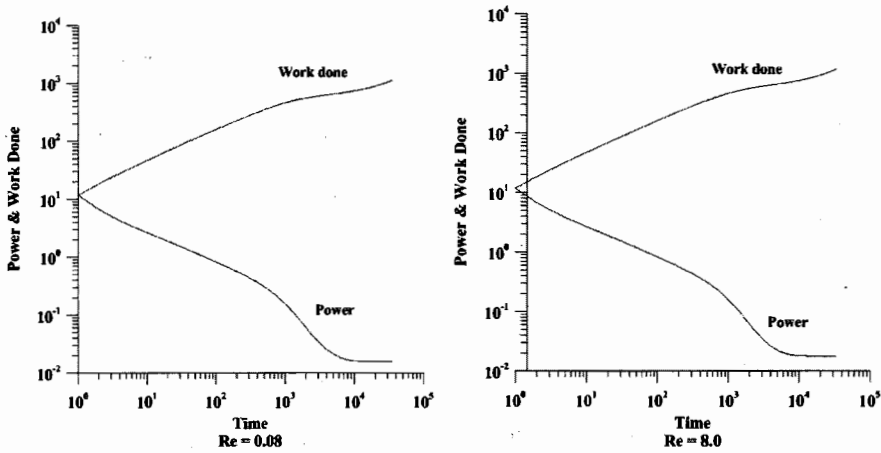


FIGURE 5. Graphs of power and work done for co-rotating stirrers with half speed for Newtonian fluid with increasing Reynolds number.

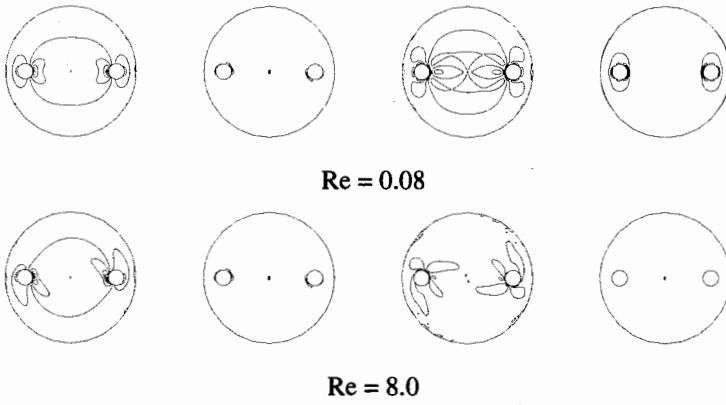


FIGURE 6. Contour plots of Velocity gradient, Shear-rate, Shear stress and Power for co-rotating stirrers with same speed for Newtonian fluid with increasing Reynolds number.

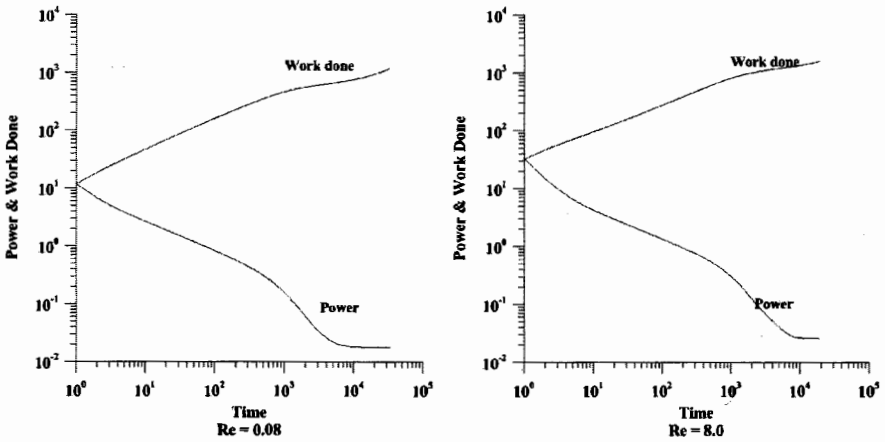


FIGURE 7. Graphs of power and work done for co-rotating stirrers with same speed for Newtonian fluid with increasing Reynolds number.

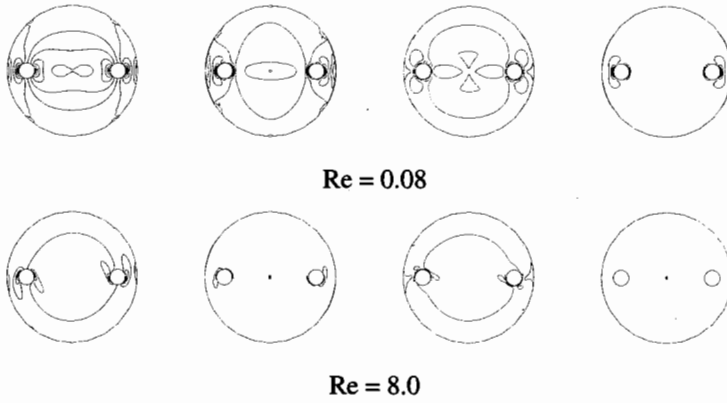


FIGURE 8. Contour plots of Velocity gradient, Shear-rate, Shear stress and Power for co-rotating stirrers with double speed for Newtonian fluid with increasing Reynolds number.

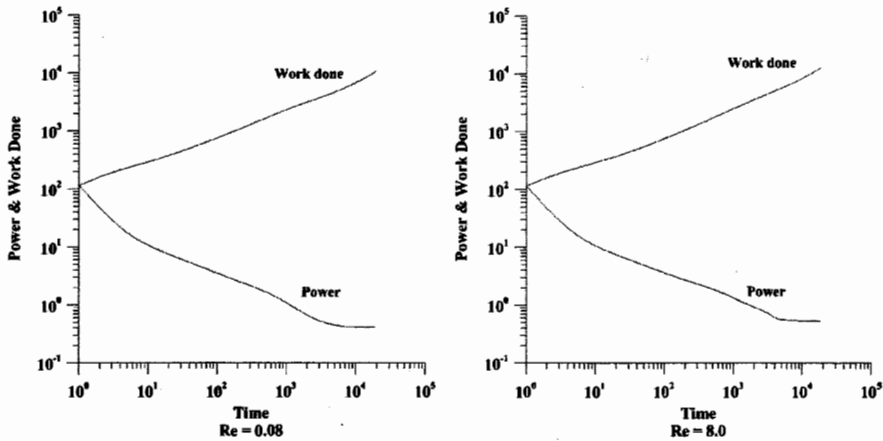


FIGURE 9. Graphs of power and work done for co-rotating stirrers with double speed for Newtonian fluid with increasing Reynolds number.

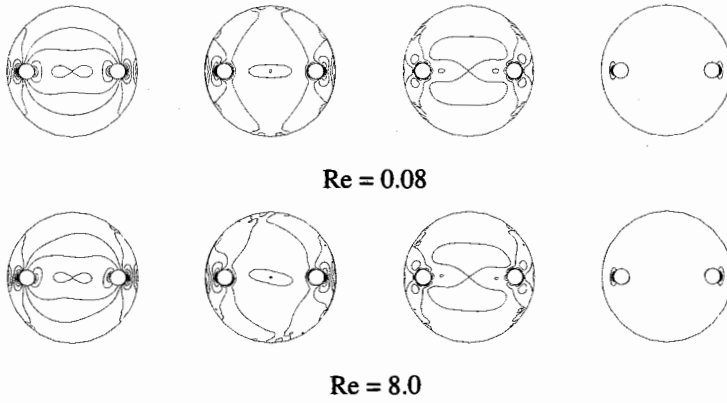


FIGURE 10. Contour plots of Velocity gradient, Shear-rate, Shear stress and Power for contra-rotating stirrers with half speed for Newtonian fluid with increasing Reynolds number.

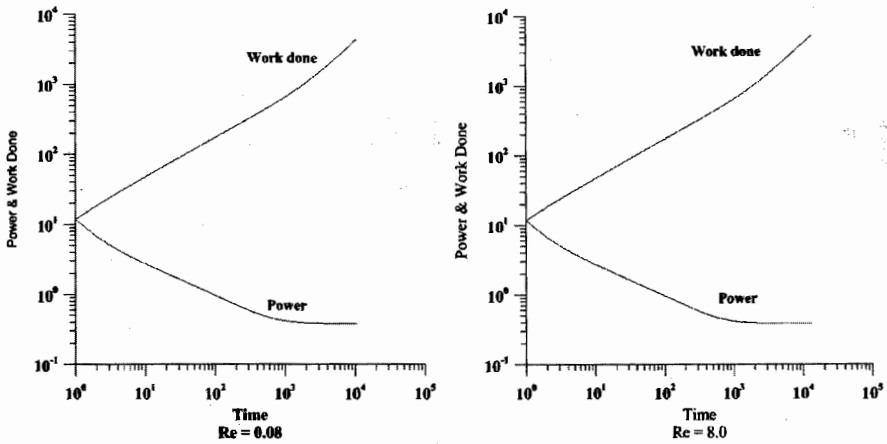


FIGURE 11. Graphs of power and work done for contra-rotating stirrers with half speed for Newtonian fluid with increasing Reynolds number.

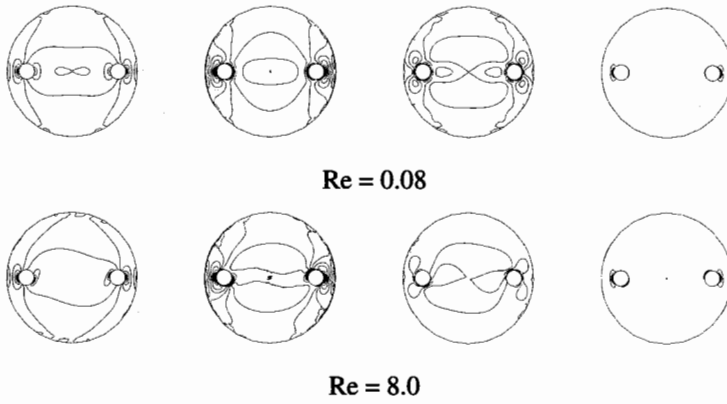


FIGURE 12. Contour plots of Velocity gradient, Shear-rate, Shear stress and Power for contra-rotating stirrers with same speed for Newtonian fluid with increasing Reynolds number.

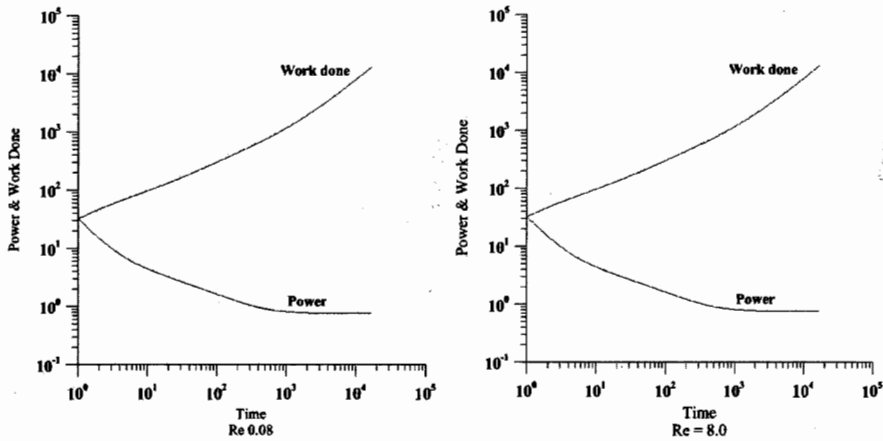


FIGURE 13. Graphs of power and work done for contra-rotating stirrers with same speed for Newtonian fluid with increasing Reynolds number.

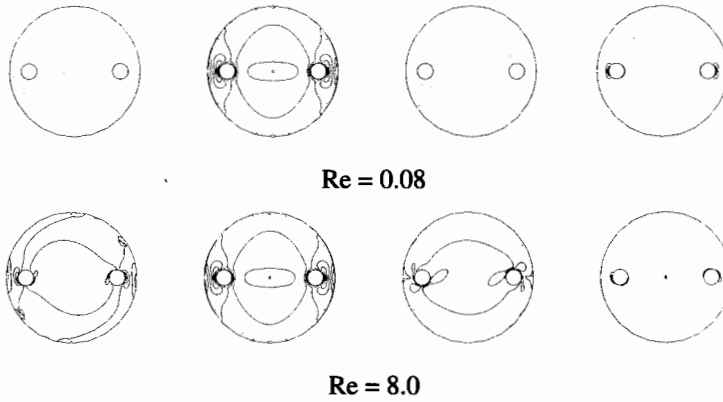


FIGURE 14. Contour plots of Velocity gradient, Shear-rate, Shear stress and Power for contra-rotating stirrers with double speed for Newtonian fluid with increasing Reynolds number.

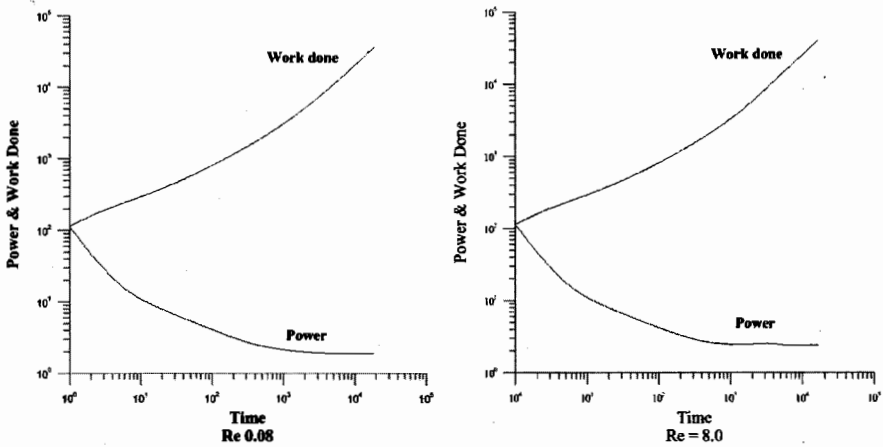


FIGURE 15. Graphs of power and work done for contra-rotating stirrers with double speed for Newtonian fluid with increasing Reynolds number.

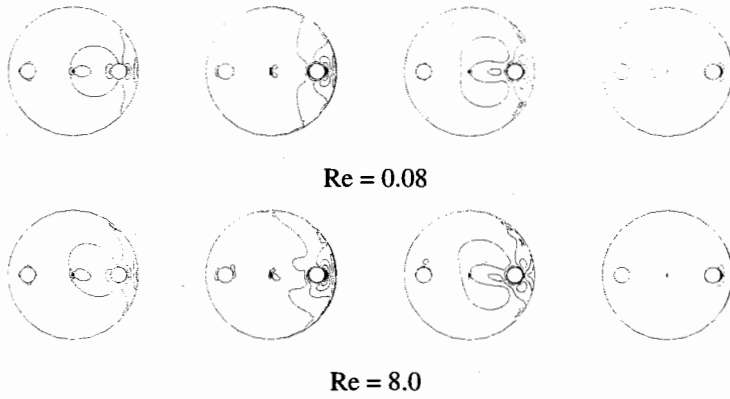


FIGURE 16. Contour plots of Velocity gradient, Shear-rate, Shear stress and Power for mix-rotating stirrers with half speed for Newtonian fluid with increasing Reynolds number.

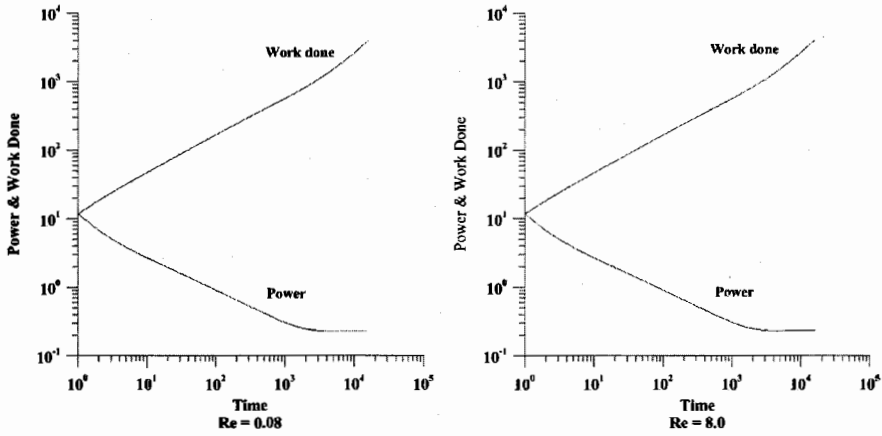


FIGURE 17. Graphs of power and work done for mix-rotating stirrers with half speed for Newtonian fluid with increasing Reynolds number.

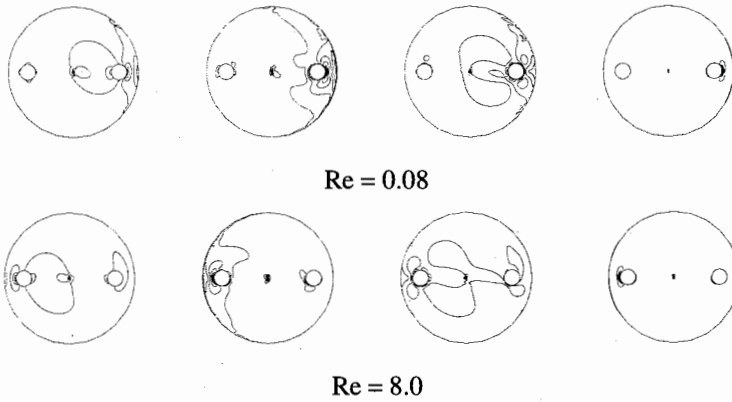


FIGURE 18. Contour plots of Velocity gradient, Shear-rate, Shear stress and Power for mix-rotating stirrers with same speed for Newtonian fluid with increasing Reynolds number.

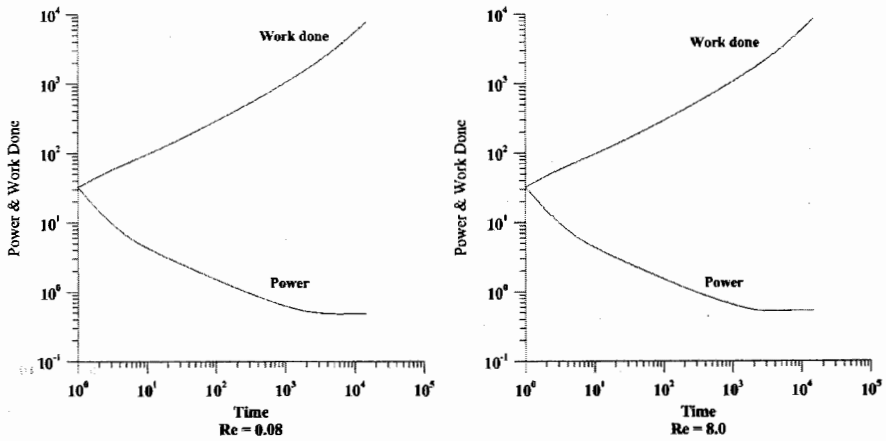


FIGURE 19. Graphs of power and work done for mix-rotating stirrers with same speed for Newtonian fluid with increasing Reynolds number.

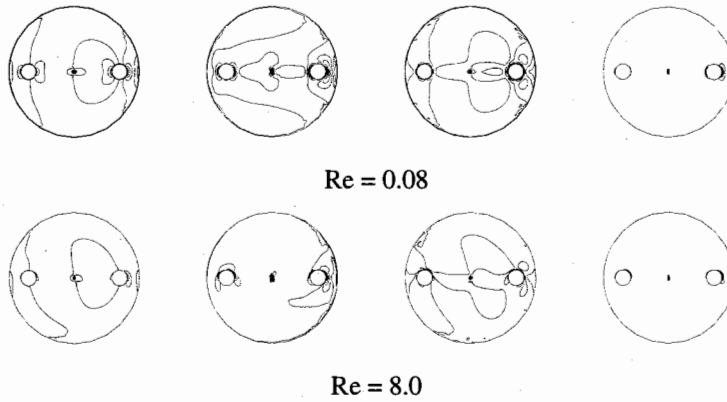


FIGURE 20. Contour plots of Velocity gradient, Shear-rate, Shear stress and Power for mix-rotating stirrers with double speed for Newtonian fluid with increasing Reynolds number.

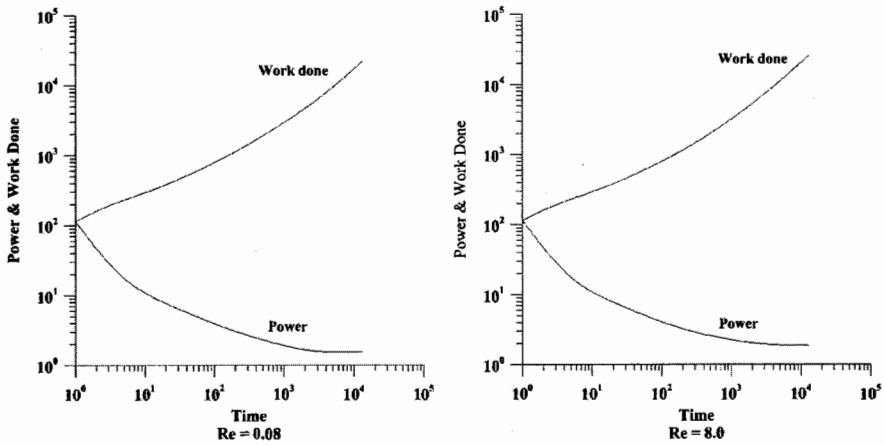
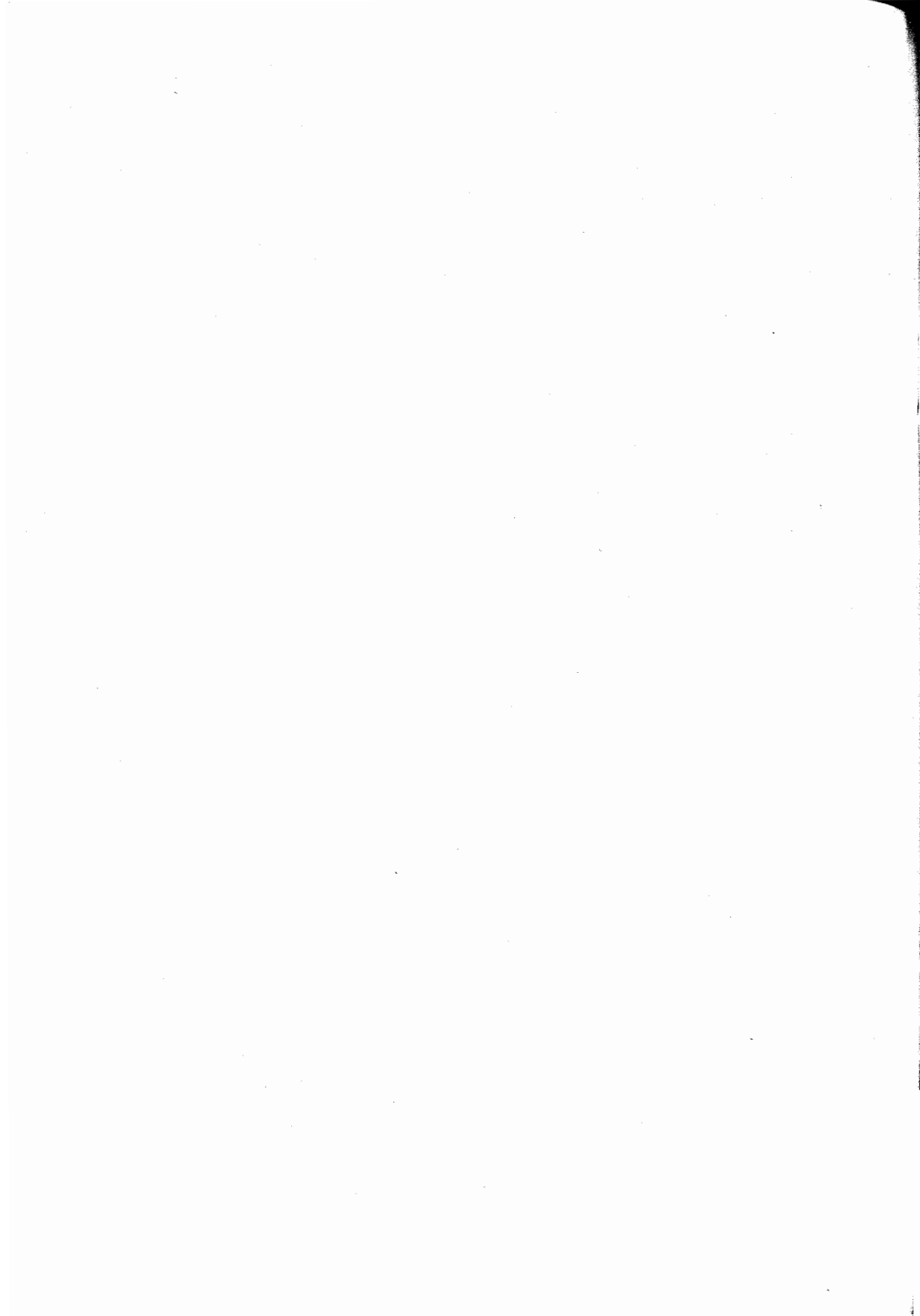


FIGURE 21. Graphs of power and work done for mix-rotating stirrers with double speed for Newtonian fluid with increasing Reynolds number.



Convolution of Salagean-type Harmonic Univalent Functions

Saurabh Porwal

Department of Mathematics

U.I.E.T. Campus, C.S.J.M. University, Kanpur-208024 (U.P.), India

E-mail: saurabhjcb@rediffmail.com

K.K. Dixit

Department of Engineering Mathematics

Gwalior Institute of Information Technology, Airport Road, Maharajpura,

Gwalior-474015 (M.P.), India

Email: kk.dixit@rediffmail.com

S.B. Joshi

Department of Mathematics

Walchand College of Engineering

Sangli-416415, Maharashtra, India

Email: joshisb@hotmail.com

Abstract. A recent result of Yalcin [9] appeared in Applied Mathematics Letters (2005), concerning the convolution of two harmonic univalent functions in class $\bar{S}_H(m, n, \alpha)$ is improved.

AMS (MOS) Subject Classification Codes: 30C45

Key Words: Harmonic, Univalent, Salagean derivative, Convolution.

1. INTRODUCTION

A continuous complex-valued function $f = u + iv$ defined in a simply connected complex domain D is said to be harmonic in D if both u and v are real harmonic in D . In any simply connected domain we can write $f = h + \bar{g}$, where h and g are analytic in D . We call h the analytic part and g the co-analytic part of f . A necessary and sufficient condition for f to be locally univalent and sense-preserving in D is that $|h'(z)| > |g'(z)|$, $z \in D$. See Clunie and Sheil-Small [2], for more basic results on harmonic functions one may refer to the following standard introductory text book Duren [3], see also Ahuja [1] and Ponnusamy and Rasila ([6], [7]). Denote by S_H the class of functions $f = h + \bar{g}$ that are harmonic univalent and sense-preserving in the unit disc $U = \{z : |z| < 1\}$ for which $f(0) = f_z(0) - 1 = 0$. Then for $f = h + \bar{g} \in S_H$ we may express the analytic functions h and g as

$$h(z) = z + \sum_{k=2}^{\infty} a_k z^k, \quad g(z) = \sum_{k=1}^{\infty} b_k z^k, \quad |b_1| < 1. \quad (1.1)$$

The differential operator D^m was introduced by Salagean [8]. For $f = h + \bar{g}$ given by (1.1), Jahangiri et al. [4] defined the modified Salagean operator of f as

$$D^m f(z) = D^m h(z) + (-1)^m \overline{D^m g(z)} \quad (1.2)$$

where

$$D^m h(z) = z + \sum_{k=2}^{\infty} k^m a_k z^k \text{ and } D^m g(z) = \sum_{k=1}^{\infty} k^m b_k z^k.$$

For $0 \leq \alpha < 1$, $m \in N$, $n \in N_0$, $m > n$ and $z \in U$, suppose $S_H(m, n, \alpha)$ denote the family of harmonic functions f of the form (1.1) such that

$$\operatorname{Re} \left\{ \frac{D^m f(z)}{D^n f(z)} \right\} > \alpha \quad (1.3)$$

where $D^m f$ is defined by (1.2).

Further, let the subclass $\bar{S}_H(m, n, \alpha)$ consist of harmonic functions $f_m = h + \bar{g}_m$ in $\bar{S}_H(m, n, \alpha)$ so that h and g_m are of the form

$$h(z) = z - \sum_{k=2}^{\infty} a_k z^k, \quad g_m(z) = (-1)^{m-1} \sum_{k=1}^{\infty} b_k z^k, \quad a_k, b_k \geq 0. \quad (1.4)$$

The classes $S_H(m, n, \alpha)$ and $\bar{S}_H(m, n, \alpha)$ were studied by Yalcin [9].

Let us define the convolution of two harmonic functions. For harmonic functions of the form

$$f_m(z) = z - \sum_{k=2}^{\infty} a_k z^k + (-1)^{m-1} \sum_{k=1}^{\infty} b_k \bar{z}^k$$

and

$$F_m(z) = z - \sum_{k=2}^{\infty} A_k z^k + (-1)^{m-1} \sum_{k=1}^{\infty} B_k \bar{z}^k$$

we define the convolution of two harmonic functions f_m and F_m as

$$(f_m * F_m)(z) = f_m(z) * F_m(z) = z - \sum_{k=2}^{\infty} a_k A_k z^k + (-1)^{m-1} \sum_{k=1}^{\infty} b_k B_k \bar{z}^k. \quad (1.5)$$

Recently Yalcin [[9], Theorem 6] has obtained the following result for convolution of two functions in class $\bar{S}_H(m, n, \alpha)$.

Theorem A. For $0 \leq \beta \leq \alpha < 1$ let $f_m \in \bar{S}_H(m, n; \alpha)$ and $F_m \in \bar{S}_H(m, n; \beta)$. Then $f_m * F_m \in \bar{S}_H(m, n; \alpha) \subseteq \bar{S}_H(m, n; \beta)$.

In the present paper, motivated with the work of Kumar [5], we prove the following theorem and then we critically observed that it improves the above stated theorem of Yalcin [9].

Theorem 1. Let the functions

$$f_m(z) = z - \sum_{k=2}^{\infty} a_k z^k + (-1)^{m-1} \sum_{k=1}^{\infty} b_k \bar{z}^k \quad (a_k, b_k \geq 0)$$

and

$$F_m(z) = z - \sum_{k=2}^{\infty} A_k z^k + (-1)^{m-1} \sum_{k=1}^{\infty} B_k \bar{z}^k \quad (A_k, B_k \geq 0)$$

belong to the classes $\bar{S}_H(m, n; \alpha)$ and $\bar{S}_H(m, n; \beta)$ respectively. Then $(f_m * F_m)(z) \in \bar{S}_H(2m, m+n; \alpha)$ (if m is an even integer) and $(f_m * F_m)(z) \in \bar{S}_H(2m-1, m+n-1; \alpha)$ (if m is an odd integer).

To prove this theorem we require the following lemmas. Lemma 1 and 2 are due to Yalcin [9].

Lemma 2. A function $f_m(z)$ of the form (1.4) belongs to the class $\overline{S}_H(m, n; \alpha)$ if and only if

$$\sum_{k=2}^{\infty} \frac{k^m - \alpha k^n}{1 - \alpha} a_k + \sum_{k=1}^{\infty} \frac{k^m - (-1)^{m-n} \alpha k^n}{1 - \alpha} b_k \leq 1.$$

Lemma 3. $\overline{S}_H(m, n; \alpha) \subseteq \overline{S}_H(m, n; \beta)$, if $0 \leq \beta \leq \alpha < 1$.

Lemma 4. (i) $\overline{S}_H(2m, m + n; \alpha) \subseteq \overline{S}_H(m, n; \alpha)$, (if m is an even integer).

(ii) $\overline{S}_H(2m - 1, m + n - 1; \alpha) \subseteq \overline{S}_H(m, n; \alpha)$, (if m is an odd integer).

Proof. **Proof of Lemma 4(i)**

Let $f_m \in \overline{S}_H(2m, m + n; \alpha)$ then by using Lemma 2 we have

$$\begin{aligned} & \sum_{k=2}^{\infty} \frac{k^{2m} - \alpha k^{m+n}}{1 - \alpha} a_k + \sum_{k=1}^{\infty} \frac{k^{2m} - (-1)^{2m-(m+n)} \alpha k^{m+n}}{1 - \alpha} b_k \leq 1 \\ \Rightarrow & \sum_{k=2}^{\infty} \frac{k^m(k^m - \alpha k^n)}{1 - \alpha} a_k + \sum_{k=1}^{\infty} \frac{k^m(k^m - (-1)^{m-n} \alpha k^n)}{1 - \alpha} b_k \leq 1. \end{aligned} \tag{1.6}$$

Now

$$\begin{aligned} & \sum_{k=2}^{\infty} \frac{k^m - \alpha k^n}{1 - \alpha} a_k + \sum_{k=1}^{\infty} \frac{k^m - (-1)^{m-n} \alpha k^n}{1 - \alpha} b_k \\ & \leq \sum_{k=2}^{\infty} \frac{k^m(k^m - \alpha k^n)}{1 - \alpha} a_k + \sum_{k=1}^{\infty} \frac{k^m(k^m - (-1)^{m-n} \alpha k^n)}{1 - \alpha} b_k \\ & \leq 1, \quad [\text{Using (1.6)}]. \end{aligned}$$

Thus $f_m \in \overline{S}_H(m, n; \alpha)$.

The proof of Lemma 4(i) is established. □

Proof. **Proof of Lemma 4(ii)** The proof of Lemma 4(ii) is similar to that of Lemma 4(i), hence it will be omitted. □

2. PROOF OF THE THEOREM 1.

Here we only prove the Theorem 1 for the case when m is an even integer. For the case when m is an odd integer one can prove the Theorem 1 in similar way. Therefore it is omitted.

Proof. Since $f_m(z) \in \overline{S}_H(m, n; \alpha)$, then by using Lemma 2 we have

$$\sum_{k=2}^{\infty} \frac{k^m - \alpha k^n}{1 - \alpha} a_k + \sum_{k=1}^{\infty} \frac{k^m - (-1)^{m-n} \alpha k^n}{1 - \alpha} b_k \leq 1. \tag{2.1}$$

Similarly $F_m(z) \in \overline{S}_H(m, n; \beta)$, we have

$$\sum_{k=2}^{\infty} \frac{k^m - \beta k^n}{1 - \beta} A_k + \sum_{k=1}^{\infty} \frac{k^m - (-1)^{m-n} \beta k^n}{1 - \beta} B_k \leq 1.$$

Therefore $\frac{k^m - \beta k^n}{1 - \beta} A_k \leq 1, \forall k = 2, 3, \dots$

$$\frac{k^m - \beta k^n}{1 - \beta} A_k \leq 1, \forall k = 2, 3, \dots$$

and

$$\frac{k^m - (-1)^{m-n} \beta k^n}{1 - \beta} B_k \leq 1, \forall k = 1, 2, 3, \dots$$

Now, for the convolution function $f_m * F_m$ we have

$$\begin{aligned} & \sum_{k=2}^{\infty} \frac{k^{2m} - \alpha k^{m+n}}{1 - \alpha} a_k A_k + \sum_{k=1}^{\infty} \frac{k^{2m} - (-1)^{2m-(m+n)} \alpha k^{m+n}}{1 - \alpha} b_k B_k \\ &= \sum_{k=2}^{\infty} \frac{k^m (k^m - \alpha k^n)}{1 - \alpha} a_k A_k + \sum_{k=1}^{\infty} \frac{k^m (k^m - (-1)^{m-n} \alpha k^n)}{1 - \alpha} b_k B_k \\ &\leq \sum_{k=2}^{\infty} \left(\frac{k^m - \beta k^n}{1 - \beta} \right) A_k \left(\frac{k^m - \alpha k^n}{1 - \alpha} \right) a_k \\ &+ \sum_{k=1}^{\infty} \left(\frac{k^m - (-1)^{m-n} \beta k^n}{1 - \beta} \right) B_k \left(\frac{k^m - (-1)^{m-n} \alpha k^n}{1 - \alpha} \right) b_k \\ &\leq \sum_{k=2}^{\infty} \frac{k^m - \alpha k^n}{1 - \alpha} a_k + \sum_{k=1}^{\infty} \frac{k^m - (-1)^{m-n} \alpha k^n}{1 - \alpha} b_k \\ &\leq 1, \text{ [Using (2.1)].} \end{aligned}$$

Therefore, we have

$(f_m * F_m)(z) \in \overline{S}_H(2m, m+n; \alpha)$ (if m is an even integer).

Similarly

$(f_m * F_m)(z) \in \overline{S}_H(2m-1, m+n-1; \alpha)$ (if m is an odd integer). \square

IMPROVEMENT OF YALCIN'S RESULT

In this section, we consider the following two cases and in each case, we observe that our result improves the result of Yalcin [[9], Theorem 6].

Case (i) When m is an even integer.

Case (ii) When m is an odd integer.

Here we discuss these cases one by one.

Case (i) When m is an even integer our Theorem states that $(f_m * F_m)(z) \in \overline{S}_H(2m, m+n; \alpha)$, whereas result of Yalcin gives $(f_m * F_m)(z) \in \overline{S}_H(m, n; \alpha)$. But by Lemma 3 and 4(i) we have $\overline{S}_H(2m, m+n; \alpha) \subseteq \overline{S}_H(m, n; \alpha) \subseteq \overline{S}_H(m, n; \beta)$. Therefore our result provides smaller class in comparison to the class given by Yalcin to which $(f_m * F_m)(z)$ belongs.

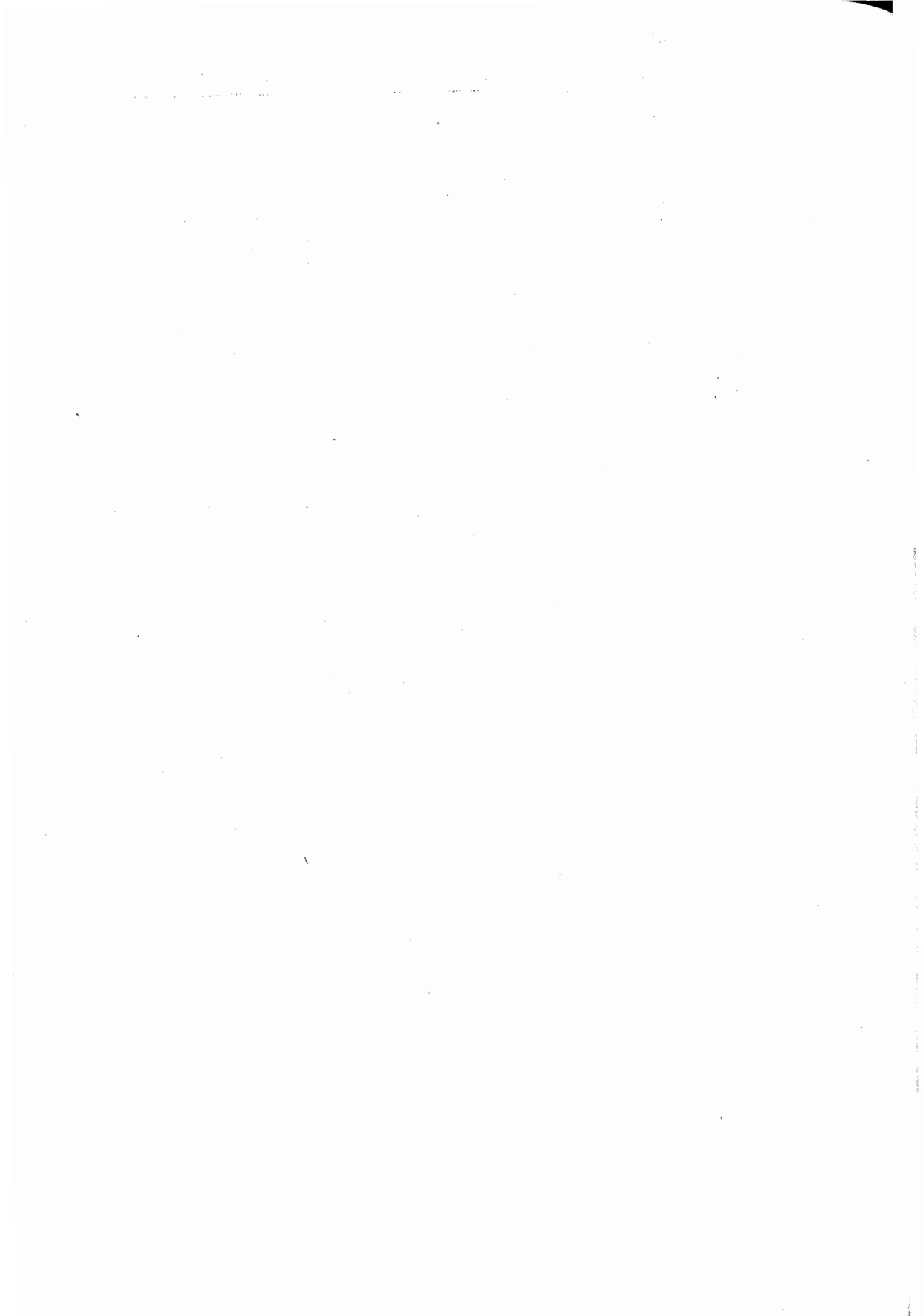
Case (ii) When m is an odd integer we use our result $(f_m * F_m)(z) \in \overline{S}_H(2m-1, m+n-1; \alpha)$. Since $\overline{S}_H(2m-1, m+n-1; \alpha) \subseteq \overline{S}_H(m, n; \alpha) \subseteq \overline{S}_H(m, n; \beta)$ (by Lemma 3 and 4(ii)). Our result provides better estimate in this case also.

Hence we conclude that for all values of $m \in N = \{1, 2, 3, \dots\}$ our result improves the result of Yalcin [[9], Theorem 6].

Acknowledgement: The authors are thankful for the referee for his valuable comments and suggestions.

REFERENCES

- [1] O.P. AHUJA, *Planar harmonic univalent and related mappings*, J. Inequal. Pure Appl. Math., **6** (4) (2005), Art. 122, 1-18.
- [2] J. CLUNIE AND T. SHEIL-SMALL, *Harmonic univalent functions*, Ann. Acad. Sci. Fen. Series AI Math., **9** (1984), 3-25.
- [3] P. DUREN, *Harmonic mappings in the plane*, Camb. Univ. Press, (2004).
- [4] J.M. JAHANGIRI, G. MURUGUSUNDARAMOORTHY AND K. VIJAYA, *Salagean-type harmonic univalent functions*, Southwest J. Pure Appl. Math., **2** (2002), 77-82.
- [5] V. KUMAR, *Hadamard product of certain starlike functions*, J. Math. Anal. Appl., **110** (1985), 425-428.
- [6] S. PONNUSAMY AND A. RASILA, *Planar harmonic mappings*, Mathematics Newsletters, **17** (2) (2007), 40-57.
- [7] S. PONNUSAMY AND A. RASILA, *Planar harmonic and quasiconformal mappings*, Mathematics Newsletters, **17** (3) (2007), 85-101.
- [8] G.S. SALAGEAN, *Subclasses of univalent functions*, Complex Analysis-Fifth Romanian Finish Seminar, Bucharest, **1** (1983), 362-372.
- [9] SIBEL YALCIN, *A new class of Salagean-type harmonic univalent functions*, Appl. Math. Lett., **18** (2005), 191-198.



G -Subsets and G -Orbits of $Q^*(\sqrt{n})$ Under Action of the Modular Group

M. Aslam Malik
 Department of Mathematics
 University of the Punjab
 Lahore, Pakistan.
 Email: malikpu@yahoo.com

M. Riaz
 Department of Mathematics
 University of the Punjab
 Lahore, Pakistan.
 Email: mriaz@math.pu.edu.pk

Abstract. It is well known that $G = \langle x, y : x^2 = y^3 = 1 \rangle$ represents the modular group $PSL(2, \mathbb{Z})$, where $x : z \rightarrow \frac{-1}{z}, y : z \rightarrow \frac{z-1}{z}$ are linear fractional transformations. Let $n = k^2m$, where k is any non zero integer and m is square free positive integer. Then the set

$$Q^*(\sqrt{n}) := \left\{ \frac{a + \sqrt{n}}{c} : a, c, b = \frac{a^2 - n}{c} \in \mathbb{Z} \text{ and } (a, b, c) = 1 \right\}$$

is a G -subset of the real quadratic field $Q(\sqrt{m})$ [12]. We denote $\alpha = \frac{a + \sqrt{n}}{c}$ in $Q^*(\sqrt{n})$ by $\alpha(a, b, c)$. For a fixed integer $s > 1$, we say that two elements $\alpha(a, b, c), \alpha'(a', b', c')$ of $Q^*(\sqrt{n})$ are s -equivalent if and only if $a \equiv a' \pmod{s}, b \equiv b' \pmod{s}$ and $c \equiv c' \pmod{s}$. The class $[a, b, c] \pmod{s}$ contains all s -equivalent elements of $Q^*(\sqrt{n})$ and E_s^n denotes the set consisting of all such classes of the form $[a, b, c] \pmod{s}$. In this paper we investigate proper G -subsets and G -orbits of the set $Q^*(\sqrt{n})$ under the action of Modular Group G .

AMS (MOS) Subject Classification Codes: 05C25, 11E04, 20G15

Keywords: Real quadratic irrational number, congruences, quadratic residues, linear fractional transformations.

1. INTRODUCTION

An integer $m > 0$ is said to be square free if its prime decomposition contains no repeated factors. It is well known that every irrational member of $Q(\sqrt{m})$ can be uniquely expressed as $\frac{a + \sqrt{n}}{c}$, where $n = k^2m$ for some integer k and $a, \frac{a^2 - n}{c}$ and c are relatively prime integers.

The set $Q^*(\sqrt{n}) = \left\{ \frac{a + \sqrt{n}}{c} : a, c, b = \frac{a^2 - n}{c} \in \mathbb{Z} \text{ and } (a, b, c) = 1 \right\}$ is a proper G -subset of $Q(\sqrt{m})$ [12]. If $\alpha = \frac{a + \sqrt{n}}{c}$ and $\bar{\alpha} = \frac{a - \sqrt{n}}{c}$ have different signs, then α is called

an ambiguous number. These ambiguous numbers play an important role in the study of action of G on $\mathbb{Q}(\sqrt{m}) \cup \{\infty\}$, as $\text{Stab}_\alpha(G)$ are the only non-trivial stabilizers and in the orbit α^G , there is only one (up to isomorphism).

G. Higman (1978) introduced the concept of the coset diagrams for the modular group $PSL(2, \mathbb{Z})$ and Q. Mushtaq (1983) laid its foundation. By using the coset diagrams for the orbit of the modular group $G = \langle x, y : x^2 = y^3 = 1 \rangle$ acting on the real quadratic fields Mushtaq [12] showed that for a fixed non-square positive integer n , there are only a finite number of ambiguous numbers in $\mathbb{Q}^*(\sqrt{n})$, and that the ambiguous numbers in the coset diagram for the orbit α^G form a closed path and it is the only closed path contained in it. Let $\mathcal{C}' = \mathcal{C} \cup \{\pm\infty\}$ be the extended complex plane. The action of the modular group $PSL(2, \mathbb{Z})$ on an imaginary quadratic field, subsets of \mathcal{C}' , has been discussed in [11]. The action of the modular group on the real quadratic fields, subsets of \mathcal{C}' , has been discussed in detail in [2], [12] and [13]. The exact number of ambiguous numbers in $\mathbb{Q}^*(\sqrt{n})$ has been determined in [7], [15] as a function of n . The ambiguous length of an orbit α^G is the number of ambiguous numbers in the same orbit [7], [15]. The Number of Subgroups of $PSL(2, \mathbb{Z})$ when acting on $F_p \cup \{\infty\}$ has been discussed in [14] and the subgroups of the classical modular group has been discussed in [10].

A classification of the elements $(a + \sqrt{p})/c$, $b = (a^2 - p)/c$, of $\mathbb{Q}^*(\sqrt{p})$, p an odd prime, with respect to odd-even nature of a, b, c has been given in [3]. M. Aslam Malik et al. [8] proved, by using the notion of congruence, that for each non-square positive integer $n > 2$, the action of the group G on a subset $\mathbb{Q}^*(\sqrt{n})$ of the real Quadratic field $\mathbb{Q}(\sqrt{m})$ is intransitive.

If p is an odd prime, then $t \not\equiv 0 \pmod{p}$ is said to be a quadratic residue of p if there exists an integer u such that $u^2 \equiv t \pmod{p}$.

The quadratic residues of p form a subgroup R of the group of nonzero integers modulo p under multiplication and $|R| = (p - 1)/2$. [1]

Lemma 1. *If $r_1, r_2 \in R$, $n_1, n_2 \notin R$ (r_1, r_2 are quadratic residues, and n_1, n_2 are quadratic non-residue, Then*

(a) $n_1 r_1$ is a quadratic non-residue.

(b) $n_1 n_2$ is a quadratic residue.

(c) $r_1 r_2$ is a quadratic residue.

In the sequel, q, r and q, nr will stand for quadratic residue and quadratic non-residue respectively. The Legendre symbol (a/p) is defined as 1 if a is a quadratic residue of p otherwise it is defined by -1 . [1]

We denote the element $\alpha = \frac{a + \sqrt{n}}{c}$ of $\mathbb{Q}^*(\sqrt{n})$ by $\alpha(a, b, c)$ and say that two elements $\alpha(a, b, c)$ and $\alpha'(a', b', c')$ of $\mathbb{Q}^*(\sqrt{n})$ are s -equivalent (and write $\alpha(a, b, c) \sim_s \alpha'(a', b', c')$ or $\alpha \sim_s \alpha'$) if and only if $a \equiv a' \pmod{s}$, $b \equiv b' \pmod{s}$ and $c \equiv c' \pmod{s}$. Clearly the relation \sim_s is an equivalence relation, so for each integer $s > 1$, we get different equivalence classes $[a, b, c]$ modulo s of $\mathbb{Q}^*(\sqrt{n})$. [8]

Let E_s denote the set consisting of classes of the form $[a, b, c] \pmod{s}$, n modulo s whereas if $n \equiv i \pmod{s}$ for some fixed $i \in \{0, 1, \dots, s - 1\}$ and the set consisting of elements of the form $[a, b, c]$ with $n \equiv i \pmod{s}$ is denoted by E_p^i (or E_s^n). Obviously $\bigcup_{i=1}^{s-1} E_s^i = E_s$ and $E_s^i \cap E_s^j = \phi$ for $i \neq j$. [6]

The classification of the real quadratic irrational numbers by taking prime modulus is very helpful in studying the modular group action on the real quadratic fields. Thus it becomes

interesting to determine the proper G -subsets of $Q^*(\sqrt{n})$ by taking the action of G on the set $Q^*(\sqrt{n})$ and hence to find the G -orbits of $Q^*(\sqrt{n})$ for each non square n .

2. MODULAR GROUP G ACTING ON $Q^*(\sqrt{n})$.

In [8], it was shown that the action of the group on $Q^*(\sqrt{2})$ is transitive, whereas the action of G on $Q^*(\sqrt{n})$, $n \neq 2$ is intransitive. Specifically, it was proved with the help of classes $[a, b, c] \pmod{2^2}$ of the elements of $Q^*(\sqrt{n})$ that $Q^*(\sqrt{n})$, $n \not\equiv 2 \pmod{4}$, has two proper G -subsets.

Q. Mushtaq [12], In the case of $PSL(2, 13)$, showed one G -orbit of length 13 in the coset diagram for the natural action of $PSL(2, \mathbb{Z})$ on any subset of the real projective line. In [6] it was proved that there exist two proper G -subsets of $Q^*(\sqrt{n})$ when $n \equiv 0 \pmod{p}$ and four G -subsets of $Q^*(\sqrt{n})$ when $n \equiv 0 \pmod{pq}$. In the present studies, with the help of the idea of quadratic residues, we generalize this result and prove some crucial results which provide us proper G -subsets and G -orbits of $Q^*(\sqrt{n})$.

We extend this idea to determine four proper G -subsets of $Q^*(\sqrt{n})$ with $n \equiv 0 \pmod{2pq}$.

Lemma 2. *Let $n \equiv 0 \pmod{2pq}$ where p and q are two distinct odd primes, then the sets $S_1 = \{\alpha \in Q^*(\sqrt{n}) : (c/pq) = 1 \text{ or } (b/pq) = 1\}$, $S_2 = \{\alpha \in Q^*(\sqrt{n}) : (c/p) = -1 \text{ or } (b/p) = -1 \text{ with } (c/q) = 1 \text{ or } (b/q) = 1\}$, $S_3 = \{\alpha \in Q^*(\sqrt{n}) : (c/p) = 1 \text{ or } (b/p) = 1 \text{ with } (c/q) = -1 \text{ or } (b/q) = -1\}$, and $S_4 = \{\alpha \in Q^*(\sqrt{n}) : (c/p) = -1 \text{ or } (b/p) = -1 \text{ with } (c/q) = -1 \text{ or } (b/q) = -1\}$ are four proper G -subsets of $Q^*(\sqrt{n})$.*

Proof. Let $\frac{a+\sqrt{n}}{c} \in Q^*(\sqrt{n})$ and $n \equiv 0 \pmod{2pq}$, then

$$a^2 \equiv bc \pmod{2pq} \tag{2. 1}$$

where a, b, c are belonging to the complete residue system $\{0, 1, 2, \dots, 2\bar{p}q - 1\}$. The congruence (2. 1) implies $a^2 \equiv bc \pmod{2}$, $a^2 \equiv bc \pmod{p}$ and $a^2 \equiv bc \pmod{q}$. Since 1 is the only quadratic residue of 2 and there is no quadratic non-residue of 2. Thus by Lemma 1.1 the quadratic residues and quadratic non residues of pq and $2pq$ are the same. We know that, if $(t, m) = 1$ and $m = 2pq$, then the congruence $x^2 \equiv t \pmod{m}$ is solvable and has four incongruent solutions if and only if t is quadratic residue of m [1], and in this case congruence (2. 1) is solvable and has exactly four incongruent solutions. If $a = b = c$ and each of a, b, c are quadratic residue of pq then there exist four distinct classes

$$[a, b, c], [-a, b, c], [a, -b, -c], [-a, -b, -c] \pmod{pq}$$

Thus for each member $[a, b, c] \pmod{pq}$, we have four cases.

case(i) The classes $[a, b, c] \pmod{pq}$ with $(b/pq) = 1$, Then all these classes are contained in S_1 .

case(ii) The classes $[a, b, c] \pmod{pq}$ with $(b/p) = -1$, $(b/q) = 1$, Then all these classes are contained in S_2 .

case(iii) The classes $[a, b, c] \pmod{pq}$ with $(b/p) = 1$, $(b/q) = -1$, Then all these classes are contained in S_3 .

case(iv) The classes $[a, b, c] \pmod{pq}$ with $(b/p) = -1$, $(b/q) = -1$, Then all these classes are contained in S_4 .

As $x(\alpha) = \frac{-a+\sqrt{n}}{b} = \frac{a_1+\sqrt{n}}{c_1}$, where $a_1 = -a$, $b_1 = c$, $c_1 = b$ and $y(\frac{a+\sqrt{n}}{c}) = \frac{-a+b+\sqrt{n}}{b} = \frac{a_2+\sqrt{n}}{c_2}$, where

$$a_2 = -a + b, b_2 = -2a + b + c, \text{ and } c_2 = b$$

then by the congruence (2.1) we have

$$(-a + b)^2 \equiv (-2a + b + c)b \pmod{p} \quad (2.2)$$

Since the modular group $PSL(2, \mathbb{Z})$ has the representation $G = \langle x, y : x^2 = y^3 = 1 \rangle$ and every element of G is a word in the generators x, y of G , to prove that S_1 is invariant under the action of G , it is enough to show that every element of S_1 is mapped onto an element of S_1 under x and y . Thus clearly by the congruences (2.1) and (2.2) the sets S_1, S_2, S_3 and S_4 are G -subsets of $\mathbb{Q}^*(\sqrt{n})$. \square

Remark 3. Since the quadratic residues and quadratic non residues of pq and $2pq$ are the same. Therefore the number of G -subsets of $\mathbb{Q}^*(\sqrt{n})$ when $n \equiv 0 \pmod{pq}$ or $n \equiv 0 \pmod{2pq}$ are same.

Example 1. In the coset diagram for $\mathbb{Q}^*(\sqrt{15})$ there are four G -orbits namely

$$(\sqrt{15})^G, (-\sqrt{15})^G, \left(\frac{\sqrt{15}}{3}\right)^G \text{ and } \left(\frac{\sqrt{15}}{-3}\right)^G$$

and similarly there are four G -orbits for $\mathbb{Q}^*(\sqrt{30})$ namely

$$(\sqrt{30})^G, (-\sqrt{30})^G, \left(\frac{\sqrt{30}}{2}\right)^G \text{ and } \left(\frac{\sqrt{30}}{-2}\right)^G$$

In the closed path lying in the orbit $(\sqrt{15})^G$, the transformation

$$g = (yx)^3(y^2x)(yx)^3$$

fixes $k = \sqrt{15}$ that is $((yx)^3(y^2x)(yx)^3)(k) = k$, and so gives the quadratic equation $k^2 - 15 = 0$, the zeros, $\pm\sqrt{15}$, of this equation are fixed points of the transformations g .

Let k is an ambiguous number then $x(k)$ is also ambiguous but one of the numbers $y(k)$ or $y^2(k)$ is ambiguous. The orientation of edges in the coset diagram is associated with the involution x and the small triangles with y which has order 3. One of k and $x(k)$ is positive and other is negative but one of $k, y(k)$ or $y^2(k)$ is negative and the other two are positive. We use an arrow head on an edge to indicate its direction from negative to a positive vertex. The table 1 shows the details of the orbits α^G , transformations which fixes α , and the ambiguous lengths of each orbit.

TABLE 1. The Orbits of $\alpha \in \mathbb{Q}^*(\sqrt{n})$.

G -orbits	Transformations	Ambiguous Length
$(\sqrt{15})^G$	$(yx)^3(y^2x)(yx)^3$	14
$(-\sqrt{15})^G$	$(yx)^3(y^2x)(yx)^3$	14
$\left(\frac{\sqrt{15}}{3}\right)^G$	$(yx)(y^2x)^3(yx)$	10
$\left(\frac{\sqrt{15}}{-3}\right)^G$	$(yx)(y^2x)^3(yx)$	10
$(\sqrt{30})^G$	$(yx)^5(y^2x)^2(yx)^5$	24

G-orbits	Transformations	Ambiguous Length
$(-\sqrt{30})^G$	$(yx)^5(y^2x)^2(yx)^5$	24
$(\frac{\sqrt{30}}{2})^G$	$(yx)^2(y^2x)(yx)^2(y^2x)(yx)^2$	16
$(\frac{\sqrt{30}}{-2})^G$	$(yx)^2(y^2x)(yx)^2(y^2x)(yx)^2$	16

Now we extend this idea when $n \equiv 0 \pmod{p_1p_2\dots p_r}$.

Theorem 4. Let $n \equiv 0 \pmod{p_1p_2\dots p_r}$, where p_1, p_2, \dots, p_r are distinct odd primes, then there are exactly 2^r , G-subsets of $\mathbb{Q}^*(\sqrt{n})$.

Proof. Let $\frac{a+\sqrt{n}}{c} \in \mathbb{Q}^*(\sqrt{n})$ and $n \equiv 0 \pmod{p_1p_2\dots p_r}$ where p_1, p_2, \dots, p_r are distinct odd primes, then $a^2 - n = bc$ gives

$$a^2 \equiv bc \pmod{p_1p_2\dots p_r} \tag{2.3}$$

The congruence (2.3) implies $a^2 \equiv bc \pmod{p_1}$,

$$a^2 \equiv bc \pmod{p_2}, \dots, \text{ and } a^2 \equiv bc \pmod{p_r}.$$

We know that, if $(t, m) = 1$ and $m = p_1p_2\dots p_r$, then the congruence $x^2 \equiv t \pmod{m}$ is solvable if and only if t is quadratic residue of m [1], and in this case congruence (2.3) is solvable and has exactly 2^r incongruent solutions. Since all values of b or c which are quadratic residues and quadratic non-residues of m lie in the distinct G-subsets and m is the product of r distinct primes, Thus consequently we obtain 2^r , G-subsets of $\mathbb{Q}^*(\sqrt{n})$. □

Corollary 5. Let $n \equiv 0 \pmod{2p_1p_2\dots p_r}$ where p_1, p_2, \dots, p_r are distinct odd primes, then there are exactly 2^r , G-subsets of $\mathbb{Q}^*(\sqrt{n})$.

Proof. Let $\frac{a+\sqrt{n}}{c} \in \mathbb{Q}^*(\sqrt{n})$ and $n \equiv 0 \pmod{2p_1p_2\dots p_r}$ where p_1, p_2, \dots, p_r are distinct odd primes, then

$$a^2 \equiv bc \pmod{2p_1p_2\dots p_r} \tag{2.4}$$

The congruence (2.4) implies $a^2 \equiv bc \pmod{2}$, $a^2 \equiv bc \pmod{p_1}$,

$$a^2 \equiv bc \pmod{p_2}, \dots, \text{ and } a^2 \equiv bc \pmod{p_r}$$

Since 1 is the only quadratic residue of 2 and there is no quadratic non-residue of 2. Thus by Lemma 1 the quadratic residues and quadratic non residues of $p_1p_2\dots p_r$ and $2p_1p_2\dots p_r$ are same. Hence the result follows by the Theorem 4 □

Remark 6. The number of G-orbits of $\mathbb{Q}^*(\sqrt{n})$ when $n \equiv 0 \pmod{p_1p_2\dots p_r}$ or $n \equiv 0 \pmod{2p_1p_2\dots p_r}$ are same.

Example 2. Take $n = 3.5.7.11 = 1155$, Under the action of G on $\mathbb{Q}^*(\sqrt{1155})$ there are sixteen G-orbits of $\mathbb{Q}^*(\sqrt{1155})$ namely

$$(\sqrt{1155})^G, \left(\frac{\sqrt{1155}}{-1}\right)^G, \left(\frac{\sqrt{1155}}{3}\right)^G, \left(\frac{\sqrt{1155}}{-3}\right)^G,$$

$$\begin{aligned} & \left(\frac{\sqrt{1155}}{5}\right)^G, \left(\frac{\sqrt{1155}}{-5}\right)^G, \left(\frac{\sqrt{1155}}{7}\right)^G, \left(\frac{\sqrt{1155}}{-7}\right)^G, \\ & \left(\frac{\sqrt{1155}}{11}\right)^G, \left(\frac{\sqrt{1155}}{-11}\right)^G, \left(\frac{\sqrt{1155}}{15}\right)^G, \left(\frac{\sqrt{1155}}{-15}\right)^G, \\ & \left(\frac{\sqrt{1155}}{21}\right)^G, \left(\frac{\sqrt{1155}}{-21}\right)^G, \left(\frac{\sqrt{1155}}{33}\right)^G, \left(\frac{\sqrt{1155}}{-33}\right)^G. \end{aligned}$$

Similarly for $n = 2.3.5.7.11 = 2310$, Under the action of G on $\mathcal{Q}^*(\sqrt{2310})$ there are sixteen G -orbits of $\mathcal{Q}^*(\sqrt{2310})$ namely

$$\begin{aligned} & (\sqrt{2310})^G, \left(\frac{\sqrt{2310}}{-1}\right)^G, \left(\frac{\sqrt{2310}}{2}\right)^G, \left(\frac{\sqrt{2310}}{-2}\right)^G, \\ & \left(\frac{\sqrt{2310}}{5}\right)^G, \left(\frac{\sqrt{2310}}{-5}\right)^G, \left(\frac{\sqrt{2310}}{7}\right)^G, \left(\frac{\sqrt{2310}}{-7}\right)^G, \\ & \left(\frac{\sqrt{2310}}{10}\right)^G, \left(\frac{\sqrt{2310}}{-10}\right)^G, \left(\frac{\sqrt{2310}}{11}\right)^G, \left(\frac{\sqrt{2310}}{-11}\right)^G, \\ & \left(\frac{\sqrt{2310}}{14}\right)^G, \left(\frac{\sqrt{2310}}{-14}\right)^G, \left(\frac{\sqrt{2310}}{22}\right)^G, \left(\frac{\sqrt{2310}}{-22}\right)^G. \end{aligned}$$

Theorem 7. Let $h = 2k + 1 \geq 3$ then there are exactly two G -orbits of $\mathcal{Q}^*(\sqrt{2^h})$ namely $(2^k\sqrt{2})^G$ and $\left(\frac{2^k\sqrt{2}}{-1}\right)^G$.

Proof. Let $\frac{a+\sqrt{n}}{c} \in \mathcal{Q}^*(\sqrt{2^h})$. Then we have $a^2 - 2^h \equiv bc \pmod{2^h}$. This implies that $a^2 \equiv bc \pmod{2^h}$. We know by [1] that the congruence $a^2 \equiv bc \pmod{2^h}$ is solvable if and only if $bc \equiv 1 \pmod{8}$, Moreover the quadratic residue of 2^h , $h \geq 3$ are those integers of the form $8l + 1$ which are less than 2^h . Since all values of b or c which are quadratic residues and quadratic non-residues of 2^h lie in the distinct orbits. Thus the classes $[a, b, c]$ (modulo 2^h) with b or c quadratic residues of 2^h lie in the orbit $(2^k\sqrt{2})^G$ and similarly the classes $[a, b, c]$ (modulo 2^h) with b or c quadratic non-residues of 2^h lie in the orbit $\left(\frac{2^k\sqrt{2}}{-1}\right)^G$, This proves the result. \square

Example 3. There are exactly two G -orbits of $\mathcal{Q}^*(\sqrt{2^7})$ namely $(2^3\sqrt{2})^G$ and $\left(\frac{2^3\sqrt{2}}{-1}\right)^G$, In the closed path lying in the orbit $(2^3\sqrt{2})^G$, the transformation $(yx)^{11}(y^2x)^3(yx)^5(y^2x)^3(yx)^{11}$ fixes $2^3\sqrt{2}$. Similarly in the closed path lying in the orbit $\left(\frac{2^3\sqrt{2}}{-1}\right)^G$, the transformation $(yx)^{11}(y^2x)^3(yx)^5(y^2x)^3(yx)^{11}$ fixes $\frac{2^3\sqrt{2}}{-1}$.

3. ACTION OF THE SUBGROUP $G^* = \langle yx \rangle$ AND $G^{**} = \langle yx, y^2x \rangle$ ON $\mathcal{Q}^*(\sqrt{n})$.

Let us suppose that $G^* = \langle yx \rangle$ and $G^{**} = \langle yx, y^2x \rangle$ are two subgroups of G . In this section, we determine the G -subsets and G -orbits of $\mathcal{Q}^*(\sqrt{n})$ by subgroup G^* and G^{**} acting on $\mathcal{Q}^*(\sqrt{n})$. Let $yx(\alpha) = \alpha + 1$ and $y^2x(\alpha) = \frac{\alpha}{\alpha+1}$. Thus $yx\left(\frac{a+\sqrt{n}}{c}\right) = \frac{a_1+\sqrt{n}}{c_1}$, with $a_1 = a+c$, $b_1 = 2a+b+c$, $c_1 = c$ and $y^2x\left(\frac{a+\sqrt{n}}{c}\right) = \frac{a_2+\sqrt{n}}{c_2}$, with $a_2 = a+b$, $b_2 = b$, and $c_2 = 2a+b+c$.

In the next Lemma we see that the transformation yx fixes the classes $[0, 0, c]$ (modulo p) and the chain of these classes help us in finding G^* -subsets of $\mathcal{Q}^*(\sqrt{n})$.

Lemma 8. Let p be any prime, $n \equiv 0 \pmod{p}$, Then for any $k \geq 1$, $(yx)^k[0, 0, c] = [kc, k^2c, c] \pmod{p}$ and in particular $(yx)^p[0, 0, c] = [0, 0, c] \pmod{p}$.

Proof. Let $\alpha = [0, 0, c] \pmod p$ be a class contained in E_p^0 . Applying the linear fractional transformation yx on α successively we see $yx[0, 0, c] = [c, c, c]$, $(yx)^2[0, 0, c] = [2c, 4c, c]$, $(yx)^3[0, 0, c] = [3c, 9c, c]$ continuing this process k -times we obtain $(yx)^k[0, 0, c] = [kc, k^2c, c] \pmod p$

In particular for $k = p$, $kp \equiv 0 \pmod p$ and $k^2p \equiv 0 \pmod p$. Thus we get $(yx)^p[0, 0, c] = [0, 0, c] \pmod p$. □

Lemma 9. Let p be an odd prime, $n \equiv 0 \pmod p$ and $G^* = \langle yx \rangle$, Then the sets

$A_1 = \{\alpha \in Q^*(\sqrt{n}) : (c/p) = 1\}$, $A_2 = \{\alpha \in Q^*(\sqrt{n}) : (c/p) = -1\}$,

$C_1 = \{\alpha \in Q^*(\sqrt{n}) : c \equiv 0 \pmod p \text{ with } (b/p) = 1\}$, $C_2 = \{\alpha \in Q^*(\sqrt{n}) : c \equiv 0 \pmod p \text{ with } (b/p) = -1\}$,

are G^* -subsets of $Q^*(\sqrt{n})$.

Proof. For any $\alpha = \frac{a+\sqrt{n}}{c} \in A_1$ with $n \equiv 0 \pmod p$, then

$$a^2 \equiv bc \pmod p \tag{3.5}$$

We have two cases.

(i) If $a \equiv 0 \pmod p$, The congruence (3.5) forces that $bc \equiv 0 \pmod p$, Then either $b \equiv 0 \pmod p$ or $c \equiv 0 \pmod p$ but not both. So in this case α belongs to the class $[0, b, 0]$ or $[0, 0, c]$ modulo p .

(ii) If $a \not\equiv 0 \pmod p$, $a^2 \equiv bc \pmod p$, Then (3.5) forces that either both b, c are quadratic residues of p or both quadratic non-residues of p .

As $yx : [a, b, c] \rightarrow [a + c, 2a + b + c, c]$, Then it is clear that the set A_1 is invariant under the action of the mapping yx , So the set A_1 is a G^* -subset $Q^*(\sqrt{n})$. Similarly the set A_2 is G^* -subset of $Q^*(\sqrt{n})$.

Again for any $\alpha = \frac{a+\sqrt{n}}{c} \in C_1$ by congruence (3.5) $c \equiv 0 \pmod p \Rightarrow a \equiv 0 \pmod p$, with $b \not\equiv 0 \pmod p$, so the classes belonging to the set C_1 are of the form $[0, b, 0]$ with b quadratic residue of p . Since the mapping yx fixes the classes $[0, b, 0]$. Thus clearly the set C_1 is a G^* -subsets. Similarly the set C_2 is G^* -subsets of $Q^*(\sqrt{n})$. □

In the next theorem we determine two G -subsets of $Q^*(\sqrt{n})$ by using A_1, A_2, C_1 and C_2 as given in Lemma 9

Theorem 10. The sets $S_1 = A_1 \cup C_1$ and $S_2 = A_2 \cup C_2$ are two G -subsets of $Q^*(\sqrt{n})$.

Proof. Let $\alpha = \frac{a+\sqrt{n}}{c} \in S_1$ then either $\alpha \in A_1$ or $\alpha \in C_1$ with $n \equiv 0 \pmod p$. Thus it is clear that the classes $[a, b, c] \pmod p$ with b or c quadratic residues of p is contained in $A_1 \cup C_1$. By Lemma 3.1 yx fixes the classes $[0, 0, c] \pmod p$. Also the classes belonging to A_1, A_2 are connected to the classes belonging to C_1, C_2 , respectively under x . Since the modular group $PSL(2, \mathbb{Z})$ has the representation $G = \langle x, y : x^2 = y^3 = 1 \rangle$ and every element of G is a word in its generators x, y , to prove that S_1 is invariant under the action of G , it is enough to show that every element of S_1 is mapped onto an element of S_1 under x and y . Thus clearly we see that $S_1 = A_1 \cup C_1$ and $S_2 = A_2 \cup C_2$ are both G -subsets of $Q^*(\sqrt{n})$. □

In view of the above theorem we observe that for $n = 2$ the action of G on $Q^*(\sqrt{n})$ is transitive. Since 1 is the only quadratic residue of 2 and there is no quadratic non-residue of 2, Therefore the set S_2 becomes empty and S_1 is the only G -subset of $Q^*(\sqrt{2})$. While the action of G on $Q^*(\sqrt{n})$, $n \neq 2$ is intransitive.

Example 4. Let $\alpha = \frac{a+\sqrt{n}}{c} \in \mathcal{Q}^*(\sqrt{n})$, with $n \equiv 0 \pmod{5}$, be of the form $[a, b, c] \pmod{5}$. In modulo 5, the squares of the integers 1, 2, 3, 4 are

$$1^2 \equiv 4^2 \equiv 1 \text{ and } 2^2 \equiv 3^2 \equiv 4$$

Consequently, the quadratic residues of 5 are 1, 4, and the non residues are 2, 3. Thus A_1 consists of elements of $\mathcal{Q}^*(\sqrt{n})$ of the form

$$[0, 0, 1], [0, 0, 4], [1, 1, 1], [4, 1, 1], [2, 4, 1], [2, 1, 4], [3, 1, 4], [3, 4, 1], [1, 4, 4], [4, 4, 4] \pmod{5}.$$

Then A_1 is invariant under yx , Thus A_1 is G^* -subset of $\mathcal{Q}^*(\sqrt{n})$.

The elements of A_2 are of the form

$$[0, 0, 2], [0, 0, 3], [2, 2, 2], [3, 2, 2], [2, 3, 3], [4, 3, 2], [4, 2, 3], [1, 2, 3], [1, 3, 2] \text{ and } [3, 3, 3] \pmod{5} \text{ only.}$$

Again A_2 is invariant under yx , Thus A_2 is also G^* -subset of $\mathcal{Q}^*(\sqrt{n})$.

The elements of C_1 are of the form $[0, 1, 0]$ and $[0, 4, 0]$, and the elements of C_2 are of the form $[0, 2, 0]$ and $[0, 3, 0]$ Thus C_1 and C_2 are G^* -subsets.

Then clearly the sets $S_1 = A_1 \cup C_1$ and $S_2 = A_2 \cup C_2$ are two G -subsets of $\mathcal{Q}^*(\sqrt{n})$.

In the next lemma we find the conditions when n is quadratic residue of p .

Lemma 11. For any $\alpha(a, b, c) \in \mathcal{Q}^*(\sqrt{n})$, then the following statements are equivalent

(i) n is quadratic residue of p

(ii) b or $c \equiv 0 \pmod{p}$.

Proof. Let $\alpha = \frac{a+\sqrt{n}}{c} \in \mathcal{Q}^*(\sqrt{n})$, then

$$a^2 - n \equiv bc \pmod{p} \tag{3.6}$$

Let b or $c \equiv 0 \pmod{p}$

Then congruence (3.6) implies that $a^2 \equiv n \pmod{p}$. This shows that n is quadratic residue of p .

Conversely let n be quadratic residue of p then the congruence $a^2 \equiv n \pmod{p}$ must be solvable. Now the congruence (6) holds only if b or $c \equiv 0 \pmod{p}$. \square

Further we see the action of $G^{**} = \langle yx, y^2x \rangle$ on $\mathcal{Q}^*(\sqrt{n})$ with n quadratic residue of p and determine four proper G^{**} -subsets of $\mathcal{Q}^*(\sqrt{n})$.

Theorem 12. Let p be an odd prime and n is quadratic residue of p , let $\alpha = \frac{a+\sqrt{n}}{c} \in \mathcal{Q}^*(\sqrt{n})$ and $G^{**} = \langle yx, y^2x \rangle$, then the sets

$$G_1 = \{\alpha \in \mathcal{Q}^*(\sqrt{n}) : (c/p) = 1\}, G_2 = \{\alpha \in \mathcal{Q}^*(\sqrt{n}) : (c/p) = -1\},$$

are both G^{**} -subsets of $\mathcal{Q}^*(\sqrt{n})$.

Proof. Let $\alpha = \frac{a+\sqrt{n}}{c} \in \mathcal{Q}^*(\sqrt{n})$, with $a^2 - n \equiv bc \pmod{p}$, and a, b, c modulo p are belonging to the set $\{0, 1, 2, \dots, p-1\}$.

Let p be an odd prime with n quadratic residue of p , then by Lemma 11 either $b \equiv 0 \pmod{p}$ or $c \equiv 0 \pmod{p}$.

Since $yx : [a, b, c] \rightarrow [a+c, 2a+b+c, c]$ and $y^2x : [a, b, c] \rightarrow [a+b, b, 2a+b+c]$, Since every element of G^{**} is a word in its generators yx, y^2x , Then clearly the sets G_1, G_2 , are two G^{**} -subsets of $\mathcal{Q}^*(\sqrt{n})$. \square

It is important to note that 37 is the smallest prime which have four G -orbits and all odd primes less than 37 has exactly two G -orbits.

Example 5. In the coset diagram for $Q^*(\sqrt{37})$, There are exactly four G-orbits of $Q^*(\sqrt{37})$ given by $(\sqrt{37})^G$, $(\frac{1+\sqrt{37}}{2})^G$, $(\frac{1+\sqrt{37}}{-3})^G$, $(\frac{-1+\sqrt{37}}{-3})^G$.

The Set S_1 containing three orbits $(\sqrt{37})^G$, $(\frac{1+\sqrt{37}}{-3})^G$, $(\frac{-1+\sqrt{37}}{-3})^G$ is a G-subset, While the set S_2 containing only one orbit $(\frac{1+\sqrt{37}}{2})^G$ is another G-subset.

In the closed path lying in the orbit $(\sqrt{37})^G$, the transformation

$$g_1 = (yx)^6(y^2x)^{12}(yx)^6$$

fixes $k = \sqrt{37}$, that is $g_1(k) = ((yx)^6(y^2x)^{12}(yx)^6)(k) = k$, and so gives the quadratic equation $k^2 - 37 = 0$, the zeros, $\pm\sqrt{37}$, of this equation are fixed points of the transformations g_1 .

In the closed path lying in the orbit $(\frac{1+\sqrt{37}}{2})^G$, the transformations

$$g_2 = (yx)^3(y^2x)(yx)(y^2x)^5(yx)(y^2x)(yx)^2$$

fixes $l = \frac{1+\sqrt{37}}{2}$ and so gives the quadratic equation $l^2 - l - 9 = 0$, the zeros, $\frac{1\pm\sqrt{37}}{2}$, of this equation are fixed points of g_2 .

Similarly in the closed path lying in the orbit $(\frac{1+\sqrt{37}}{-3})^G$ the transformation

$$g_3 = (yx)^2(y^2x)^2(yx)(y^2x)^3(yx)^2(y^2x)(yx)$$

fixes $(\frac{1+\sqrt{37}}{-3})$ and corresponding to the closed lying in the orbit $(\frac{-1+\sqrt{37}}{-3})^G$, the transformation

$$g_4 = (yx)(y^2x)(yx)^2(y^2x)^3(yx)(y^2x)^2(yx)^2$$

fixes $(\frac{-1+\sqrt{37}}{-3})$.

By [7], [15] we see that $\tau^*(37) = 124$, That is there are 124 ambiguous numbers in the coset diagram for $Q^*(\sqrt{37})$ while the ambiguous length of the orbits $(\sqrt{37})^G$, $(\frac{1+\sqrt{37}}{2})^G$, $(\frac{1+\sqrt{37}}{-3})^G$, and $(\frac{-1+\sqrt{37}}{-3})^G$ are 48, 28, 24 and 24 respectively.

REFERENCES

- [1] Andrew Adler and John E. Coury: *The Theory of Numbers*. Jones and Barlett Publishers, Boston London (1995).
- [2] G. Higman and Q. Mushtaq: Coset Diagrams and Relations for $PSL(2, \mathbb{Z})$. Gulf J.Sci. Res. (1983) 159-164.
- [3] I. Kouser, S.M. Husnine, A. Majeed: A classification of the elements of $Q^*(\sqrt{p})$ and a partition of $Q^*(\sqrt{p})$ Under the Modular Group Action. PUJM, Vol.31 (1998) 103-118.
- [4] I. N. Herstein: *Topics in Algebra*. John Wiley and Sons, Second Edition (1975).
- [5] J. H. Conway, R. T. Curtis, S. P. Norton, R. A. Parker, and R. A. Wilson: *An Atlas of Finite Groups*. Oxford Univ. Press, Oxford, (1985).
- [6] M. Aslam Malik, M. Asim Zafar: Real Quadratic Irrational Numbers and Modular Group Action. South East Asian Bulletin of Mathematics, Vol.35(3) (2011).
- [7] M. Aslam Malik, S. M. Husnine and A. Majeed: Modular Group Action on Certain Quadratic Fields. PUJM, Vol.28 (1995) 47-68.
- [8] M. Aslam Malik, S. M. Husnine and A. Majeed: Intransitive Action of the Modular Group $PSL(2, \mathbb{Z})$ on a subset $Q^*(\sqrt{k^2m})$ of $Q(\sqrt{m})$. PUJM, Vol.37, (2005) 31-38.
- [9] M. Aslam Malik, S. M. Husnine, and A. Majeed: Properties of Real Quadratic Irrational Numbers under the action of group $H = \langle x, y : x^2 = y^4 = 1 \rangle$. Studia Scientiarum Mathematicarum Hungarica Vol.42(4) (2005) 371-386.
- [10] M. H. Millington: Subgroups of the classical modular group. J. London Math. Soc. 1:351-357 (1970) 133-146.
- [11] Muhammad Ashiq and Q. Mushtaq: Actions of a subgroup of the Modular Group on an imaginary Quadratic Field. QuasiGroups and Related Systems Vol. 14, (2006) 133-146.

- [12] Q. Mushtaq: Modular Group acting on Real Quadratic Fields. Bull. Austral. Math. Soc. Vol. 37, (1988) 303-309, 89e: 11065.
- [13] Q. Mushtaq: On word structure of the Modular Group over finite and real quadratic fields. Discrete Mathematics 179 (1998). 145-154.
- [14] S. Anis, Q. Mushtaq: The Number of Subgroups of $PSL(2, \mathbb{Z})$ when acting on $F_p \cup \{\infty\}$. Communication in Algebra, Vol 36 4276-4283 (2008).
- [15] S. M. Husnine, M. Aslam Malik, and A. Majeed: On Ambiguous Numbers of an invariant subset $\mathbb{Q}^*(\sqrt{k^2m})$ of $\mathbb{Q}(\sqrt{m})$ under the action of the Modular Group $PSL(2, \mathbb{Z})$. Studia Scientiarum Mathematicarum Hungarica Vol.42(4) (2005) 401-412.

Anti Fuzzy Implicative Ideals in BCK-Algebras

Nora.O.Al-Shehri
Department of mathematics
Faculty of Sciences for Girls
King Abdulaziz University
Jeddah, Saudi Arabia
Email: n.alshehry@yahoo.com

Abstract.The aim of this paper is to introduce the notion of anti fuzzy implicative ideals of BCK -algebras and to investigate their properties. We give several characterizations of anti fuzzy implicative ideals. We also introduce the notion of anti Cartesian product of anti fuzzy implicative ideals, and then we study related properties.

AMS (MOS) Subject Classification Codes: 06F35, 03G25

Key Words: Anti fuzzy ideal, Anti fuzzy implicative ideal, BCK -algebra.

1. INTRODUCTION

The main problem in fuzzy mathematics is how to carry out the ordinary concepts to the fuzzy case. The difficulty lies in how to pick out the rational generalization from the large number of available approaches. It is worth noting that fuzzy ideals are different from ordinary ideals in the sense that one cannot say which BCK -algebra element belongs to the fuzzy ideal under consideration and which one does not. The concept of fuzzy sets was introduced by Zadeh [13]. Since then these ideas have been applied to other algebraic structures such as semigroups, groups, rings, modules, vector spaces and topologies. In 1991, Xi [12] applied the concept of fuzzy sets to BCK -algebras which are introduced by Imai and Iséki [5]. In [1], Biswas introduced the concept of anti fuzzy subgroups of groups. Modifying his idea, in [4], S. M. Hong and Y. B. Jun applied the idea to BCK -algebras. They introduced the notion of anti fuzzy ideals of BCK -algebras. In this paper, we introduce the notion of anti fuzzy implicative ideal of BCK -algebras, and investigate some related properties. We show that in an implicative BCK -algebra, a fuzzy subset is an anti fuzzy ideal if and only if it is an anti fuzzy implicative ideal. We show that a fuzzy subset of a BCK -algebra is a fuzzy implicative ideal if and only if the complement of this fuzzy subset is an anti fuzzy implicative ideal. Moreover, we discuss the pre-image of anti fuzzy implicative ideals. Finally, we introduce the notion of anti Cartesian product of anti fuzzy implicative ideals, and then we characterize anti fuzzy implicative ideals by it.

2. PRELIMINARIES

In this section we cite the fundamental definitions that will be used in the sequel:

Definition 1. [6] An algebra $(X, *, 0)$ of type $(2, 0)$ is called a *BCK* - algebra if it satisfies the following axioms for all $x, y, z \in X$:

- (i) $((x * y) * (x * y)) * (x * y) = 0$,
- (ii) $(x * (x * y)) * y = 0$,
- (iii) $x * x = 0$,
- (iv) $0 * x = 0$,
- (v) $x * y = 0$ and $y * x = 0$ imply $x = y$

We can define a partial ordering \leq on X by $x \leq y$ if and only if $x * y = 0$.

Proposition 2. [6] In any *BCK*-algebra X , the following hold for all $x, y, z \in X$:

- (i) $(x * y) * z = (x * z) * y$,
- (ii) $x * y \leq x$,
- (iii) $x * 0 = x$,
- (iv) $(x * z) * (y * z) \leq x * y$,
- (v) $x * (x * (x * y)) = x * y$,
- (vi) $x \leq y$ implies $x * z \leq y * z$ and $z * y \leq z * x$.

A *BCK*-algebra is said to be implicative if $x * (y * x) = x$ for all $x, y \in X$ (see[6,9]).

Definition 3. [8] A non-empty subset I of a *BCK*-algebra X is called an ideal of X if it satisfies

- (I₁) $0 \in I$
- (I₂) $x * y \in I$ and $y \in I$ imply $x \in I$.

Definition 4. [8] A non-empty subset I of a *BCK*-algebra X is called an implicative ideal of X if it satisfies (I₁) and (I₃) $x \in I$ whenever $(x * (y * x)) * z \in I$ and $z \in I$ for all $x, y, z \in X$.

Definition 5. [13] Let S be a non-empty set. A fuzzy subset A of S is a function $A : S \rightarrow [0,1]$. Let A be a fuzzy subset of S . Then for $t \in [0,1]$, the t -level cut of A is the set $A_t = \{x \in S \mid A(x) \geq t\}$ and the complement of A , denoted by A^c is the fuzzy subset of S given by $A^c(x) = 1 - A(x)$ for all $x \in S$.(see [2,3,7]).

Definition 6. [12] A fuzzy subset A of a *BCK*-algebra is called a fuzzy subalgebra of X if $A(x * y) \geq \min \{A(x), A(y)\}$ for all $x, y \in X$.

Definition 7. [12] Let X be a *BCK*-algebra. A fuzzy subset A of X is called a fuzzy ideal of X if

- (F₁) $A(0) \geq A(x)$,
- (F₂) $A(x) \geq \min \{A(x * y), A(y)\}$, for all $x, y \in X$.

Definition 8. [10] A fuzzy subset A of a *BCK*-algebra X is called a fuzzy implicative ideal of X if it satisfies

- (F₁) and (F₃) $A(x) \geq \min \{A((x * (y * x)) * z), A(z)\}$ for all $x, y, z \in X$.

Definition 9. [4] A fuzzy subset A of a *BCK*-algebra X is called an anti fuzzy subalgebra of X if

$$A(x * y) \leq \max \{A(x), A(y)\} \text{ for all } x, y \in X.$$

Definition 10. [4] A fuzzy subset A of a *BCK*-algebra X is called an anti fuzzy ideal of X if

- (A₁) $A(0) \leq A(x)$,
- (A₂) $A(x) \leq \max \{A(x * y), A(y)\}$, for all $x, y \in X$.

Proposition 11. [4] Every anti fuzzy ideal of a BCK-algebra X is an anti fuzzy subalgebra of X .

Definition 12. [4] Let A be a fuzzy subset of a BCK-algebra. Then for $t \in [0, 1]$ the lower t -level cut of A is the set

$$A^t = \{x \in X \mid A(x) \leq t\}$$

Definition 13. [4] Let A be a fuzzy subset of a BCK-algebra. The fuzzification of $A^t, t \in [0, 1]$ is the fuzzy subset μ_{A^t} of X defined by

Definition 14. [11] Let $f : X \rightarrow Y$ be a mapping of BCK-algebras and A be a fuzzy subset of Y . The map A^f is the inverse image of A under f if $A^f(x) = A(f(x)) \forall x \in X$.

3. ANTI FUZZY IMPLICATIVE IDEAL

Definition 15. A fuzzy subset A of a BCK-algebra X is called an anti fuzzy implicative ideal of X if it satisfies

$$(A_1) \text{ and } (A_3) \ A(x) \leq \max \{A((x * (y * x)) * z), A(z)\} \text{ for all } x, y, z \in X.$$

Example 1. (1) Every constant function $A : X \rightarrow [0, 1]$ is an anti fuzzy implicative ideal of X (2) Let $X = \{0, a, b, c\}$ be a BCK-algebra with Cayley table as follows:

*	0	a	b	c
0	0	0	0	0
a	a	0	0	a
b	b	a	0	b
c	c	c	c	0

Let t_0, t_1 be such that $t_0 < t_1$. Define $A : X \rightarrow [0, 1]$ by $A(0) = A(a) = A(b) = t_0$ and $A(c) = t_1$. Routine calculations give that A is an anti fuzzy implicative ideal.

Proposition 16. Every anti fuzzy implicative ideal of a BCK-algebra X is order preserving.

Proof. Let A be an anti fuzzy implicative ideal of a BCK-algebra X and let $x, y \in X$ be such that $x \leq y$. Then

$$\begin{aligned} A(x) &\leq \max \{A((x * (z * x)) * y), A(y)\}, \\ &= \max \{A((x * y) * (z * x)), A(y)\}, \\ &= \max \{A(0 * (z * x)), A(y)\}, \\ &= \max \{A(0), A(y)\} = A(y). \end{aligned} \quad \square$$

Proposition 17. Every anti fuzzy implicative ideal of a BCK-algebra X is an anti fuzzy ideal.

Proof. Let A be an anti fuzzy implicative ideal of a BCK-algebra X , so for all $x, y, z \in X$:

$$A(x) \leq \max \{A((x * (y * x)) * z), A(z)\},$$

Putting in $y = x$, and $z = y$:

$$\begin{aligned} A(x) &\leq \max \{A((x * x) * y), A(y)\} \\ &= \max \{A(x * y), A(y)\}. \end{aligned} \quad \square$$

Combining Proposition 2.11 and 3.4 yields the following result.

Proposition 18. Every anti fuzzy implicative ideal of a BCK-algebra X is an anti fuzzy subalgebra of X .

Remark 19. An anti fuzzy ideal (subalgebra) of a BCK-algebra X may not be an anti fuzzy implicative ideal of X as shown in the following example:

Example 2. Let X be the BCK-algebra in Example 3.2(2) and let $t_0, t_1, t_2 \in [0, 1]$ be such that $t_0 < t_1 < t_2$. Define $A : X \rightarrow [0, 1]$ by $A(0) = t_0, A(a) = A(b) = t_1$ and $A(c) = t_2$. Routine calculations give that A is an anti fuzzy ideal (subalgebra) of X , but not an anti fuzzy implicative ideal of X because

$$\begin{aligned} A(a) &= t_1 > \max \{A((a * (b * a)) * 0), A(0)\} \\ &= \max \{A(0), A(0)\} = t_0. \end{aligned}$$

Proposition 20. If X is implicative BCK-algebra, then every anti fuzzy ideal of X is an anti fuzzy implicative ideal of X .

Proof. Let A be an anti fuzzy ideal of an implicative BCK-algebra X , so for all $x, z \in X$:

$$A(x) \leq \max \{A(x * z), A(z)\},$$

Since X is an implicative, then $x * (y * x) = x$ for all $x, y \in X$. Hence

$$A(x) \leq \max \{A((x * (y * x)) * z), A(z)\},$$

This shows that A is an anti fuzzy implicative ideal of X . □

By applying Proposition 17 and 20, we have

Theorem 21. If X is an implicative BCK-algebra, then a fuzzy subset A of X is an anti fuzzy ideal of X if and only if it is an anti fuzzy implicative ideal of X .

Proposition 22. A fuzzy subset A of a BCK-algebra X is a fuzzy implicative ideal of X if and only if its complement A^c is an anti fuzzy implicative ideal of X .

Proof. Let A be a fuzzy implicative ideal of a BCK-algebra X , and let $x, y, z \in X$. Then

$$\begin{aligned} A(0) &= 1 - A(0) \leq 1 - A(x) = A^c(x) \text{ and} \\ A^c(x) &= 1 - A(x) \leq 1 - \min \{A((x * (y * x)) * z), A(z)\}, \\ &= 1 - \min \{1 - A^c((x * (y * x)) * z), 1 - A^c(z)\}, \\ &= \max \{A^c((x * (y * x)) * z), A^c(z)\}. \end{aligned}$$

So, A^c is an anti fuzzy implicative ideal of X . Now let A^c is an anti fuzzy implicative ideal of X , and let $x, y, z \in X$. Then

$$\begin{aligned} A(0) &= 1 - A^c(0) \geq 1 - A^c(x) = A(x) \text{ and} \\ A(x) - 1A^c(x) &\leq 1 - \max \{A^c((x * (y * x)) * z), A^c(z)\}, \\ &= 1 - \max \{1 - A((x * (y * x)) * z), 1 - A(z)\}, \\ &= \min \{A((x * (y * x)) * z), A(z)\}. \end{aligned}$$

Thus, A is a fuzzy implicative ideal of X . □

Theorem 23. Let A be an anti fuzzy implicative ideal of a BCK-algebra X . Then the set

$$X_A = \{x \in X \mid A(x) = A(0)\},$$

is an implicative ideal of X .

Proof. Clearly $0 \in X$. Let $x, y, z \in X_A$ be such that $(x * (x * y)) * z \in X$ and $z \in X_A$. Then

$$A((x * (y * x)) * z) = A(z) = A(0).$$

It follows that

$$\begin{aligned} A(x) &\leq \max \{A((x * (y * x)) * z), A(z)\} \\ &= \max \{A(0), A(0)\} = A(0). \end{aligned}$$

Combining Definition 15(A₁), we get $A(x) = A(0)$ and hence $x \in X$. □

Theorem 24. Let A be a fuzzy subset A of a BCK-algebra X . Then A is an anti fuzzy implicative ideal of X if and only if for each $t \in [0, 1], t \geq A(0)$, the lower t -level cut A^t is an implicative ideal of X .

Proof. Let A be an anti fuzzy implicative ideal of X and let $t \in [0, 1]$ with $t \geq A(0)$. Clearly $0 \in A^t$. Let $x, y, z \in X$ be such that $(x * (y * x)) * z \in A^t$ and $z \in A^t$. Then $A((x * (y * x)) * z) \leq t$, $A(z) \leq t$,

hence

$$A(x) \leq \max\{A((x * (y * x)) * z), A(z)\} \leq t.$$

And so $x \in A^t$. Hence A^t is an implicative ideal of X .

Conversely, let A^t is an implicative ideal of X , we first show $A(0) \leq A(x)$ for all $x \in X$. If not, then there exists $x_0 \in X$ such that $A(0) \not\leq A(x_0)$. Putting $t_0 = \frac{1}{2}\{A(0) + A(x_0)\}$ then $0 \leq A(x_0)$; $t_0 \leq A(0) \leq 1$. Hence $x_0 \in A^{t_0}$, so that $A^{t_0} \neq \emptyset$. But A^{t_0} is an implicative ideal of X . Thus $0 \in A^{t_0}$, or $A(0) \leq t_0$, a contradiction. Hence $A(0) \leq A(x)$ for all $x \in X$. Now we prove that $A(x) \leq \max\{A((x * (y * x)) * z), A(z)\}$ for all $x, y, z \in X$. If not, then there exists $x_0, y_0, z_0 \in X$, such that

$$A(x_0) > \max\{A((x_0 * (y_0 * x_0)) * z_0), A(z_0)\},$$

Taking $s_0 = \frac{1}{2}\{A(x_0) + \max\{((x_0 * (y_0 * x_0)) * z_0), A(z_0)\}\}$;

then $s_0 \leq A(x_0)$ and

$$0 \leq \max\{A((x_0 * (y_0 * x_0)) * z_0), A(z_0)\} \leq s_0.$$

Thus we have $s_0 \leq A((x_0 * (y_0 * x_0)) * z_0)$ and $s_0 \leq A(z_0)$. Which imply that $(x_0 * (y_0 * x_0)) * z_0 \in A^{s_0}$ and $z_0 \in A^{s_0}$. But A^{s_0} is an implicative ideal of X . Thus $x_0 \in A^{s_0}$ or $A(x_0) \leq s_0$. This is a contradiction, ending the proof. \square

Theorem 25. *If A is an anti fuzzy implicative ideal of a BCK-algebra X . Then μ_{A^t} is also an anti fuzzy implicative ideal of X where $t \in [0, 1]$, $t \geq A(0)$.*

Proof. From Theorem 24, it is sufficient to show that $(\mu_{A^t})^s$ is an implicative ideal of X , where $s \in [0, 1]$ and $s \geq \mu_{A^t}(0)$. Clearly, $0 = (\mu_{A^t})^s$. Let $x, y, z \in X$ be such that $(x * (y * x)) * z \in (\mu_{A^t})^s$ and $z \in (\mu_{A^t})^s$,

hence

$$\mu_{A^t}((x * (y * x)) * z) \leq s,$$

and

$\mu_{A^t}(z) \leq s$. We claim that $x \in (\mu_{A^t})^s$ or $\mu_{A^t}(x) \leq s$. If $(x * (y * x)) * z \in A^t$ and $z \in A^t$, then $x \in A^t$ because A^t is an implicative ideal of X . Hence,

$$\begin{aligned} \mu_{A^t}(x) &= A(x) \\ &\leq \max\{A((x * (y * x)) * z), A(z)\}, \\ &= \max\{\mu_{A^t}((x * (y * x)) * z), \mu_{A^t}(z)\} \leq s. \end{aligned}$$

and so $x \in (\mu_{A^t})^s$ if $(x * (y * x)) * z \notin A^t$ or $z \notin A^t$, then $\mu_{A^t}((x * (y * x)) * z) = 0$ or $\mu_{A^t}(z) = 0$ then clearly $\mu_{A^t}(x) \leq s$, and so $x \in (\mu_{A^t})^s$. Therefore $(\mu_{A^t})^s$ is an implicative ideal of X . \square

Theorem 26. *Theorem 3.13. Let $f : X \rightarrow Y$ be a homomorphism of BCK-algebras. If A is an anti fuzzy implicative ideal of Y , then A^f is an anti fuzzy implicative ideal of X .*

Proof. Since A is an anti fuzzy implicative ideal of Y , then $A(0') \leq A(f(x))$ for any $x \in X$, and so, $A^f(0) = A(f(0)) = A(0') \leq A(f(x)) = A^f(x)$. For any $x, y, z \in X$, we have:

$$\begin{aligned} A^f(x) &= A(f(x)) \leq \max\{A((f(x) * (f(y) * f(x))) * f(z)), A(f(z))\}, \\ &= \max\{A((f(x) * (f(y * x))) * f(z)), A(f(z))\}, \\ &= \max\{A((f(x * (y * x))) * f(z)), A(f(z))\}, \\ &= \max\{A(f((x * (y * x)) * z)), A(f(z))\}, \\ &= \max\{A^f((x * (y * x)) * z), A^f(z)\}. \end{aligned}$$

This completes the proof. \square

Theorem 27. Theorem 3.14. Let $f : X \rightarrow Y$ be an epimorphism of BCK-algebras. If A^f is an anti fuzzy implicative ideal of X , then A is an anti fuzzy implicative ideal of Y .

Proof. Let $y \in Y$, there exists $x \in X$ such that $f(x) = y$. Then

$$A(y) = A(f(x)) = A^f(x) \geq A^f(0) = A(0').$$

Let $x', y', z' \in Y$. Then there exist $x, y, z \in X$ such that $f(x) = x', f(y) = y'$ and $f(z) = z'$. It follows that

$$\begin{aligned} A(x') &= A(f(x)) = A^f(x) \leq \max \{A^f((x * (y * x)) * z), A^f(z)\}, \\ &= \max \{A(f((x * (y * x)) * z)), A(f(z))\}, \\ &= \max \{A((f(x) * (f(y * x))) * f(z)), A(f(z))\}, \\ &= \max \{A((f(x) * (f(y) * f(x))) * f(z)), A(f(z))\}, \\ &= \max \{A((x' * (y' * x')) * z'), A(z')\}. \end{aligned}$$

Hence A is an anti fuzzy implicative ideal of Y . \square

4. ANTI CARTESIAN PRODUCT OF ANTI FUZZY IMPLICATIVE IDEALS

Definition 28. Let λ and μ be the fuzzy subsets in a set X . The anti Cartesian product $\lambda \times \mu : X \times X \rightarrow [0, 1]$ is defined by $(\lambda \times \mu)(x, y) = \max \{\lambda(x), \mu(y)\}$ for all $x, y \in X$.

Theorem 29. If λ and μ are anti fuzzy implicative ideals of a BCK-algebra X , then $\lambda \times \mu$ is an anti fuzzy implicative ideal of $X \times X$.

Proof. Let $x, x' \in X$

$$\begin{aligned} (\lambda \times \mu)(0, 0) &= \max \{\lambda(0), \mu(0)\} \\ &\leq \max \{\lambda(x), \mu(x)\} = (\lambda \times \mu)(x, x') \end{aligned}$$

For any $(x, x'), (y, y'), (z, z') \in X \times X$ we have

$$\begin{aligned} (\lambda \times \mu)(x, x') &= \max \{\lambda(x), \mu(x')\} \\ &\leq \max \{\max \{\lambda(x * (y * x)) * z, \lambda(z)\}, \max \{\mu(x' * (y' * x')) * z', \mu(z')\}\}, \\ &= \max \{\max \{\lambda(x * (y * x)) * z, \mu(x' * (y' * x')) * z'\}, \max \{\lambda(z), \mu(z')\}\}, \\ &= \max \{(\lambda \times \mu)((x, x') * ((y, y') * (x, x'))) * (z, z'), (\lambda \times \mu)(z, z')\}. \end{aligned}$$

Hence $\lambda \times \mu$ is an anti fuzzy implicative ideal of $X \times X$ \square

Theorem 30. Let λ and μ be fuzzy subsets in a BCK-algebra X such that $\lambda \times \mu$ is an anti fuzzy implicative ideal of $X \times X$ Then:

- (i) either $\lambda(x) \geq \lambda(0)$ or $\mu(x) \leq \mu(0)$ for all $x \in X$;
- (ii) if $\lambda(x) \geq \lambda(0)$ for all $x \in X$, then either $\lambda(x) \geq \mu(0)$ or $\mu(x) \geq \mu(0)$;
- (iii) if $\mu(x) \geq \mu(0)$ for all $x \in X$, then either $\lambda(x) \geq \lambda(0)$ or $\mu(x) \geq \lambda(0)$.

Proof. (i) Suppose that $\lambda(x) < \lambda(0)$ and $\mu(y) < \mu(0)$ for some $x, y \in X$. Then

$$(\lambda \times \mu)(x, y) = \max \{\lambda(x), \mu(y)\} < \max \{\lambda(0), \mu(0)\} = (\lambda \times \mu)(0, 0).$$

This is a contradiction and we obtain (i).

(ii) Assume that there exist $x, y \in X$ such that $\lambda(x) < \mu(0)$ and $\mu(x) < \mu(0)$. Then

$$(\lambda \times \mu)(0, 0) = \max \{\lambda(0), \mu(0)\} = \mu(0).$$

It follows that

$$(\lambda \times \mu)(x, y) = \max \{\lambda(x), \mu(y)\} < \mu(0) = (\lambda \times \mu)(0, 0),$$

which is a contradiction. Hence (ii) holds.

(iii) Similar to (ii). \square

Theorem 31. Let λ and μ be fuzzy subsets in a BCK-algebra X such that $\lambda \times \mu$ is an anti fuzzy implicative ideal of $X \times X$. Then either μ or λ is an anti fuzzy implicative ideal of X .

Proof. By Theorem 30(i), without loss of generality we assume that $\mu(x) \geq \mu(0)$ for all $x \in X$. From (iii) it follows that either $\lambda(x) \geq \lambda(0)$ or $\mu(x) \geq \lambda(0)$. If $\mu(x) \geq \lambda(0)$ for all $x \in X$, then $(\lambda \times \mu)(0, x) = \max\{\lambda(0), \mu(x)\} = \mu(x)$. Let $(x, x'), (y, y'), (z, z') \in X \times X$, since $\lambda \times \mu$ is an anti fuzzy implicative ideal of $X \times X$. We have $(\lambda \times \mu)(x, x') \leq \max\{(\lambda \times \mu)((x, x') * (y, y') * (x, x')) * (z, z'), (\lambda \times \mu)(z, z')\}$,
 $= \max\{\lambda \times \mu((x * (y * x)) * z, (x' * (y' * x')) * z'), (\lambda \times \mu)(z, z')\}$.

Putting $x = y = z = 0$, then

$$\begin{aligned} \mu(x') &= (\lambda \times \mu)(0, x') \leq \max\{(\lambda \times \mu)(0, (x' * (y' * x')) * z'), (\lambda \times \mu)(0, z')\}, \\ &= \max\{\max\{\lambda(0), \mu((x' * (y' * x')) * z')\}, \max\{\lambda(0), \mu(z')\}\}, \\ &= \max\{\mu((x' * (y' * x')) * z'), \mu(z')\}. \end{aligned}$$

This proves that μ is an anti fuzzy implicative ideal of X . The second part is similar. This completes the proof. \square

5. CONCLUSION

We discussed the notion of anti fuzzy implicative ideals of *BCK*-algebras and gave several characterizations. Also, we introduced the notion of anti cartesian product of anti fuzzy implicative ideals. Our definitions probably can be applied in other kinds of anti ideals of *BCK*-algebras.

REFERENCES

- [1] R. Biswas, Fuzzy subgroups and anti fuzzy subgroups, *Fuzzy Sets and systems*, 35(1990), 121-124.
- [2] P. S. Das, Fuzzy groups and level subgroups, *Math. Anal. Appl.* 84(1981), 264-269.
- [3] J. A. Goguen, L-fuzzy sets, *J. Math. Anal. Appl.* 18(1967), 145-179.
- [4] S. M. Hong and Y. B. Jun, Anti fuzzy ideals in *BCK*-algebras, *Kyungpook Math. J.* 38(1998), 145-150.
- [5] Y. Imai and K. Iseki, On axiom systems of propositional calculi, *Proc. Japan Academy*, 42(1966), 19-22.
- [6] K. Iseki and S. Tanaka, An introduction to the theory of *BCK*-algebras, *Math. Japon.* 23(1978), 1-26.
- [7] Y. B. Jun, Characterization of fuzzy ideals by their level ideals in *BCK(BCI)*-algebras, *Math. Japon.* 38(1993), 67-71.
- [8] J. Meng, On ideals in *BCK*-algebras, *Math. Japon.* 40(1994), 143-154.
- [9] J. Meng and Y. B. Jun, *BCK*-algebras, Kyung Moon Sa Co., Seoul Korea 1994.
- [10] J. Meng, Y. B. Jun and H. S. Kim, Fuzzy implicative ideals of *BCK*-algebras, *Fuzzy Sets and systems*, 89(1997), 243-248.
- [11] A. Rosenfeld, Fuzzy groups, *J. Math. Anal. Appl.*, 35(1971), 512-517.
- [12] O. G. Xi, Fuzzy *BCK*-algebras, *Math. Japon.* 36(1991), 935-942.
- [13] L. A. Zadeh, Fuzzy sets, *Inform. Control*, 8(1965), 338-353.



Instructions for Author

1. The journal is meant for publication of research papers and review articles covering state of the art in a particular area of mathematical science.
2. Manuscripts should be in suitable form for publication. As far as possible, the use of complicated notations should be avoided. Illustrations and diagrams should be submitted on separate sheets and not included in the text. They should be of good quality.
3. The contributors are required to provide a soft copy (in pdf form) of the paper composed in Latex/Tex at the following addresses
shahid_siddiqi@math.pu.edu.pk
shahidsiddiqimath@yahoo.co.uk
or the same may be sent in triplicate to the Chief Editor, PUJM,
Department of Mathematics, University of the Punjab, Quaid-e-Azam
Campus, Lahore 54590, Pakistan.
If the paper is accepted, the source file of the paper in Latex/Tex AMS
format will be required.
4. Reference should be given at the end of the paper and be referred by numbers in serial order on square brackets, e.g. [3]. Reference should be typed as follows:
Reference to Paper:
[3] C.S. Hoo, *BCI-algebras with conditions*, Math. Japonica 32, No. 5 (1987) 749-756.
Reference to Book:
B. Mitchel: *Theory of categories*, New York: Academic Press, 1965.
5. The decision to accept or reject a paper for publication in the Journal rests fully with the Editorial Board.
6. Authors, whose papers will be published in the Journal, will receive free reprints of their papers and a copy of the issue containing their contributions.
7. The Journal which is published annually will be supplied free of cost in exchange with other Journals of Mathematics.

CONTENTS

- Chromatic Uniqueness of Complete Bipartite Graphs with Certain Edges Deleted II 1-8
by R. Hasni and Y.H. Peng
- Newton-Like Methods with At least Quadratic Order of Convergence for the Computation of Fixed Points 9-18
by Ioannis K. Argyros
- On the Semilocal Convergence of Werner's Method for Solving Equations Using Recurrent Functions 19-28
by Ioannis K. Argyros and Said Hilout
- Simulation of Rotational Flows in Cylindrical Vessel with Double Rotating Stirrers; Part-A: Analysis of Flow Structure and Pressure Differentials 29-45
by Ahsanullah Baloch, Rafique Ahmed Memon and M.A. Solangi
- Analysis of Stresses and Power Consumption of Mixing Flow in Cylindrical Container 46-67
by Ahsanullah Baloch, Rafique Ahmed Memon and M.A. Solangi
- Convolution of Salagean-type Harmonic Univalent Functions 69-73
by Saurabh Porwal, K. K. Dixit and S. B. Joshi
- G-Subsets and G-Orbits of $Q^*(\sqrt{n})$ Under Action of the Modular Group 75-84
by M. Riaz and M. Aslam Malik
- Anti Fuzzy Implicative Ideals in BCK-Algebras 85-91
by Nora. O. Al-Shehri